

**Analysis of  
A Disintegrin and Metalloprotease 17 (ADAM17)  
in the metastatic niche  
of the lung**

Dissertation  
zur Erlangung des Doktorgrades  
der Mathematisch-Naturwissenschaftlichen Fakultät  
der Christian-Albrechts-Universität  
zu Kiel

vorgelegt von

Marija Stevanovic

Kiel, 2013

Referent/in: Prof. Dr. Stefan Rose-John  
Korreferent/in: Prof. Dr. Thomas Röder  
Tag der mündlichen Prüfung: 10.02.2014  
Zum Druck genehmigt: Kiel, .....  
Der Dekan

*To the strongest women in my life:  
to my mother and my grandmother...*

*To the bravest men who had a courage to follow them:  
to my father and my grandfather.*

*To the greatest support and love of my life, to Aleksandar.*

<b>Index</b> .....	I
<b>Register of figures</b> .....	VI
<b>1 Introduction</b> .....	1
1.1 Cancer and metastasis .....	1
1.2 A Disintegrin and Metalloprotease 17 (ADAM17) .....	2
1.3 ADAM17 in cancer and metastasis .....	5
1.3.1 The impact of ADAM17 on epidermal growth factor receptor (EGFR)..	5
1.3.2 The implication of ADAM17 in Notch signaling.....	6
1.4 Nuclear factor-kappa B (NF-κB) in cancer .....	10
1.5 Immune response in cancer and metastasis .....	15
<b>2 Aim of this study</b> .....	21
<b>3 Materials and Methods</b> .....	22
3.1 Materials .....	22
3.1.1 Solutions and buffers .....	22
3.1.2 Primers .....	26
3.1.3 Primary Antibodies .....	28
3.1.3 Secondary Antibodies .....	28
3.1.4 Recombinant proteins .....	29
3.1.5 Enzyme Linked Immunosorbent Assay (ELISA) .....	30
3.1.6 FACS Antibodies .....	30
3.1.7 Immunohistology .....	31
3.1.8 Proteome Profiler Antibody Array .....	32
3.2 Methods .....	32
3.2.1 RNA Isolation .....	32
3.2.2 shADAM17_pLeGO_C/BSD vector .....	33
3.2.3 Generation of LLC cells with stable ADAM17 knock down .....	34
3.2.4 Cell culture and cell lines .....	36
3.2.5 Proliferation Assay .....	37
3.2.6 Protein extraction from tissues and cultured cells .....	37
3.2.7 SDS-polyacrylamide gel electrophoresis (SDS-PAGE) .....	38
3.2.8 Immunoblotting Analysis .....	38
3.2.9 Generation of Bone Marrow Derived Neutrophils (BMDNs) .....	38
3.2.10 Generation of Bone Marrow Derived Macrophages (BMDMs) .....	39



3.2.11 Enzyme Linked Immunosorbent Assay (ELISA) .....	39
3.2.12 Animal breeding .....	40
3.2.13 Model of experimental metastasis .....	40
3.2.14 FACS analysis of tumor bearing lung tissue .....	40
3.2.15 Immunohistochemistry .....	41
3.2.16 Proteome Profiler™ Array - Mouse Cytokine Array .....	42
3.2.17 Proteome Profiler™ - Mouse Phospho-RTK Array .....	42
<b>4 Results</b> .....	<b>44</b>
4.1 ADAM17 <sup>ex/ex</sup> mice are protected in a model of experimental metastasis ....	44
4.2 ADAM17 in the metastatic niche supports metastatic progression.....	47
4.3 The early phase of metastasis is marked by accumulation of Ly6G/Gr1 <sup>+</sup> but not F4/80 <sup>+</sup> cells .....	50
4.4 Tumor-bearing lungs of ADAM17 <sup>ex/ex</sup> mice produce less factors implicated in MDSCs expansion and survival .....	51
4.5 TNF- $\alpha$ is released from the surface of Ly6G/Gr1 <sup>+</sup> cells at the early phase of metastasis .....	55
4.6 ADAM17 generates proliferatory signals during lung metastasis .....	57
4.7 ADAM17 is required for Notch activation at early phases of metastasis.....	61
4.8 IL-6 trans-signaling does not promote lung metastasis.....	62
4.9 ADAM17 in tumor cells contributes to tumor cell growth <i>in vitro</i> and metastatic growth <i>in vivo</i> .....	65
<b>5 Discussion</b> .....	<b>69</b>
5.1 ADAM17 in a model of experimental metastasis .....	69
5.2 ADAM17 in the metastatic niche is important for inflammatory signals .....	70
5.3 ADAM17 enhances metastatic progression via proliferatory stimuli .....	75
5.4 IL-6 trans-signaling does not play a protective role in LLC induced lung metastasis .....	77
5.5 ADAM17 in tumor cells is necessary for tumor cell growth <i>in vitro</i> and <i>in vivo</i> .....	78
<b>6 Summary</b> .....	<b>80</b>
<b>6 Zusammenfassung</b> .....	<b>81</b>
<b>7 References</b> .....	<b>82</b>
<b>8 Appendix</b> .....	<b>95</b>
<b>9 Publications</b> .....	<b>102</b>

**Index**

---

**10 Acknowledgement** ..... 103  
**11 Statutory Declaration** ..... 104  
**12 Curriculum vitae** ..... 105

### Register of Figures

Figure 1.1.1 Tumor-stroma interaction in primary tumor development. ....	1
Figure 1.2.1 ADAM17 domain structure .....	3
Figure 1.2.2 The implication of ADAM17 in inflammatory and proliferatory stimuli.....	4
Figure 1.3.1 Classic Notch signaling .....	8
Figure 1.3.2 Angiocrine Notch signaling .....	9
Figure 1.4.1 Complexity of TNF- $\alpha$ signaling .....	12
Figure 1.4.2 IL-6 classic and trans-signaling .....	14
Figure 1.5.1 Cytotoxic T lymphocyte cytotoxicity .....	16
Figure 4.1.1 Metastasis to the lungs and liver after LLC inoculation. ....	44
Figure 4.1.2 Metastasis to the lungs, liver and kidneys 21 days after B16F1 inoculation .....	45
Figure 4.1.3 Quantification of tumor burden in B16F1 injected animals .....	46
Figure 4.1.4 Survival rate of LLC injected animals.....	46
Figure 4.2.1 Infiltration of Gr1 <sup>+</sup> myeloid cells depends on ADAM17 in the metastatic niche .....	47
Figure 4.2.2 ADAM17 <sup>wt/wt</sup> tumor bearing lungs reveal increased infiltration of Ly6G/Gr1 <sup>+</sup> myeloid cells .....	48
Figure 4.2.3 ADAM17 <sup>wt/wt</sup> tumor bearing lungs display stronger infiltration of MDSCs..	49
Figure 4.3.1 Myeloid infiltrations in the lungs of ADAM17 <sup>wt/wt</sup> and ADAM17 <sup>ex/ex</sup> mice 7 days after LLC cells injection .....	50
Figure 4.3.2 ADAM17 <sup>wt/wt</sup> mice show increased myeloid infiltration 14 days after LLC cells injection.....	51
Figure 4.4.1 Tumors of ADAM17 <sup>wt/wt</sup> mice sustain inflammatory status via production of inflammatory cytokines and chemokines .....	52
Figure 4.4.2 CCL2/MCP-1 is predominantly produced by tumor cells .....	53

## Register of Figures

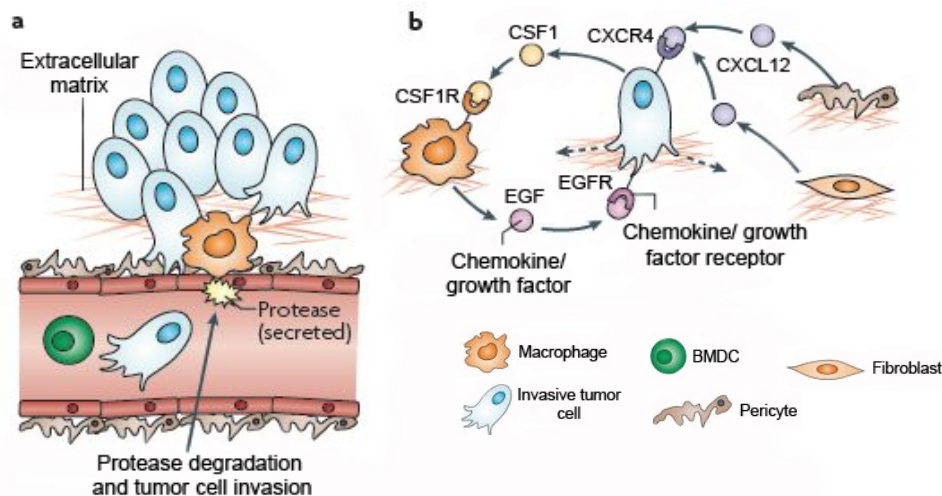
---

Figure 4.4.3 Tumor bearing lungs of ADAM17 <sup>wt/wt</sup> mice show high mRNA expression of CCL2/MCP-1 .....	53
Figure 4.4.4 Early phase of metastasis is characterized by an increased transcription of inflammatory chemokines .....	54
Figure 4.5.1 TNF- $\alpha$ and IL-1 $\beta$ are upregulated in early time points of metastasis .....	55
Figure 4.5.2 BMDN and BMDM produce TNF- $\alpha$ upon stimulation with LLC cell supernatant .....	56
Figure 4.6.1 ADAM17 in the host contributes to cell proliferation .....	57
Figure 4.6.2 TNF- $\alpha$ induces proliferation of wild type LLC cells at early time points....	58
Figure 4.6.3 Tumor bearing lungs of ADAM17 <sup>wt/wt</sup> mice show activation of ERK kinase	59
Figure 4.6.4 Phospho-RTK antibody array from lung tissue of ADAM17 <sup>wt/wt</sup> and ADAM17 <sup>ex/ex</sup> mice 2 and 3 weeks after LLC cells injection .....	60
Figure 4.7.1 ADAM17 <sup>ex/ex</sup> mice show decreased activation of Notch signaling at early phase of metastasis .....	61
Figure 4.7.2 ADAM17 <sup>ex/ex</sup> mice show decreased activation of Notch signaling at early phase of metastasis .....	62
Figure 4.8.1 Experimental metastasis with LLC cells and sgp130Fc and C57Bl6/N mice .....	63
Figure 4.8.2 sgp130Fc and C57Bl6/N mice show same tumor burden .....	64
Figure 4.9.1 ADAM17 protein and mRNA expression in different kdADAM17-LLC clones .....	65
Figure 4.9.2 kdADAM17-LLC cells grow significantly slower than wild type LLC cells	66
Figure 4.9.3 ADAM17 in tumor cells is necessary for tumor growth <i>in vivo</i> .....	67
Figure 4.9.4 mRNA expression of mCherry in the lungs of C57Bl6/N mice injected with kdADAM17-LLC cells .....	68
Figure 5.1 ADAM17 contribution to lung metastasis .....	70

# 1 Introduction

## 1.1 Cancer and Metastasis

In 2000 Hanahan and Weinberg determined six hallmarks of cancer, which are required for multistep development of tumors: sustaining proliferative signaling, evading growth suppression, resisting programmed cell death, enabling replicative immortality, inducing angiogenesis, activating invasion and metastasis (Hanahan and Weinberg, 2000). During the past decade, remarkable discoveries and progress towards understanding each hallmark of cancer have been made. Defining tumors not only as masses of proliferating cancer cells, but as complex tissues composed of a variety of cell types implicated in mutual interaction (Figure 1.1.1), led to revision and modification of formulations originally postulated. Therefore, in 2011 Hanahan and Weinberg, next to existing six hallmarks of cancer, included four new hallmarks: avoiding immune destruction, genome instability and mutation, deregulating cellular energetics and tumor-promoting inflammation (Hanahan and Weinberg, 2011).



**Figure 1.1.1 Tumor-stroma interactions in primary tumor development.** **a** For intravasation of cancer cells into the bloodstream the presence of perivascular macrophages and BMDCs is necessary. Macrophages and BMDCs supply the surrounding tissue with proteases for vascular basement membrane degradation and endothelial cell contact disruption, which is required for tumor cells to escape into the bloodstream, **b** Migration of cancer cells is accompanied with cross-talk between tumor cells, macrophages, fibroblast and pericytes. Cancer cells produce CSF1, which stimulates macrophages to secrete growth factors like e.g. EGF. Furthermore, cancer cells express CXCR4 on their surface, which is activated by CXCL12 produced by fibroblasts and pericytes. This cross-talk induces tumor cell movement towards macrophages, fibroblasts and pericytes (marked with dashed arrows); **CSF1** - colony stimulating factor 1, **CXCR4** - C-X-C chemokine receptor 4, **CXCL12** - C-X-C chemokine 12, **EGF** - epidermal growth factor, **EGFR** - epidermal growth factor receptor, **CSF1R** - colony-stimulating factor 1 receptor, **BMDC** - bone marrow derived cells. Picture was adopted from Joyce and Pollard, 2009.

Most cancer cells fail to undergo metastasis because of one or more deficiencies during this process (Fidler, 2003). Metastasis-competent cancer cells should be able to invade locally through surrounding extracellular matrix, intravasate into the lumina of blood vessels, survive the rigors of transport through the vasculature and arrest at distant organ sites. At distant organs they have to extravasate into the parenchyma, initially survive in these foreign microenvironments in order to form micrometastasis and reinitiate their proliferative capability at metastatic sites (Valastyan and Weinberg, 2011). As the end product of this multistep process – metastasis at distant organ, takes place.

Stephen Paget, the creator of the „seed and soil“ hypothesis, postulated in 1889 that metastasis does not occur by chance, but that rather certain tumor cells with metastatic activity („seed“), choose a specific organ („soil“) for the growth-enhancing milieu. This hypothesis survived until today, with more profound explanations why metastasis-competent cells have particular preferences towards specific tissues. Nowadays, it is known that gene expression in certain organs can guide cancer cells to metastatic colonization. Breast cancer cells e.g. metastasize specifically to the lungs (Minn et al., 2005) or the liver (Tabaries et al., 2011).

Metastatic seeding can be enhanced by the action of primary tumors, that secrete factors, which „prepare“ distant organs for upcoming of cancer cells, thus forming a pre-metastatic niche (Kaplan et al., 2005). Kaplan and colleagues demonstrated that Lewis Lung Carcinoma (LLC) cells, that metastasize to the lungs and occasionally to the liver, and B16 melanoma cells, which possess a more widely disseminating metastatic potential, secrete vascular endothelial growth factor (VEGF) and placental growth factor (PIGF). VEGF and PIGF, produced by the primary tumor, can attract bone marrow-derived haematopoietic progenitor cells (BMDCs) via engagement of vascular endothelial growth factor receptor 1 (VEGFR1). BMDCs that are VEGFR1<sup>+</sup>, can home to tumor-specific pre-metastatic sites and form cellular clusters before the arrival of tumor cells.

### **1.2 A Disintegrin and Metalloprotease 17 (ADAM17)**

ADAM17 was characterized and cloned in 1997 as a protease responsible for the cleavage of the membrane bound form of tumor necrosis factor-alpha, proTNF- $\alpha$  (Black and White, 1997), it was there initially termed TNF- $\alpha$  converting enzyme (TACE). It belongs

## Introduction

---

to the family of metalloproteases with high sequence homology to the snake venom metalloproteinases (SVMPs) (Blobel, 1997).

ADAM17 is a type I transmembrane protein with a domain structure (Figure 1.2.1). It consists of pro-domain, catalytic, disintegrin, membrane proximal, transmembrane and cytoplasmic domains. Each domain has unique functions. ADAM17 pro-domain acts as an inhibitor of the protease activity and it is only present when ADAM17 is in an inactive state (cleavage of pro-domain is regulated by furin protease in late Golgi compartment). The catalytic domain contains the  $Zn^{2+}$ -binding consensus motif H-E-X-G-H-X-X-G-X-X-H-D involved in coordinating  $Zn^{2+}$  with histidine residues and creating the active site of the enzyme (Stöcker et al., 1995). A disintegrin domain is important for the interaction with integrins while membrane proximal domain is necessary for the recognition of substrates and dimerization. The transmembrane domain is responsible for localization in the lipid rafts. Cytoplasmic domain is necessary for subcellular localization, trafficking and activation via phosphorylation (Scheller et al., 2011).

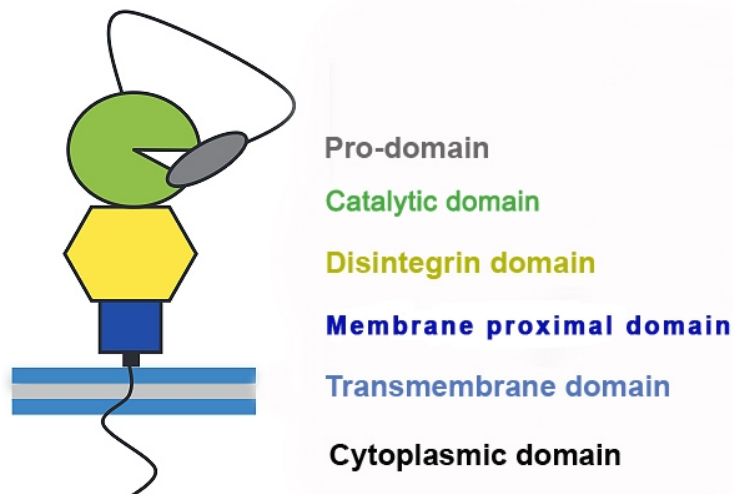


**Figure 1.2.1 ADAM17 domain structure.** ADAM17 has six domains, each with unique functions. Picture was modified from Scheller et al., 2011.

ADAM17 has emerged as a sheddase with an extremely broad substrate range. ADAM17 generates soluble proteins from their membrane-bound precursors in a process termed protein ectodomain shedding. ADAM17 is responsible for the membrane release of TNF- $\alpha$  and its receptors: tumor necrosis factor alpha receptor I and II (TNFR I and TNFR II). Furthermore, ADAM17 is responsible for the proteolytic release of epidermal growth factor receptor (EGFR) ligands like e.g. amphiregulin (AR), transforming growth factor-alpha

## Introduction

(TGF- $\alpha$ ), heparin binding-epidermal growth factor (HB-EGF) (Sahin et al., 2004). Soluble forms of these proteins have a pivotal role in cell development, inflammation, migration, cell proliferation, angiogenesis and invasion (Figure 1.2.2).

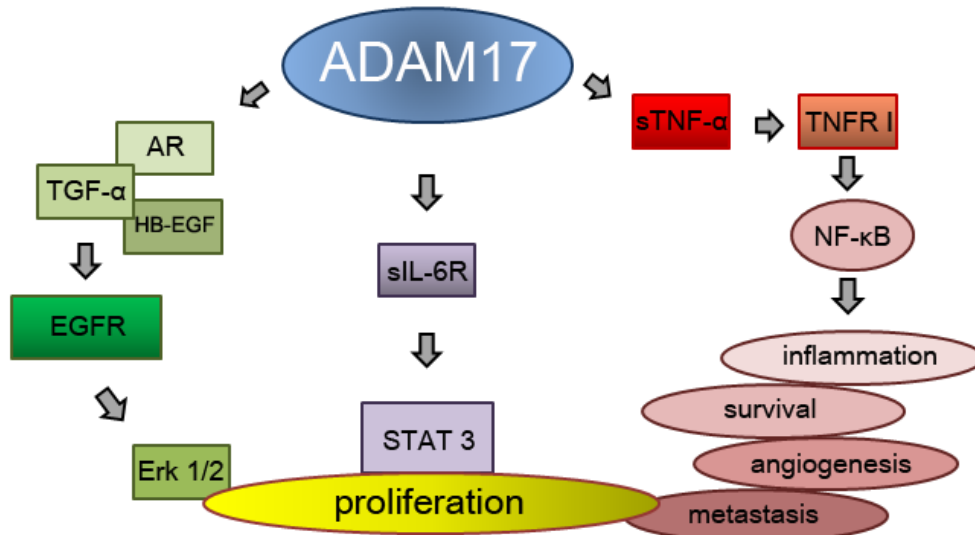


**Figure 1.2.2 The implication of ADAM17 in inflammatory and proliferative stimuli.** ADAM17 releases soluble ligands from the membrane surface, in the process denoted as „ectodomain shedding“. sTNF- $\alpha$  activates TNFR I, and induces activation and translocation of transcription factor NF- $\kappa$ B to the nucleus where it activates transcription of genes implicated in inflammation. EGFR can be activated with different ligands like AR, TGF- $\alpha$ , HB-EGF. Activation of EGFR induces cell survival and proliferation via Erk kinase signaling. The generation of sIL-6R is a prerequisite for IL-6 trans-signaling (explained in detail in section 1.4). IL-6 trans-signaling activates phosphorylation and dimerization of STAT 3 proteins which are important for cell proliferation; **ADAM17** - A Disintegrin and Metalloprotease 17, **sTNF- $\alpha$**  - soluble tumor necrosis factor alpha, **TNFR I** - Tumor Necrosis Factor Receptor I, **NF- $\kappa$ B** - Nuclear Factor kappa B, **sIL-6R** - soluble interleukin-6 receptor, **STAT3** - Signal transducer and activator of transcription 3, **EGF** - epidermal growth factor, **TGF- $\alpha$**  - transforming growth factor alpha, **HB-EGF** - heparin binding epidermal growth factor, **EGFR** - epidermal growth factor receptor, **Erk 1/2** - extracellular-signal-regulated kinases.

ADAM17 deficient mice (ADAM17<sup>-/-</sup>) showed embryonic lethality between embryonic day 17.5 and the first day of birth (Peschon et al., 1998). ADAM17 deficient embryos displayed defects reminiscent of those in TGF- $\alpha$  deficient mice, with additional defects similar to those caused by the lack of EGFR.

Chalaris and colleagues succeeded in generating viable mice with barely detectable levels of ADAM17 in all tissues (Chalaris et al., 2010). They introduced a novel strategy called exon-induced translational stop (EXITS), which is based on the insertion of an artificial exon in the *ADAM17* gene. This extra exon, named exon 11a, was inserted between



exon 11 and exon 12. The inserted exon contained an in frame translational stop codon and it was flanked by splice donor/acceptor sites, which slightly deviated from the canonical consensus sequence. Homozygous mice, denoted as ADAM17<sup>ex/ex</sup> mice (named **ex/ex** for the **EXITS** strategy), expressed only ~5% of ADAM17 protein in all cell types compared to wild type mice. ADAM17<sup>ex/ex</sup> mice had macroscopically visible eye and hair defects, reminiscent to TGF- $\alpha$  knock out mice. Interestingly, ADAM17<sup>ex/ex</sup> mice showed abrogated generation of soluble TNF- $\alpha$  and significantly reduced shedding of TNFR I and TNFR II, indicating impaired ADAM17 activity.

### **1.3. ADAM17 in cancer and metastasis**

Over the last few years ADAM17 has been associated with tumorigenesis and tumor progression. A very common and vastly investigated type of human lung cancer is Non-Small Cell Lung Cancer (NSCLC). NSCLC comprises any type of epithelial lung cancer except small cell lung carcinoma (SCLC). NSCLC is the leading cause of cancer-related deaths in the United States and Europe with very limited treatment options. The most common types of NSCLC are adenocarcinoma, large cell carcinoma and squamous cell carcinoma. In a recent study, Ni and colleagues could demonstrate that ADAM17 expression in NSCLC correlated with patients poor prognosis (Ni et al., 2013). They performed quantitative real time PCR to assess the ADAM17 mRNA expression from tissues of 124 patients with clinicopathologically characterized NSCLC. Furthermore, they analyzed the expression of ADAM17 by immunohistochemistry. They discovered that ADAM17 mRNA and protein expression levels in NSCLC tissues were both significantly higher than those in non-cancerous tissues. Interestingly, Ni and colleagues demonstrated that high expression of ADAM17 significantly correlated with tumor size, tumor grade, lymph node metastasis, aggressive progression and poor prognosis. They suggested that ADAM17 could be an important molecular marker for predicting carcinogenesis, progression and prognosis of NSCLC.

#### **1.3.1 The impact of ADAM17 on epidermal growth factor receptor (EGFR)**

All EGFR ligands are produced as membrane-associated molecules that require proteolytic processing by ADAM17 and A Disintegrin and Metalloprotease 10 (ADAM10) for the generation of the active forms. Upon binding of its active ligand, EGFR dimerizes and becomes activated. EGFR dimerization stimulates its intrinsic intracellular tyrosine kinase

activity, which leads to its autophosphorylation, and subsequently to downstream activation of several signal transduction cascades. Principally the cascades are the MAPK/Erk (Mitogen-activated protein kinases/Extracellular signal-regulated kinases), Akt (also known as Protein kinase B) and JNK (c-Jun NH(2)-terminal kinase) pathways. These pathways are implicated in cell proliferation, survival, migration and invasion.

EGFR activation has been implicated in cancer development, growth and metastasis (Olayioye et al., 2000). Shedding of TGF- $\alpha$  was necessary for tumor formation in a model of ovarian cancer (Borrell-Pages et al., 2003). Namely, Borrell-Pages and colleagues could demonstrate that the transmembrane form of TGF- $\alpha$  (proTGF- $\alpha$ ) interacted with, but did not activate the EGFR. They made a series of proTGF- $\alpha$  deletion constructs affecting the ADAM17 cleavage site and stably transfected these constructs in Chinese hamster ovary (CHO) cells. As a control for unimpaired ADAM17 shedding, they stably transfected CHO cells with a construct containing wild type proTGF- $\alpha$ . Interestingly, they demonstrated that over-expression of wild type proTGF- $\alpha$  in CHO cells allowed vigorous growth of CHO xenografts in nude mice. In contrast, deletion constructs in CHO cells resulted in significantly reduced tumor growth of CHO xenografts in nude mice. They demonstrated that ectodomain shedding of proTGF- $\alpha$  by ADAM17 is required for activation of the EGFR and for maximal tumor growth *in vivo*, thus indicating a crucial role for ADAM17 in tumorigenesis.

### 1.3.2 The implication of ADAM17 in Notch signaling

One of evolutionary the most conserved pathways involved in cell development and cell self-renewal is Notch signaling. It has been reported that Notch signaling participates in tumor-stroma and tumor-endothelium interactions in primary tumors and in metastasis (Pannuti et al., 2010). ADAM17, next to ADAM10, has a prominent role in activation of Notch signaling (Brou et al., 2000). There are four transmembrane Notch receptors (Notch-1, Notch-2, Notch-3 and Notch-4) and five transmembrane ligands (Delta-like [DLL] 1, DLL 2, DLL 3, DLL 4, Jagged-1 and Jagged-2).

Notch receptors are synthesized as precursor proteins, which are subjected to three proteolytic cleavages. In signal-receiving cells, Notch precursor proteins are processed in the trans-Golgi apparatus by furin-like convertases to generate a mature receptor.

## Introduction

---

This cleavage is marked as S1 cleavage (Figure 1.3.1). The mature receptor is a heterodimer consisting of Notch extracellular and Notch transmembrane parts. The mature receptor is then translocated to the cell membrane where it can be engaged with membrane associated ligands from the signal-sending cell. Upon binding of a ligand to the Notch receptor, S2 cleavage occurs.

Interestingly, ADAM10 cleaves Notch in ligand-dependent activation, while ADAM17 can cleave Notch receptor in ligand-independent activation (Bozkulak et al., 2009). Bozkulak and colleagues demonstrated that ADAM17 cannot cleave Notch-1 in response to ligand. Performing coimmunoprecipitation, they demonstrated that ADAM17 does not interact with endogenous Notch-1, explaining that perhaps ADAM17 and Notch-1 occupy distinct cell surface microdomains. However, they were able to coimmunoprecipitate ADAM17 with ectopically expressed Notch-1. Furthermore, they could show that ADAM17 activation of ectopically expressed Notch-1 did not require ligand interaction as well as ectodomain shedding, thus excluding the possibility that ADAM17 cleaves Notch-1 at the cell surface. Although it was unclear where in the cell ADAM17 cleaves and activates Notch-1, they speculated that ADAM17 and Notch-1 accumulate at high levels intracellularly. This accumulation could enhance interactions between these two proteins, and subsequently activate Notch-1 receptor.

After S2 cleavage, the extracellular part of Notch receptor bound to its ligand is endocytosed in the signal-sending cell and degraded. S3 cleavage, which is mediated by  $\gamma$ -secretase at the plasma membrane, results in the release of the active Notch Intracellular Domain (NICD). NICD translocates into the nucleus where it recruits transcriptional regulators, and forms the "Notch transcriptional complex" leading to the transcription of genes like e.g. Hairy/Enhancer and Split 1 or 5 (Hes 1, Hes 5) or Hairy/enhancer-of-split related YRPW motif like protein 1 (Hey1). This signaling is known as classic Notch signaling.

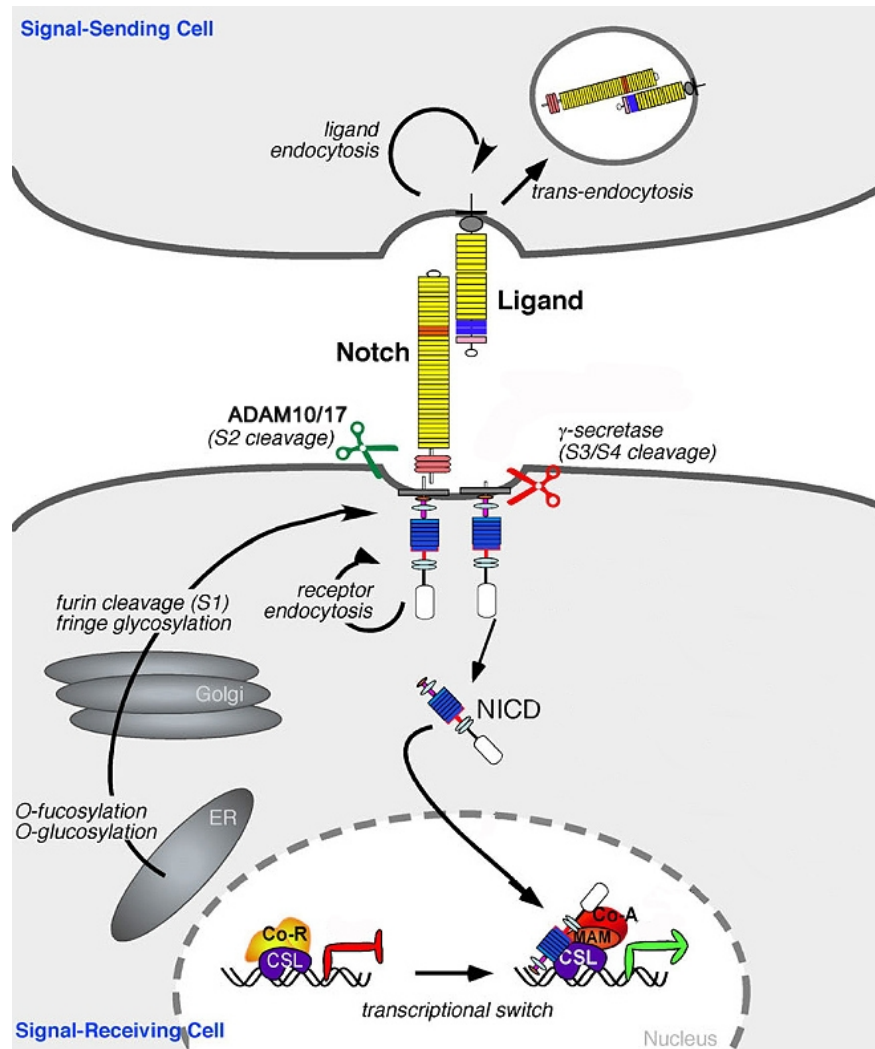


**Figure 1.3.1 Classic Notch signalling.** Notch precursor is processed in the Golgi apparatus to generate a mature form of Notch (S1 cleavage). After S1 cleavage, mature Notch is translocated to the cell surface. After binding a ligand, extracellular part of Notch receptor is cleaved by ADAM10/ADAM17 (S2 cleavage). Intracellular NICD is generated through the third (S3) cleavage by  $\gamma$ -secretase. NICD forms a complex with the transcriptional regulators Co-A, MAM and CSL, and acts as transcription factor; **NICD** - Notch Intracellular Domain, **ER** - Endoplasmic Reticulum, **Co-R** – transcriptional co-repressors, **CSL** - DNA-binding protein, **MAM** - co-activator. Picture was adopted from Kopan and Liagan, 2009.

Baumgart and colleagues pointed out that ADAM17 contributes to tumor growth via Notch-1-mediated up-regulation of EGFR expression in NSCLC (Baumgart et al., 2010). They demonstrated that ADAM17 knock down in NSCLC cells abrogated tumor growth in nude mice. Interestingly, they managed to identify Notch-1 signaling as the main pathway responsible for such significant tumor reduction in mice. Moreover, knock down of Notch-1 in tumor cells lead to reduced EGFR expression. They could show that inhibition of Notch-1 and ADAM17, but not of EGFR, resulted in tumor cell death. Until now, targeting the EGFR in NSCLC was considered to be a promising therapy. Unfortunately, the

## Introduction

majority of NSCLC patients do not respond to EGFR targeted therapy. The study of Baumgart et al. for the first time demonstrated that ADAM17 mediated Notch signaling contributes to the expression of EGFR. This finding marked ADAM17 and Notch-1 as a promising targets for the treatment of NSCLC.

In a recent publication Lu and colleagues could demonstrate that for promotion of colorectal cancer metastasis angiocrine Notch signaling is necessary (Lu et al., 2013). Hereby, the soluble Notch ligand Jagged-1 is liberated by ADAM17 from the surface of endothelial cells. Soluble Jagged-1 can interact with Notch receptor on the surface of cancer cell and stimulate  $\gamma$ -secretase-mediated release of NICD into the cytoplasm. NICD activates the transcription of genes necessary for the transformation of cancer cells into cancer-stem cells (Figure 1.3.2). Cancer-stem cells (CSCs) possess properties like self-renewal, which drives tumorigenesis and resistance to cell death, which leads towards tumor progression. This finding marked ADAM17 as a potential target for eradication of CSCs.

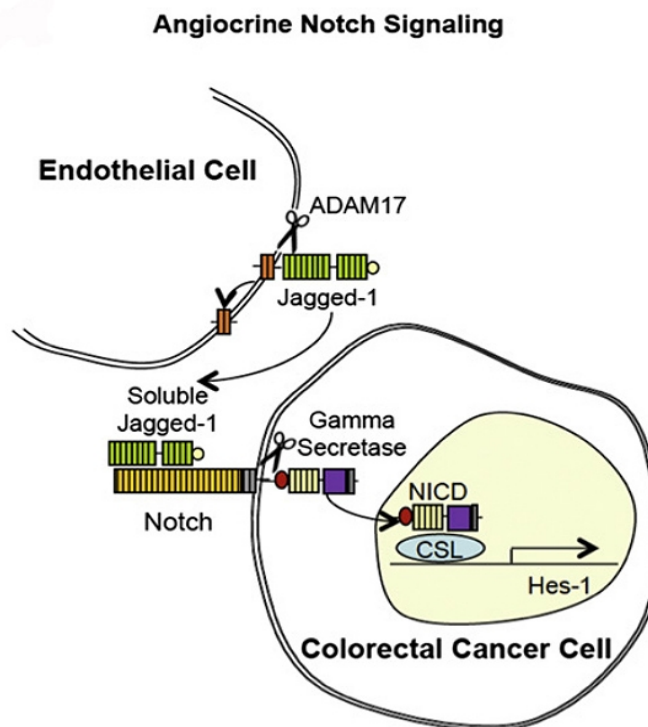


**Figure 1.3.2 Angiocrine Notch signaling.** Extracellular part of Jagged-1 is released from the surface of endothelial cells by ADAM17 mediated cleavage. Soluble Jagged-1 can interact with Notch receptor on the surface of cancer cell and activate transcription of Notch genes e.g. Hes-1 which drives transformation of cancer cell to cancer stem cell (CSC); **NICD** - Notch Intracellular Domain, **CSL** - transcriptional repressor, **Hes-1** - hairy and enhancer of split-1. Picture taken from Lu et al., 2013.

### 1.4 Nuclear factor-kappa B (NF- $\kappa$ B) in cancer

According to Weinberg and Hannahan there are ten hallmarks of cancer and the transcription factor NF- $\kappa$ B can affect six of them through the transcriptional activation of genes associated with angiogenesis, metastasis, tumor promotion, inflammation, suppression of apoptosis and cell proliferation (Baud and Karin, 2009). NF- $\kappa$ B activation can induce chemokine and cytokine expression like e.g. CXCL1, CXCL8, TNF- $\alpha$ , IL-6 and VEGF, which have been implicated in angiogenesis, or ICAM-1 and VCAM-1, which are necessary for cell adhesion. NF- $\kappa$ B can support tumor promotion via induction of matrix metalloprotease 2 (MMP2) and MMP9, which influence degradation of extracellular matrix and promotion of metastasis. There are different mechanisms of NF- $\kappa$ B activation in cancer and some of them will be discussed.

The innate immune system is evolutionary conserved and represents the first line of defense in host protection against invading microbial pathogens. Toll-like receptors (TLR) can elicit innate immune response after recognition of microbial components. TLRs are expressed on various immune cells, such as macrophages, neutrophils, dendritic and epithelial cells. TLRs are transmembrane proteins with N-terminal extracellular leucine-rich repeats, which are responsible for the recognition of pathogen-associated molecular patterns (PAMPs). The family of TLRs has 13 members with each member detecting distinct PAMPs e.g. lipopolysaccharide (LPS) is recognized by TLR4, lipoproteins by TLR2, flagelin by TLR5. After recognition of PAMPs, TLRs recruit a set of adaptor proteins in the cytoplasm, and trigger downstream signaling cascades leading to activation of NF- $\kappa$ B. Next to the induction of transcription of pro-inflammatory cytokines and chemokines, NF- $\kappa$ B influences the upregulation of co-stimulatory molecules essential for T-cell activation (Kawai et al., 2007).

Interestingly, in some cases TLRs can be activated in response to tumor cells.

In a recent report Kim and colleagues demonstrated activation of a TLR2/6 heterodimer in response to factors that are secreted by cancer cells (Kim et al., 2009). They collected serum free conditioned media from several murine cancer cell lines, placed them to bone marrow derived macrophages (BMDMs) and assessed the production of pro-inflammatory cytokines such as TNF- $\alpha$ , IL-6 and IL-1 $\beta$ . Media from two cancer cell lines, Lewis Lung Carcinoma (LLC) and the breast cancer (4T1) cell line, stimulated BMDMs and induced

## Introduction

---

secretion of TNF- $\alpha$  and IL-6. Interestingly, Kim and colleagues identified several proteins, which are components of the extracellular matrix (ECM) in conditioned medium of LLC cells: versican V1, laminin  $\beta$ 1, trombospondin 3 and pro-collagen type III  $\alpha$ 1. To investigate the role of these ECM proteins in the metastatic potential *in vivo*, they generated stable knock down LLC cells with shRNA specific to detected ECM components from the conditioned medium and injected them into wild type mice. Silencing of versican V1 in LLC cells, resulted in a significant reduction of tumor growth, while silencing the expression of other ECM components did not alter tumor growth. To determine the versican V1 mechanism of action, they assessed the production of IL-6 upon stimulation of TLR2<sup>-/-</sup>, TLR3<sup>-/-</sup>, TLR4<sup>-/-</sup> and TLR9<sup>-/-</sup> BMDMs with LLC serum free conditioned medium. They were able to show that exclusively TLR2<sup>-/-</sup> BMDMs did not produce IL-6, thus indicating that IL-6 production is fully dependent on TLR2 activation. To investigate whether TLR2 signaling contributes to LLC induced metastasis, Kim and colleagues injected wild type LLC cells into TLR2<sup>-/-</sup> mice. They were able to confirm greater survival and a significant tumor reduction in TLR2<sup>-/-</sup> lungs compared to control mice. Interestingly, TNF- $\alpha$ <sup>-/-</sup> mice displayed a markedly reduced mortality and tumor burden after LLC injection as compare to IL-6<sup>-/-</sup> and wild type mice. This work indicated that TLR2 and TNF- $\alpha$  but not IL-6 from the host are crucial for lung metastasis.

Interestingly, Pirinen and colleagues analyzed expression of versican in tumor stroma and in cancer cells from 212 patients suffering from NSCLC (Pirinen et al., 2005). They could show that high stromal staining for versican correlated with tumor recurrence, lymph node metastasis and poor prognosis, while the expression of versican in normal lung tissue was rather low.

Taking into consideration that LLC cells produce pro-metastatic factors e.g. versican V1, and that expression of versican in NSCLC in the stroma strongly correlates with recurrences and poor prognosis in patients (Isogai et al., 2005), the LLC model of experimental metastasis can give insight into molecular mechanisms of lung cancer development and metastasis.

TNF- $\alpha$  was identified in 1975 as an endotoxin-induced glycoprotein, which caused haemorrhagic necrosis of sarcomas that had been transplanted into mice (Carswell et al., 1975). TNF- $\alpha$  is produced predominantly by activated myeloid cells and

## Introduction

T-lymphocytes express a membrane bound 26 kDa protein, pro-TNF- $\alpha$ , which is cleaved from the membrane surface mainly by ADAM17. sTNF- $\alpha$  binds as a homotrimer to TNFR I (Figure 1.4.1), while membrane bound TNF- $\alpha$  binds and activates TNFR II (Grell et al., 1995). TNFR I is expressed by all tissue while TNFR II is mostly expressed in immune cells. The binding of TNF- $\alpha$  to its receptors causes the activation of two major transcription factors, NF- $\kappa$ B and AP-1. NF- $\kappa$ B is regulated primarily by phosphorylation of inhibitory proteins, the I $\kappa$ Bs, which retain NF- $\kappa$ B in the cytoplasm of non-stimulated cells. In response to TNF- $\alpha$  and other agonists, the I $\kappa$ Bs are phosphorylated by the I $\kappa$ B kinase (IKK) complex, resulting in their ubiquitination, degradation and, subsequently, in nuclear translocation of the freed NF- $\kappa$ B. AP-1 represents a complex of transcription factors consisting of Jun, Fos and ATF subunits.

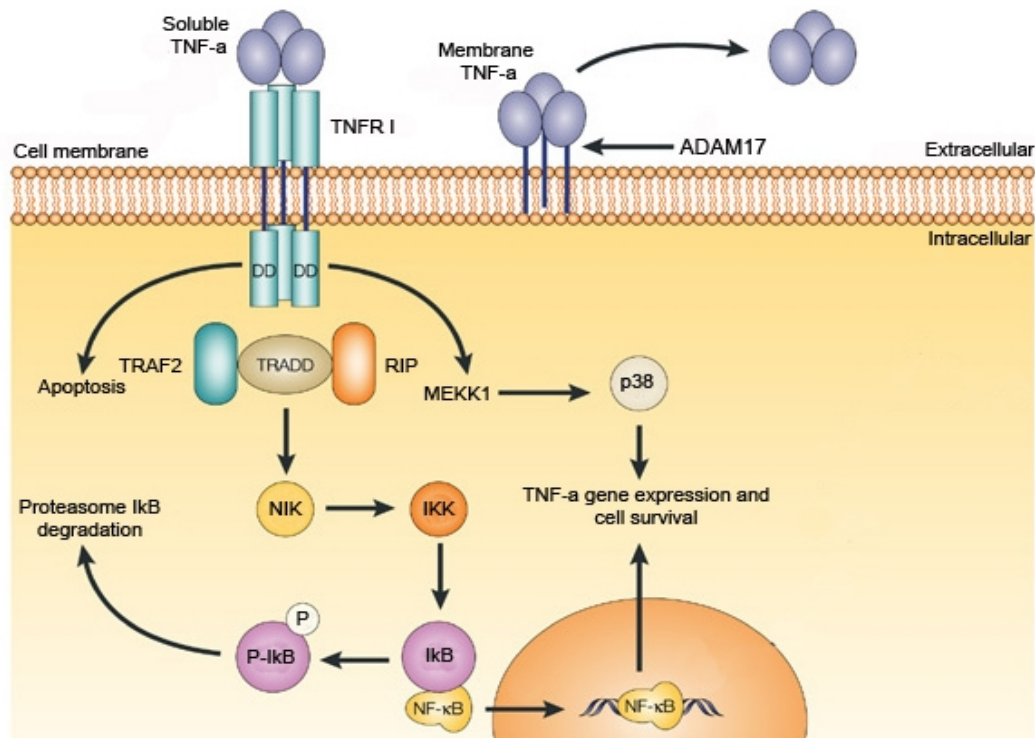


**Figure 1.4.1 Complexity of TNF- $\alpha$  signaling.** Soluble TNF- $\alpha$  (sTNF- $\alpha$ ) is generated by ADAM17 mediated cleavage. To be able to interact with and activate TNFR I, sTNF- $\alpha$  has to form homotrimers. Active TNFR I leads to downstream activation of several kinases which induce phosphorylation of NF- $\kappa$ B inhibitory subunit I $\kappa$ B, thus releasing NF- $\kappa$ B. Active NF- $\kappa$ B translocates into the nucleus and activates transcription of genes; **ADAM17** - A Disintegrin and Metalloprotease 17, **TNFR I** - Tumor Necrosis Factor Receptor I, **DD** - death domain, **TRADD** - TNFR I associated death domain containing protein, **TRAF2** - TNFR associated factor 2, **RIP** - receptor interacting protein, **MEKK1** - mitogen-activated protein kinase kinase kinase 1, **NF- $\kappa$ B** - Nuclear Factor kappa B, **NIK** - NF- $\kappa$ B-inducing kinase, **IKK** - I $\kappa$ B kinase, **I $\kappa$ B** - inhibitor of NF- $\kappa$ B. Picture was modified from Palladino et al., 2003.



## Introduction

---

Upon stimulation with TNF- $\alpha$ , various Mitogen activated protein kinases (MAPKs) enter the nucleus to phosphorylate DNA-bound transcription factors, like Jun, and induce AP-1 activity. The TNF- $\alpha$  promoter itself contains NF- $\kappa$ B and AP-1 binding sites and is a subject to positive autoregulation. TNF- $\alpha$  can mediate inflammation in the immune system, which is therapeutic if the inflammation is acute, short-term without permanent tissue damage. If the inflammation is chronic or long-term, it can cause a damage that is more likely to lead to chronic disease such as cancer. Therefore, TNF- $\alpha$  can be defined as a „double-edged sword“ cytokine.

IL-6 is a multifunctional cytokine initially found to be a B-cell differentiation factor which induces immunoglobulin production (Muraguchi et al., 1988). Nowadays, it is known that IL-6 regulates immune response, acute phase response and inflammation. IL-6 is secreted by various lymphoid cell types such as T-cells, B-cells, macrophages and monocytes (Kishimoto et al, 1995) and its production can be induced by NF- $\kappa$ B activation. On target cells, IL-6 in a complex with membrane bound IL-6R interacts with two gp130 molecules and induces activation of JAK/STAT (Janus kinase/Signal transducer and activator of transcription) pathway (Rose-John, 2012). This is called IL-6 classic signaling (Figure 1.4.2). Only few cell types like hepatocytes, some leukocytes and some epithelial cells express membrane bound IL-6R, while gp130 molecule is expressed by all cells of the body. Cells, which do not express IL-6R, are unresponsive to IL-6 alone, since gp130 has no affinity to IL-6, but only to its complex with IL-6R. Interestingly, the soluble isoform of the IL-6R can be generated by alternative splicing or by proteolytic cleavage of the membrane-bound precursor. For the constitutive shedding of IL-6R appears to be responsible ADAM10, while ADAM17 accounts for the stimulated shedding of IL-6R (Matthews et al., 2003). sIL-6R can associate with IL-6 and form IL-6/sIL-6R complex, which can interact with gp130 molecule, induce its dimerization and subsequently activate JAK/STAT pathway. This is called IL-6 trans-signaling (Figure 1.4.2). IL-6 trans-signaling drastically enlarges the spectrum of IL-6 target cells.

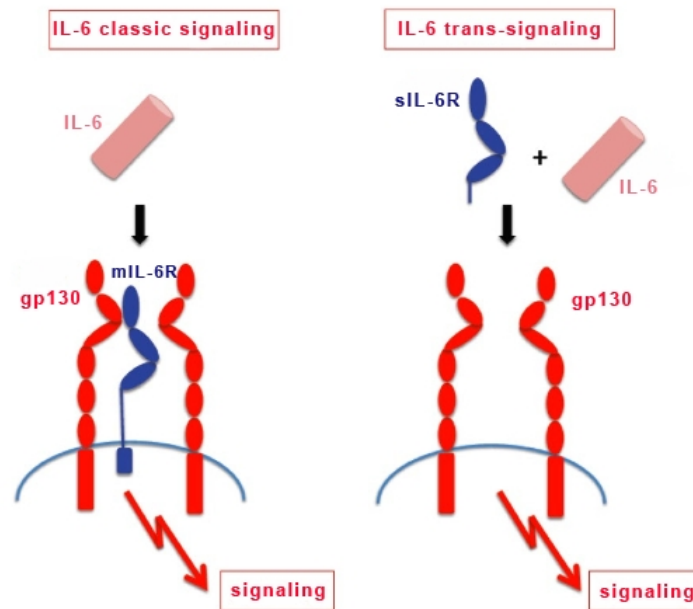


**Figure 1.4.2 IL-6 classic and trans-signaling.** IL-6 classic signaling is limited to hepatocytes, some leukocytes and some epithelial cells. For IL-6 classic signaling engagement of membrane bound IL-6R is required. Complex between IL-6 and mIL-6R induces dimerization and activation of signal-transducing gp130 molecules. IL-6 trans-signaling can be activated in all cell types in the body and it requires engagement of soluble IL-6R. Complex between IL-6 and sIL-6R can activate signaling downstream of dimerized gp130 molecules. **IL-6** - interleukin 6, **sIL-6R** - soluble interleukin 6 receptor, **mIL-6R** – membrane bound interleukin-6 receptor, **gp130** - glycoprotein 130. Picture was modified from Rose-John, 2012.

In a recent publication, Yi and colleagues demonstrated importance of sIL-6R and IL-6 for the growth of cancer-stem cells (CSCs) in NSCLC (Yi et al., 2012). They isolated CSCs from H460 NSCLC and assessed proliferation rate and production of sIL-6R and IL-6 in their medium, compared to non-CSC. CSCs proliferation compared to non-CSCs proliferation, was significantly slower. Since the growth rates of CSCs and non-CSCs were substantially different, to be able to compare the amounts of produced sIL-6R and IL-6 from the cell medium, they normalized concentrations of sIL-6R and IL-6 based on the cell numbers. Normalized concentration of sIL-6R was significantly higher in CSCs than in non-CSCs medium, while the concentration of IL-6 was the same in the medium of both CSCs and non-CSCs. Interestingly, blocking IL-6 or IL-6R alone, or IL-6 and IL-6R together, resulted in diminished growth of CSCs. The authors concluded that targeting of IL-6R and IL-6 would be beneficial for the development of CSC-targeted lung cancer therapies, and suggested that IL-6R can be a potential CSC marker in NSCLC. However, authors did not comment would the inhibition of ADAM17 or ADAM10, as IL-6R sheddases, influence the growth of CSCs.

### 1.5 Immune response in cancer and metastasis

The theory of immune surveillance was introduced in the early 1900s by Ehrlich, who hypothesized that one critical function of the immune system was to detect and eliminate tumors from the host. Nowadays, it is known that T-cells are one of the crucial components of the immune system that can eliminate tumor cells (Toepfer et al., 2011).

T-cells are type of lymphocytes generated in the primary lymph organs: bone marrow and thymus. They play a central role in cell-mediated immunity. T-cell mediated immune response begins in the secondary lymph organs: spleen, lymph nodes and lymphoid tissues associated with mucosal surfaces. Secondary lymph organs have specialized T-cell rich zones where naïve T-cells are concentrated. T-cells rest in the spleen for few hours and in the lymph nodes for about 1 day, before they leave through the lymphatic vessels and reach the bloodstream. From the bloodstream T-cells again enter lymphoid organs and, if they are not activated there by antigen presenting cells, repeat the cycle or they die by neglect.

T-cells are activated via their T-cell receptor (TCR). The TCR is a protein complex consisting of  $\alpha\beta$  heterodimers, responsible for antigen recognition, and Cluster of Differentiation 3 (CD3) molecules, involved in intracellular signaling. CD3 molecules consist of several chains  $\zeta$ ,  $\delta$ ,  $\epsilon$  and  $\gamma$ , with intracellular immuno-receptor tyrosine-based activation motif (ITAMs) which initiates signal transduction.

TCR binds to antigen peptides presented on two major histocompatibility complex class molecules (MHCs), MHC class I and MHC class II, on the surface of antigen presenting-cells. Professional antigen-presenting cells (APCs) are dendritic cells (DC), macrophages and B-cells. T-cells have several subsets, which are distinguished by different lineage markers and functional activities.  $CD4^+$  T-cells recognize antigen in the context of MHC class II molecules, which are expressed on professional APCs.  $CD4^+$  T-cells produce cytokines and are marked as helper T-cells.  $CD8^+$  T-cells are activated by antigen peptides presented in the context of MHC class I molecules, which are expressed on all nucleated cells. Following the recognition of peptides presented by tumor cells in MHC class I molecules, activated  $CD8^+$  T-cells, named cytotoxic T lymphocytes (CTLs), can efficiently destroy cancer cells using one of two major apoptotic pathways:  $Ca^{2+}$  dependent

## Introduction

perforin/granzyme-mediated apoptosis or  $\text{Ca}^{2+}$ -independent Fas ligand/Fas-mediated apoptosis.  $\text{Ca}^{2+}$  dependent apoptosis is mediated by lytic granules, which contain enzymes perforin and granzyme B and proteoglycan serglycin (Figure 1.5.1). Granules are transported into target cell as one complex in endocytosed vesicle. In the membrane of endocytosed vesicle, perforin forms a pore and enables granzyme B to enter the cytosol of target cell and induce apoptosis in caspase-dependent mechanism.  $\text{Ca}^{2+}$ -independent apoptosis is initiated by binding of Fas molecule (known as CD95) on the target cell via Fas ligand (known as CD95L) on the CTL. Fas molecule is a member of TNF-receptor family with intracellular death domain, which initiates caspase-dependent apoptosis after binding to Fas ligand.

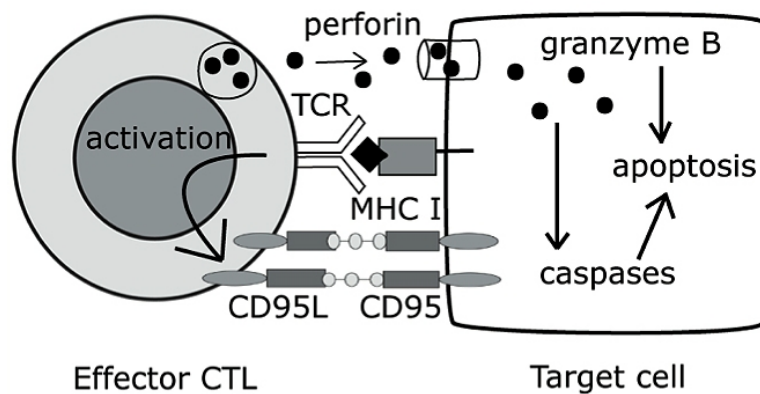


**Figure 1.5.1 Cytotoxic T lymphocyte cytotoxicity.** Cytotoxicity of CTL cells can be mediated by two distinct pathways. One pathway is induced via secretion of perforin, which creates pores in the membrane of the target cell, and granzyme B, which induces apoptosis of a target cell. The second pathway is via interaction of Fas ligand, on CTL cell, with Fas, on a target cell. This interaction induces sequential caspase activation, which leads to apoptosis; **TCR** – T cell receptor, **MHC I** – Major histocompatibility complex class I, **CTL** – cytotoxic  $\text{CD8}^+$  T-cell, **CD95** – cluster of differentiation 95, **CD95L** – cluster of differentiation 95 ligand. Picture adopted from Nijkamp and Parnham, 2011.

Peptides presented by MHC class II molecules, play also an important role in adaptive anti-cancer immunity. MHC class II molecules present peptides, which are recognized by  $\text{CD4}^+$  T-cells.  $\text{CD4}^+$  T-cells can improve the capacity of DCs to induce CTLs by cross-linking the co-stimulatory molecule CD40 on DCs with the CD40 ligand (CD40L) on activated  $\text{CD4}^+$  T-cells. Besides this, activated  $\text{CD4}^+$  T-cells can significantly boost cellular components of the innate immunity, such as macrophages, by enhanced  $\text{IFN-}\gamma$  secretion.  $\text{IFN-}\gamma$  stimulates higher expression of MHC class I molecules on antigen presenting cells thus improving the recognition capacity of  $\text{CD8}^+$  T-cells.

## Introduction

---

Despite ongoing surveillance by T-cells and other components of the immune system, tumors develop even in presence of an intact immune system and become eventually clinically detectable.

The contribution of myeloid cells to tumor pathogenesis has been recognized more than 100 years ago, but only in the last two decades their role in promoting angiogenesis, cell invasion and metastasis has been appreciated and explored in detail. Myeloid cells derive from bone marrow precursors of granulocytic lineage (Jinushi et al., 2013). They consist of various types of cells including monocytes, macrophages, dendritic cells and granulocytes. Myeloid cells are the most abundant haematopoietic cells in the body, which protect the host from pathogens, eliminate dying cells and mediate tissue remodeling. During tumor progression, tumor microenvironment recruits myeloid cells and educates them in support to tumorigenicity. Recruited myeloid cells are then converted into potent immunosuppressive cells, named myeloid-derived suppressor cells (MDSCs).

Initially, MDSCs were identified in tumor-bearing mice as cells that co-express Cluster of Differentiation 11b (CD11b) and granulocyte marker Ly6G/Gr1. CD11b mediates inflammation by regulating leukocyte adhesion and migration and has been implicated in several immune processes such as phagocytosis, cell-mediated cytotoxicity, chemotaxis and cellular activation. Expression of Ly6G/Gr1 in bone marrow correlates with granulocyte differentiation and maturation. However, the physiological role of Ly6G/Gr1, remains still unclear. Today, MDSCs are characterized as monocytic MDSCs or as polymorphonuclear/granulocytic MDSCs. The murine monocytic lineage has CD11b<sup>+</sup>Gr1<sup>low</sup>Ly6C<sup>hi</sup>Ly6G<sup>-</sup>CD49d<sup>+</sup> phenotype and the murine polymorphonuclear/granulocytic lineage has CD11b<sup>+</sup>Gr1<sup>hi</sup>Ly6C<sup>low</sup>Ly6G<sup>+</sup>CD49d<sup>-</sup> phenotype (Youn et al, 2008). Monocytic MDSCs, and monocytes/macrophages are functionally and phenotypically very distinct. Monocytic MDSCs, but not monocytes, are immunosuppressive and unlike monocytes, express high levels of iNOS and Arginase 1 (ARG1). Granulocytic MDSCs and neutrophils are functionally and phenotypically very distinct. Granulocytic MDSCs, but not neutrophils, are immunosuppressive. Compared with neutrophils, granulocytic MDSCs are less phagocytic, have increased reactive oxygen species (ROS) production and express less C-X-C chemokine receptor 1 (CXCR1) and CXCR2.

## Introduction

---

The main function of both, monocytic and granulocytic MDSCs, is to suppress T-cell activation and proliferation. This suppression can be achieved via different mechanisms, which can be grouped into four classes.

The first mechanism:

### *Depletion of nutrients required for lymphocytes*

L-arginine (L-Arg) is conditionally essential amino-acid for adult mammals, which is metabolized by arginase I, arginase II and inducible nitric oxide synthase (iNOS). At sites of prominent infiltration of MDSCs, like wounds and tumors, L-Arg is present in exceedingly low concentration in extracellular matrix. This is a consequence of increased consumption of L-Arg by infiltrated MDSCs (Albina et al., 1989). In the enzymatic reaction mediated by arginase 1, L-Arg is converted to urea and L-ornithine. In the enzymatic reaction mediated by iNOS, L-Arg degradation generates nitric (II)-oxide (NO). Decreased concentration of L-Arg and increased concentrations of urea and NO inhibit T-cell function and growth through several different mechanisms:

- decreasing the expression of CD3 zeta chain (CD3 $\zeta$ ), which is a component of TCR (Rodrigues et al., 2002)
- preventing the expression of cell cycle regulators cyclin D3 and cyclin-dependent kinase 4 (CDK4) (Rodriguez et al., 2007)
- inhibiting Major Histocompatibility Complex (MHC) class II expression on antigen presenting cells (Harari et al., 2004)
- inducing T-cell apoptosis (Rivoltini et al., 2002).

The second mechanism:

### *Generation of oxidative stress*

By the combined and cooperative activities of arginase 1 and iNOS in MDSCs, reactive oxygen species (ROS), like peroxynitrite and hydrogen peroxide, are produced. Interestingly, increased production of ROS has been detected in tumor-bearing mice and in patients suffering from cancer (Kusmartsev et al., 2004; Schmielau et al., 2001). In T-cells peroxynitrite induces post-translational modifications of proteins, like nitration and nitrosilation. Nitration and nitrosilation affect amino-acid residues like cysteine, methionine, triptophan and tyrosine (Vickers et al., 1999). Modified proteins lose their function, which in the end results in impaired cell signaling and apoptosis of T-cells.

The third mechanism:

### *Interference of lymphocyte trafficking*

Naïve T-cells circulating in the blood express adhesion molecule L-selectin (CD62L) and CC chemokine receptor 7 (CCR7). Ligands present on the endothelial cells will bind to L-selectin expressed by T-cells. This interaction induces slowing lymphocyte trafficking through the blood, their rolling and adhesion on endothelium and extravasation through high endothelial venules, into secondary lymph organs. Naive T-lymphocytes, which have not yet encountered their specific antigen, need to enter secondary lymph nodes to encounter their antigen and to be activated. If the expression of L-selectin on the surface of T-cells is diminished or lost, T-cells cannot home to lymph nodes and they become unresponsive. Interestingly, L-selectin is cleaved from the cell surface by ADAM17.

Hanson and colleagues demonstrated that the expression of L-selectin on the surface of T-cells inversely correlated with the MDSCs level in tumor bearing mice (Hanson et al., 2009). Interestingly, when they performed FACS staining for internal and for surface expression of ADAM17 in leukocytes isolated from the blood of tumor bearing mice, they were able to show that both, T-cells and MDSCs, internally expressed ADAM17. However, only MDSCs, but not T-cells, expressed ADAM17 on the cell surface. They concluded that MDSCs express on their plasma membrane ADAM17 that cleaves the ectodomain of L-selectin.

The fourth mechanism:

### *Activation and expansion of Treg cell population*

Regulatory T-cells (Treg) is a subpopulation of CD4<sup>+</sup> T-cells that maintain tolerance to self antigens. The immune system must be able to discriminate between self and non-self. When self/non-self discrimination fails, the immune system destroys cells and tissues of the body and as a result causes autoimmune diseases.

In tumors MDSCs promote the clonal expansion of antigen-specific Treg cells and also induce the conversion of naïve CD4<sup>+</sup> T-cells into induced Treg cells.

In tumor model of colon carcinoma induced with colon cancer cell line MCA26, Huang and colleagues provided the evidence that MDSCs can induce development of Treg, in IFN- $\gamma$  and IL-10 dependent mechanism (Huang et al., 2006). Namely, they isolated MDSCs from the spleens of tumor bearing mice and co-cultured them with CD4<sup>+</sup> splenocytes. They detected significant levels of IL-10 and TGF- $\beta$ , along with IFN- $\gamma$  in the cell medium of co-

## **Introduction**

---

cultured cells. IL-10 and TGF- $\beta$  have been shown to induce the development of Treg cells (Seo et al., 2001; Fu et al., 2004), but IFN- $\gamma$  was unknown actor. Therefore, they hypothesized that MDSCs can produce IL-10 and TGF- $\beta$  in response to IFN- $\gamma$ . To test this hypothesis, Huang and colleagues isolated MDSCs from mice with large tumor burdens and cultured them in presence or absence of IFN- $\gamma$ . They demonstrated that the expression of IL-10 was detectable in presence of IFN- $\gamma$ , but not in IFN- $\gamma$  absence. Interestingly, MDSCs produced TGF- $\beta$  in presence or absence of IFN- $\gamma$ .



### **2 Aim of this study**

It has become increasingly clear that inflammation can enhance tumor growth and tumor progression. ADAM17, as primary sheddase of transmembrane protein TNF- $\alpha$  and sheddase of adhesion molecules, is required for recruitment of immune cells into the tissue and is implicated in inflammatory responses. It is also shown that the metalloprotease ADAM17 is responsible for cleavage of growth factor receptors and ligands of EGFR, which are necessary for tumor growth and proliferation.

The aim of present study was to investigate the importance of ADAM17 in the tumor stroma for metastatic progression and spread. To address this, we used Lewis Lung Carcinoma (LLC) cells and ADAM17 hypomorphic mice (ADAM17<sup>ex/ex</sup> mice) in a model of experimental metastasis. In an experimental metastasis model, tumor cells are injected via the tail vein. This injection allows formation of metastatic lesions in the lungs of mice without formation of a primary tumor elsewhere in the body. At different time points we analyzed the thickness of alveolar septa, infiltration of immune cells, cytokine and chemokine expression to determine the level of lung damage in control and hypomorphic mice.

ADAM17<sup>ex/ex</sup> mice revealed significantly lower metastasis than ADAM17<sup>wt/wt</sup> mice at all followed time points. We demonstrated that ADAM17 in the host lung supports tumor growth via inflammatory and proliferatory stimuli.

### 3 Material and Methods

#### 3.1 Material

##### 3.1.1 Solutions and buffers

<b>TAE buffer (50x)</b>	242 g	Tris-HCl
	57 ml	Glacial acetic acid (17.4 M)
	18.5 g	EDTA
	to 1000 ml	ddH <sub>2</sub> O
<b>DNA sample buffer</b>	3 ml	glycerol
	1 ml	0.5 M EDTA pH 8.0
	10 mg	Br-phenolblue
	10 mg	xylencyanol
	to 10 ml	ddH <sub>2</sub> O
<b>(Ca)<sub>3</sub>(PO<sub>4</sub>)<sub>2</sub> transfection reagens</b>	2 x	HBS (precipitation buffer)
	2 M	CaCl <sub>2</sub>
<b>HBS buffer (2x)</b>	8 g	NaCl
	0.27g	Na <sub>2</sub> HPO <sub>4</sub> x 2H <sub>2</sub> O
	12 g	HEPES
	to 1 l	deionized water
<b>Transfection Medium</b>	DMEM with Gln and	high Glc
	10 %	FCS
	1 mM	Sodium Pyruvate
	20 mM	HEPES

## Material and Methods

---

	10 ml	Penicillin/Streptomycin
<b>Lysis buffer</b>	150 mM	NaCl
(Cell and tissue lysis)	2 mM	EDTA
	50 mM	Tris-HCl pH 7.4
	1% (w/v)	Triton X-100
	1% (w/v)	NP-40
added freshly:	1 mM	Na <sub>3</sub> VO <sub>4</sub>
	1 mM	NaF
	1 mM	PMSF
	1x	ABTS Tablets
<b>Erythrocyte lysis buffer</b>	8.29 g	NH <sub>4</sub> Cl
	1 g	KHCO <sub>3</sub>
	0.372 g	EDTA-Na
	to 1000 ml	ddH <sub>2</sub> O
<b>Leamli buffer (2x)</b>	4 g	SDS
	10 g	2-mercaptoethanol
	20 g	glycerol
	4 g	Br-phenolblue
	125 mM	Tris-HCl pH 6.8
	to 100ml	ddH <sub>2</sub> O
<b>Running gel (10%)</b>	2.5 ml	1.5 mM Tris-HCl pH 8.8
	0.1 ml	10% SDS

## Material and Methods

---

	0.1 ml	10% APS
	3.3 ml	30% acrylamide mix
	4 $\mu$ l	TEMED
	4 ml	ddH <sub>2</sub> O
<b>Stacking gel</b>	1.25 ml	1.5 mM Tris-HCl pH 6.8
	0.1 ml	10% SDS
	0.1 ml	10% APS
	1.7 ml	30% acrylamide mix
<b>Protein Marker</b>	Page Ruler™ Plus (Thermo Scientific)	
<b>SDS Running buffer</b>	25 mM	Tris-HCl pH 8.3
	250 mM	Glycine
	0.1%	SDS
<b>Transfer buffer</b>	25 mM	Tris-HCl pH 8.3
	192 mM	Glycine
	20 %	Methanol
<b>NETG - Blocking and Washing buffer</b>	150 mM	NaCl
	5 mM	EDTA
	50 mM	Tris-HCl pH 7.5
	0.04%	gelatine
	0.02%	Tween 20
<b>Stripping buffer</b>	15g	Glycine pH 2.2
	0.1g	SDS

## Material and Methods

---

	10ml	Tween 20
<b>Cell culture medium</b>		DMEM high glucose
	10%	FCS
	10ml	Penicilin/Streptavidin
<b>Flushing medium</b>		MEM high glucose (Glutamax)
	1 x	non-essential amino acids
	1 mM	Sodium Pyruvate
	50 $\mu$ M	$\beta$ -mercaptoethanol
<b>BMN medium</b>		MEM high glucose (Glutamax)
	20 %	FCS
	1 x	non-essential amino acids
	1mM	Sodium Pyruvate
	50 $\mu$ M	$\beta$ -mercaptoethanol
<b>Complete medium</b>		DMEM (Glutamax)
	10%	FCS
	10 ml	Penicilin/Streptavidin
	50 $\mu$ M	beta-mercaptoethanol
<b>ADAM10 inhibitor</b>	3 $\mu$ M	GI254023X
<b>ADAM17 and ADAM10 inhibitor</b>	3 $\mu$ M	GW280264X
<b>Bouin's solution</b>	5%	acetic acid
	9%	formaldehyde

## Material and Methods

---

	0.9%	Picric acid
<b>PBS (1x)</b>	137 mM	NaCl
	2.5 mM	KCl
	8.1 mM	Na <sub>2</sub> HPO <sub>4</sub>
	1.5 mM	KH <sub>2</sub> PO <sub>4</sub> pH 7.2-7.4
<b>Washing buffer</b>	0.05%	Tween-20 in PBS pH 7.2-7.4
<b>Blocking buffer/Reagent Diluent</b>	1%	BSA in PBS pH 7.2-7.4
<b>Streptavidin-HRP</b>	1:200	Solution in Blocking buffer
<b>Stop Solution</b>	1.5 M	H <sub>2</sub> SO <sub>4</sub>
<b>FACS Blocking solution per sample</b>	50 µl	PBS
	2.5 µl	FCS
	5 µl	FC Block
<b>FACS buffer per sample</b>	50 µl	PBS
	2%	FCS

### 3.1.2 Primers

All primers were purchased at Sigma.

Primer name	Primer sequence	Product size (bp)	T <sub>m</sub> (°C)	Number of cycles	Elongation time (s)
3' flox_ADAM17 (genotyp.)	5'-CTTATTATTCTCGTGGTCACC-3'	250/500	52	40	60
5' flox_ADAM17 (genotyp.)	5'-TATGTGATAGGTGTAATG-3'				

## Material and Methods

beta actin up	5'-GTGGGGCGCCCCAGGCACCA-3'	500	55	27	30
beta actin down	5'-CTCCTTAATGTCACGCACGATTTC-3'				
HES1_fw	5'-AAGCACCTCCGGAACCTGCAGC-3'	609	64	30	33
HES1_rev	5'-AGTGGCCTGAGGCTCTCAGTTCC-3'				
DLL1_fw	5'-CCTCGTTCGAGACCTCAAGGGAG-3'	550	65	30	30
DLL1_rev	5'-TAGACGTGTGGGCAGTGCCTGC-3'				
IL-6_fw	5'-TCTCTGCAAGAGACTTCCATCCAGT-3'	71	64	31	5
IL-6_rev	5'-AGTAGGAAGGCCGTGGTTGTCA-3'				
TNF-alpha_fw	5'-AGCCCACGTCGTAGCAAACCAC-3'	411	64	28	25
TNF-alpha_rev	5'-TAGACCTGCCGGACTCCGC-3'				
ICAM-1_fw	5'-GATCCCTGGGCCTGGTGATGCT-3'	740	66	28	45
ICAM-1_rev	5'-TGTGCTCTCCTGGGTCGGCA-3'				
TGF-alpha_fw	5'-GCTACTCGCCAACCGCAGGG-3'	430	65	30	28
TGF-alpha_rev	5'-GCGGAGCTGACAGCAGTGGAT-3'				
AR_fw	5'-TCACAGTGCACCTTTGGAAACGAT-3'	153	64	30	10
AR_rev	5'-TCCGGTGTGGCTTGGAATGA-3'				
MMP-9_fw	5'-TGGGCAAAGGCGTCGTGATCC-3'	893	66	29	54
MMP-9_rev	5'-AGGTGAGGGGGCGCCTGTAG-3'				
IL-1beta_fw	5'-ACGGACCCAAAAGATGAAGGGCT-3'	523	66	28	31
IL-1beta_rev	5'-TCCAGCTGCAGGTGGGTGT-3'				
PCNA_fw	5'-GCGTGAACCTCACCAGCATGTCC-3'	640	65	29	34
PCNA_rev	5'-CACGCTGGCATCTCAGGAGCA-3'				
cxcl2_fw	5'-CAGGGGCTGTTGTGGCCAGTG-3'	250	66	30	15
cxcl2_rev	5'-CCCAGGCTCCTCCTTCCAGGT-3'				
ccl4_fw	5'-TCGTGGCTGCCTTCTGTGCTC-3'	280	65	29	16
ccl4_rev	5'-CTGAAGTGGCTCCTCCTGCC-3'				
cxcl12_fw	5'-GCTCTGCATCAGTCACGGTAAACCA-3'	296	65	31	18
cxcl12_rev	5'-TGCCCTTGCATCTCCCACGGA-3'				
cx3cl1_fw	5'-GCCTGGCCGCGTTCCTCCAT-3'	170	66	31	11
cx3cl1_rev	5'-CGTCTCCAGGACAATGGCACGC-3'				
IL-10_fw	5'-GAGGCGCTGTCATCGATTCT-3'	724	60	28	44
IL-10_rev	5'-GTTTTTCAGGGATGAAGCGGC-3'				
EGF_fw	5'-CTGTTGTTGGAGGGAGCGAT-3'	330	60	28	20
EGF_rev	5'-GGGTGACCTACGTGTTCTG-3'				
HGF_fw	5'-TCGGATAGGAGCCACAAGGA-3'	370	60	29	22
HGF_rev	5'-CGAAGGCCTTGCAAGTGAAC-3'				
VEGFR_tr1_fw	5'-CCATCTGGGCCAAAGATAACC-3'	173	59	30	12
VEGFR_tr1_rev	5'-CTGGGTGTGAGAGTTCCAC-3'				
VEGFR_tr2_fw	5'-AGCTGAGAAAGACTGCAAGGC-3'	547	60	30	31
VEGFR_tr2_rev	5'-GGCCCAGAGGATTTGGAAGAA-3'				
cherry_fw	5'-GCTGTCTTCCCGAGGGCT-3'	270	66	32	15
cherry_rev	5'-TCGTAGTGGCCGCCGCTCTT-3'				

## Material and Methods

lego_17sh_fw	5'- TGGTTAGTACCGGGCCGCTCTAGAGA GGGCCTATTCCCATGATTCCTTC-3'	360	72	30	1200
lego_17sh_rev	5'- AGCTTATCGATACCGTCGACGTCGACG AATTCAAAAACCCTTGAAGAATAC-3'				

### 3.1.3 Primary Antibodies

- anti- $\beta$  actin (8H10D10) rabbit polyclonal antibody which detects endogenously expressed human  $\beta$ -actin (45kDa) with species crossreactivity to mouse (Cell Signaling, Boston, USA); WB dilution: 1:1000 in NETG buffer
- anti-STAT3 (124H6) mouse monoclonal antibody which detects endogenously expressed human STAT3 (79, 86kDa) with species crossreactivity to mouse (Cell Signaling, Boston, USA); WB dilution: 1:1000 in NETG buffer
- anti-P-STAT3 (D3A7) mouse monoclonal antibody which detects endogenously expressed human STAT3 (79, 86kDa) only when phosphorylated at tyrosine 705 with species crossreactivity to mouse (Cell Signaling, Boston, USA); WB dilution: 1:1000 in NETG buffer
- anti-ERK1/2 (L34F12) mouse monoclonal antibody which detects endogenously expressed human ERK (42, 44kDa) with species cross-reactivity to mouse (Cell Signaling, Boston, USA); WB dilution: 1:1000 in NETG buffer
- anti-P-ERK1/2 (D1H6G) mouse monoclonal antibody which detects endogenously expressed human p44 and p42 MAPK Kinase (Erk1 and Erk2) when dually phosphorylated at Thr202 and Tyr204 of Erk1 and Thr185 and Tyr187 of Erk2 and singly phosphorylated at Thr202 at Erk1, with species crossreactivity to mouse (Cell Signaling, Boston, USA); WB



## Material and Methods

---

dilution: 1:1000 in NETG buffer

anti-I-kappaB (L35A5)

mouse monoclonal antibody which detects endogenously expressed human IkappaB $\alpha$  (39kDa) with species crossreactivity to mouse (Cell Signaling, Boston, USA); WB dilution: 1:1000 in NETG buffer

anti-P-IKK (16A6)

rabbit monoclonal antibody which detects endogenously expressed human P-IKKa/b only when IKKa phosphorylated at Ser176/180 and IKKb phosphorylated at Ser177/181 (85, 87kDa) with species crossreactivity to mouse (Cell Signaling, Boston, USA); WB dilution: 1:1000 in NETG buffer

anti-ADAM17

rabbit polyclonal antibody 10.1 which recognizes the catalytic domain was used; kindly provided by Dr Athena Chalaris

### Secondary antibodies

Secondary antibodies were horseradish-peroxydase (HRP)-conjugated and used in dilution 1:5000 in NETG buffer. They were purchased from Pierce (Rockford, USA).

### 3.1.4 Recombinant proteins

**rm G-CSF**

recombinant murine Granulocyte Colony Stimulating Factor used in experiments was produced in E.coli (Immuno Tools) as a single non-glycosylated polypeptide chain with 179 amino acids and molecular mass of 19kDa

**rm M-CSF**

recombinant murine Macrophage Colony Stimulating Factor used in experiments was produced in E.coli (ImmunoTools) as a disulfide homodimer, non-glycosylated polypeptide chain with 2 x 156 amino acids and molecular mass of 36.4 kDa

**rm TNF- $\alpha$**

recombinant murine Tumor Necrosis Factor alpha used in

experiments was produced in E.coli (ImmunoTools) as a soluble 156 amino acid protein (17.3 kDa) which corresponds to C-terminal extracellular domain of the full length transmembrane protein

### 3.1.5 ELISA (Enzyme Linked Immunosorbent Assay)

TNF- $\alpha$  (DY410) and IL-6 (DY406) ELISA kits were purchased from R&D Systems (Wiesbaden-Nordenstadt, Germany). MCP-1/ccl2 (88-7391) ELISA kit was purchased from eBiosciences (San Diego, USA). ELISA microtiter plates were purchased at Thermo Scientific, USA.

### 3.1.6 FACS antibodies

Fc Block	rat anti-mouse CD16/CD32 (BD Pharmingen)
IgG2b k Isotype Control FITC	rat IgG2b, k monoclonal antibody is used as an isotype control immunoglobulin (BD Pharmingen)
anti-Ly6G/Gr1	FITC labeled rat anti-mouse Gr1 antibody reacts with mouse Ly6G, a 21-25 kDa protein (eBioscience); FACS dilution 1:100
anti-Ly6G/Gr1	Pe-Cy7 labeled rat anti-mouse Gr1 monoclonal antibody (RB6-8C5) reacts with mouse Ly-6G; a 21-25 kDa protein (eBioscience); FACS dilution 1:100
F4/80	APC labeled rat anti-mouse F4/80 antibody reacts with mouse F4/80, a 160 kDa glycoprotein (BioLegend) ; FACS dilution 1:100
CD11b	FITC labeled rat anti-mouse M1/70 monoclonal antibody reacts with mouse CD11b, a 165-170 kDa integrin $\alpha_M$ (eBioscience); FACS dilution 1:100

## Material and Methods

---

CD11c	FITC labeled rat anti-mouse CD11c (N418) monoclonal antibody reacts with mouse CD11c, the integrin $\alpha_x$ (eBioscience); FACS dilution 1:100
anti-TNF- $\alpha$	goat anti-mouse TNF- $\alpha$ monoclonal antibody (Capture antibody from TNF- $\alpha$ ELISA kit, R&D Systems) was used as a primary antibody (dilution 1:100); as the secondary antibody APC labeled anti-goat antibody was used (dilution 1:100)
anti-ADAM17	rat anti-mouse ADAM17 antibody against catalitic domain of ADAM17 was used as a primary antibody; anti-goat APC labeled antibody was used as the secondary antibody, both kindly provided by Dr Ahmad Trad; FACS dilution 1:200
<b>3.1.7 Immunohistology</b>	
HE staining	Gill3 Hematoxylin (Thermo Scientific, Cheshire, United Kingdom) and Giemsa's azur eosin methylene blue solution (Merck, Darmstadt, Germany) were used according to manufacture's instruction
anti-Ly6B.2/G1	rat anti-mouse Gr1 monoclonal antibody recognizes Ly-6B.2, a polymorphic 40 kDa antigen expressed by polymorphonuclear cells, but absent on resident tissue macrophages (AbDserotec, Duesseldorf, Germany); dilution 1:200
anti-F4/80	rat anti-mouse F4/80 monoclonal antibody recognizes Kupffer cells, Langerhans cells, peritoneal macrophages, and splenic red pulp macrophages (Caltag); dilution 1:50

## Material and Methods

---

anti-PCNA rat anti mouse PCNA monoclonal antibody recognizes PCNA p36 protein expressed in proliferating cells (Santa Cruz Biotechnology, Texas, USA); dilution 1:100

### 3.1.8 Proteome Profiler Antibody Array

For simultaneous profiling of relative levels of multiple cytokines from tissue lysates, the Mouse Cytokine Array Panel A (R&D Systems, Minneapolis, USA) was used. For simultaneous detection of the relative Receptor Tyrosine Kinase (RTK) phosphorylation in tissue lysates, the Mouse RTK Kit (R&D Systems, Minneapolis, USA) was used.

## 3.2 Methods

### 3.2.1 RNA Isolation

Total RNA from lung tissue was isolated using the NucleoSpin RNA II Kit (Macherey-Nagel GmbH, Dueren, Germany) according to the manufacturer's instructions. RNA concentration was determined using NanoDrop ND-1000 (peqLab Biotechnologie GmbH, Germany). For semiquantitative RT-PCR reaction 150 ng of RNA was used for the reverse transcription. For real time RT-PCR reaction 500 ng of RNA was used for the reversed transcription. The first strand cDNA synthesis was performed according to the manufacturer's instructions (Fisher Scientific GmbH, Schwerte, Germany):

Template RNA	total RNA	150ng-500ng
Primer	oligo(dT)	0.5 µg (100pmol)
Master Mix	ddH <sub>2</sub> O	To 13 µl
	5X reaction buffer	4µl
	dNTP Mix, 10mM each	2µl
	Revert Aid Transcriptase	1µl
	Total volume	20µl

All components were kept on ice. Each sample was mixed with the Master Mix, and incubated at 37°C for 10 min. After this time samples were heated at 60°C for 1 h and the reaction was terminated by heating at 70°C for 10 min.

## Material and Methods

---

For semi-quantitative RT-PCR reaction, the following protocol was used:

cDNA	2 $\mu$ l
Forward primer (10 $\mu$ M)	0.9 $\mu$ l
Reverse primer (10 $\mu$ M)	0.9 $\mu$ l
dNTP (10mM)	0.6 $\mu$ l
Dream taq polymerase (1U/ $\mu$ l)	0.6 $\mu$ l
Dream Taq Buffer (10x)	3 $\mu$ l
ddH <sub>2</sub> O	22 $\mu$ l
Total volume	30 $\mu$ l

### 3.2.2 shADAM17\_pLeGO\_C/BSD vector vector

The expression plasmid shADAM17-pLKO.1 containing a validated murine ADAM17 targeted shRNA under the control of the human U6 promotor, was obtained from Sigma. The shRNA cassette including the hU6 promotor was PCR amplified with primers introducing a 5' Xba I site and 3' Sal I site.

ddH <sub>2</sub> O	34.5 $\mu$ l
5 x HF buffer	10 $\mu$ l
shADAM17pLKO.1 (50 ng)	1 $\mu$ l
dNTP (10mM)	1 $\mu$ l
lego_17sh_fw	1.5 $\mu$ l
lego_17sh_rv	1.5 $\mu$ l
Phusion Hot Start II Polymerase	0.5 $\mu$ l

98°C	30 min	
98°C	10 min	
72°C	20 min	30 cycles
72°C	5 min	
4°C	infin.	

The resulting PCR product was purified from an agarose gel and Xba I/Sal I digested.

## Material and Methods

---

To remove the murine U6 promoter, the vector pLeGO-C/BSD was Xba I/Xho I digested according to the following protocol:

ddH <sub>2</sub> O	20 µl
10 x Tango buffer	6 µl
pLEGO-C/BSD (2 µg)	2 µl
Xba I	1 µl
Xho I	1 µl
Total volume	30 µl

PCR amplific. product extracted from the gel	46 µl
10 x Tango buffer	12 µl
Xba I	1 µl
Sal I	1 µl
Total volume	60 µl

The digestion products were separated on an agarose gel and the digested vector was purified by gel extraction. Digested PCR product and vector were subsequently ligated.

pLEGO-C/BSD	2.5 µl
PCR amplific. product extracted from the gel	1 µl
10 x T4 DNA Ligase buffer	2 µl
ddH <sub>2</sub> O	23.5 µl
T4 DNA Ligase	1 µl
Total volume	30 µl

The final product was termed sh17-pLeGO-C/BSD and verified by sequencing.

### 3.2.3 Generation of LLC cells with stable ADAM17 knock down

For generation of lentiviral particles following vectors were used:

## Material and Methods

---

<b>Vectors</b>	10 µg/ 10 cm dish	PMDLg/pRRE plasmid
	5 µg/ 10 cm dish	pRSV-Rev plasmid
	2 µg/ 10 cm dish	phCMV-VSV-G
	15 µg/ 10 cm dish	Adam17 pLKO.1-puro
	15 µg/ 10 cm dish	LeGO-C/BSD
	15 µg/ 10 cm dish	Sh17-pLeGO-C/BSD

### 1) Generation of lentiviral particles

#### Day 1:

In the afternoon  $5 \times 10^6$  HEK293T cells were seeded into a 10 cm dish

#### Day 2:

All the reagents and plasmids were thawed at the room temperature.

Indicated amount of plasmids was diluted in water (437.5 µl) and it was added 62.5 µl of 2 M  $\text{CaCl}_2$  solution. The 15ml falcon tube was filled with 500 µl of 2 x HBS and DNA/ $\text{CaCl}_2$  solution was added drop wise while blowing air through the solution using a pasteur pipette. This mixture was incubated for 10 – 20 min at room temperature. The medium from the cells was replaced with fresh medium, containing 25 µM Chloroquine. Subsequently DNA mixture was added, drop wise, to the cells with gentle swirling . Cells were incubated for 6 – 12h at 37°C, 5%  $\text{CO}_2$  and 95% humidity.

Medium was changed 8h later to 8 ml. From this moment on, medium was harvested every 12h.

#### Day 3:

##### Early

The supernatant (supernatant 1) was harvested and filtered through 0.45 µm or 0.22 µm filter into 2 ml tubes. For the second collection, 8 ml of fresh medium was added to the supernatant of cells. Virus containing supernatant (supernatant 1) was quickly frozen at -80°C.

##### Late

The supernatant (supernatant 2) was harvested in the same way as supernatant 1 and the new 8 ml of fresh medium was added. Successful HEK293T transfection was verified by fluorescent microscopy.

### Day 4

#### Early

The supernatant 3 was harvested, as described above in Day3.

#### Late

The supernatant 4 was harvested, as described above in Day3.

## 2) Titration of Lentiviral particles

The titration of Lentiviral particles was performed in the following way:

### Day 1

HEK293T cells, 50 000 cells per well, were seeded in a 24 well plate in a total volume of 500  $\mu$ l. Cells were left 2 – 5h to attach and then polybrene was added to a final concentration of 8  $\mu$ g/ml. Different volumes of viral particles ( 0.1  $\mu$ l, 1  $\mu$ l, 10  $\mu$ l and 100  $\mu$ l) were added in triplicates to the wells. The plate was centrifuged for 1h at 1000g and 24°C.

### Day 2

The medium was changed (1 ml per well) to medium without polybrene.

### Day 4

Cells were analysed in a BD FACS Canto™ (BD, Heidelberg, Germany) flow cytometer.

The titer was calculated from the wells showing 5 – 20% of positive cells.

Titer was calculated according to the formula:

$$T = N \cdot P / V$$

T – titer  
N – number of plated cells  
V – volume of added supernatants  
P – proportion of transduced cells

The supernatants with the best titer were used for the transduction of the LLC cells according to the protocol described above.

After transduction of LLC cells, 10 cells per ml were seeded in a 96 well plate and positive clones were identified using the fluorescent microscope. After clone expansion, the expression of ADAM17 was analysed using Western Blot Analysis, and semi-quantitative RT-PCR analysis.

### 3.2.4 Cell culture and cell lines

The murine cell lines LLC (Lewis Lung Carcinoma) and B16F1 (melanoma cell line), both



## Material and Methods

---

derived from C57Bl/6N mice, were purchased from CLS (Eppenheim, Germany). The human HEK293T cell line was purchased from DSMZ (Braunschweig, Germany).

All cell lines were cultured in the cell culture medium (see the section 3.1.1) at 37°C, 5%CO<sub>2</sub> and 95% humidity. At the confluency of 70%-80%, cells were detached from the tissue flask using trypsin/EDTA and split in a ratio 1:5.

For mice injection LLC and B16F1 cells were prepared according to the following protocol:

- 1) Cells were detached from the tissue flask and centrifuged at 1200-2000 rpm for 7 min
- 2) The cell pellet was resuspended in ice cold 1 x PBS (see the section 3.1.1) and cells were adjusted to a final concentration of  $5 \times 10^5$  cells per ml
- 3) 1ml of resuspended cells was pipeted into each eppendorf tube, centrifuged at 1200-2000 rpm for 7 min and the cell pellet was resuspended in 250µl ice cold 1 x PBS for mice injection.

### 3.2.5 Proliferation assay

Cells were counted and seeded into six well plates to a final concentration of  $5 \times 10^5$  cells per well. Cells were incubated for 4 – 6h at 37°C, 5% CO<sub>2</sub> and 95% humidity in cell culture medium (see the section 3.1.1). Subsequently, medium was changed to DMEM without FCS and cells were starved over night. The following day, cell were stimulated with rm TNF-α (see the section 3.1.4) in the final concentrations of 0.01 ng/ml, 0.03 ng/ml, 0.1 ng/ml and 0.3 ng/ml. Cells were counted 24h, 48h, 72h and 144h post stimulation.

### 3.2.6 Protein extraction from tissues and cultured cells

The same lysis buffer was used for the cell and tissue lysis (see the section 3.1.1). For the cell lysis 500µl of a lysis buffer per  $5 \times 10^5$  cells was used. Cells were scraped from the plate with the cell scraper, and subsequently transferred into eppendorf tubes and resuspended by pipetting. Lysates were cleared by centrifugation at 13,000 rpm for 10 min at 4°C. 30 µl of lysate was mixed with 5x Leammli, boiled at 95°C for 10 min and used for the SDS-polyacrylamide gel electrophoresis (SDS-PAGE) and subsequently Western Blot analysis (see the following section).

For tissue lysis 750 µl of lysis buffer per 40 mg of tissue sample was used. Tissue was lysed for 2 min at 5000 rpm using the Precellys homogenizer (PEQLAB Biotechnologie

GMBH, Erlangen, Germany). Lysate was centrifuged on 13,000 rpm for 10 min at 4°C. After centrifugation, protein concentration was determined from the supernatant using the BCA Protein Assay Kit according to manufacture's instructions (Pierce™, Rockford, USA) and 200 µg of protein lysate was used for the SDS-polyacrylamide gel electrophoresis (SDS-PAGE) and subsequently Western Blot analysis (see the sections 3.2.7 and 3.2.8).

### 3.2.7 SDS-polyacrylamide gel electrophoresis (SDS-PAGE)

Proteins were separated on a polyacrylamide gel, according to their molecular weight, using the Mini-Protein III system (BioRad). The gels were run for 90 min at 120 V const.

### 3.2.8 Immunoblotting Analysis

After the proteins were separated by SDS-PAGE, they were transferred onto a PVDF membrane (GE Healthcare, Uppsala, Sweden) using MINI TRANSBLOT apparatus (BioRad Laboratories GmbH, München, Germany). After the protein transfer for 90 min at 100V const, the PVDF membranes were placed into a plastic container in NETG buffer (see the section 3.1.1) and blocked for 1h at room temperature. Subsequently, membranes were incubated with primary antibody for 1h at room temperature or over night at 4°C. The excess of the primary antibody was removed by washing the membrane in NETG buffer 3 times for 10 min, after which the membrane was incubated for 1 h with the secondary antibody followed by 3 times washing in NETG. ECL-Plus Western blotting Detection Kit (Piers, Massachusetts, USA) was used for the protein detection with the CCD camera system LAS-1000 (Fujifilm, USA).

### 3.2.9 Generation of Bone Marrow Derived Neutrophils (BMDNs)

7-11 weeks old mice were killed via cervical dislocation, and femora and tibia were dissected. The ends of the bones were removed and the bone marrow was flushed through a 70 µm cell mesh with the flushing medium (see the section 3.1.1) into the collection tube. The pellet from the collection tube was resuspended in BMN medium (see the section 3.1.1) to a final concentration of  $1 \times 10^6$  cells per ml. rm G-CSF (see the section 3.1.4) was added to a final concentration of 5 ng/ml. Finally, the cells were seeded into the 24-well plate with 1ml per well.

After 4-5 days additional 500µl of fresh BMN medium was added. Cells were differentiated after 9 days. To ascertain the purity of differentiated cells after 9 days, extracellular FACS

staining was performed using anti-CD11b and anti-Gr-1 antibodies.

### **3.2.10 Generation of Bone Marrow Derived Macrophages (BMDMs)**

7-11 weeks old mice were killed via cervical dislocation, femura and tibia bones were dissected, the ends of the bones were removed and the bone marrow was flushed with 5ml of ice cold 1 x PBS (see the section 3.1.1) into a 50 ml falcon tube. Cell suspension was passed through a 70  $\mu$ m cell strainer and subsequently centrifuged at 300 x g for 10 min at 4°C. Supernatant was discarded. The pellet was resuspended in 5 ml ice cold erythrocyte lysis buffer and incubated for 5 min at 4°C. After incubation, 45 ml of PBS was added and centrifuged as above. Cell pellet was resuspended into the complete medium (see the section 3.1.1) supplemented with rm M-CSF in final concentration of 50 ng/ml, and cell density was adjusted to  $7.5 \times 10^5$  cells per ml. Cells were seeded into 10 cm bacteria dishes, for less adherence, and cultured for 3 days. After 3 days, 5 ml of complete medium was added. After 5-6 days macrophages were differentiated and ready to use. To detach macrophages from the plate, 1-2 ml of 1% EDTA in 1 x PBS was used and the plates were placed at 37°C in the incubator for 25 min. After 25 min detached cells were resuspended into 10 ml of ice cold 1 x PBS and centrifuged at 300 x g for 10 min at 4°C. Cell were resuspended in the complete medium (see the section 3.1.1) and plated for the experiment.

### **3.2.11 Enzyme Linked Immunosorbent Assay (ELISA)**

To determine the precise concentration of the protein of interest from the cell culture supernatants or of the tissue homogenates, the sandwich ELISA was used. The ELISA microtiter plate was coated with 100 $\mu$ l of Capture Antibody diluted in PBS according to the manufacture's protocol. Plate was sealed and incubated overnight at room temperature. The following day, the excess of the Capture Antibody was removed by washing 3-5 times in the Washing buffer (section 3.1.1) with complete removal of liquid at each step. The plate was blocked with the 300 $\mu$ l Reagent Diluent for 1h at room temperature. Plates were washed 3-5 times with Washing buffer to remove the excess of Capture antibody. After aspiration, 100 $\mu$ l of sample or Standard, diluted in the Reagent Diluent according to the manufacture's recommendation, was added to the wells (each sample was measured in the duplicate or triplicate) and incubated for 2h at the room temperature. The aspiration/wash step was repeated. Detection Antibody was diluted in Reagent Diluent

## Material and Methods

---

according to the manufacture's protocol and 100µl was added to each well and incubated for 2h at the room temperature. Streptavidin conjugated to horseradish-peroxidase and peroxidase substrate (Roche, Mannheim, Germany) were used for the subsequent detection in the colorimetric reaction. Absorption was measured at 475nm in an ELISA plate reader TECAN RainBow (Tecan GmbH, Carlsheim, Germany).

### 3.2.12 Animal breedings

Hypomorphic male C57Bl/6N ADAM17<sup>ex/ex</sup> mice (Chalaris 2010), ADAM17<sup>wt/wt</sup> littermates, sgp130Fc transgenic mice and C57Bl/6N (Charles River, Sulzfeld, Germany) male mice were used in this study. ADAM17<sup>ex/ex</sup> mice were backcrossed to the C57Bl/6N background 9 times. sgp130 mice were backcrossed to the C57Bl/6N background 8 times. Mice were maintained at a 12 hour light-dark cycle under standard conditions, provided with food and water ad libitum.

### 3.2.13 Model of experimental metastasis

For all animal experiments male mice 9-12 weeks of age were used. All experiments were performed according to the German guidelines for animal care and protection.

Hypomorphic ADAM17<sup>ex/ex</sup> mice and ADAM17<sup>wt/wt</sup> littermates, sgp130 and C57Bl/6N mice were injected through the tail vein with LLC or B16F1 cells, prepared as previously described (see the section 3.2.4). Mice were sacrificed via cervical dislocation at 20h, 7, 14 and 21 days post injection, organs were excised and frozen in liquid nitrogen for further analysis.

### 3.2.14 FACS analysis of tumor bearing lung tissue

The lungs were excised, cut in pieces and digested in 5 ml of 0.1% Collagenase Type IV (Serva, Electrophoresis GmbH, Heidelberg, Germany) diluted in PBS at room temperature for 2h. A single cell suspension was generated by sucking through a 26G needle and passing through 70 µm cell strainer (BD Falcon, Germany). Cells were centrifuged for 8 min at 400 g at 4°C, the pellet was resuspended in 5 ml of erythrocyte lysis buffer (see the section 3.1.1) and incubated at 37°C for 5 min. Cell lysis was stopped by adding a 10 fold volume of ice cold 1 X PBS. After sedimentation for 8 min at 400 g, cells were resuspended in the FACS buffer, stained and analysed with Flow Cytometer BD FACS Canto™ (BD, Heidelberg, Germany).

## Material and Methods

---

### 3.2.15 Immunohistochemistry

Tissue samples were incubated in 4% formaldehyde over night at 4°C. The next day samples were washed and kept in water for 3-5 hours at room temperature. After washing, they were incubated in 50% ethanol over night, and then it was proceeded with the alcohol dehydration series according to the protocol:

1	70% ethanol	60 min
2	96% ethanol I	30 min
4	100% ethanol I	60 min
5	100% ethanol II	30 min
6	Xylol I	120 min
7	Xylol II	120 min
8	Paraffin I	30 min
9	Paraffin II	60 min or over night
10	Paraffin III	60 min

After paraffin embedding, sections were cut to 5 µm thickness and stained according to the following protocols:

**HE staining** - Tissue sections were incubated for 10 min in Gill3 Hematoxylin, differentiated in 0.5% acetic acid, rinsed in tap water and counterstained with Giemsa's azur eosin methylene blue solution.

**Neutrophil and Macrophage stainings** - Tissue sections were deparaffined and rehydrated according to the protocol:

1	Xylol	3 x 5 min
2	100% Ethanol	2 x 5 min
3	95% Ethanol	2 x 5 min
4	70% Ethanol	1 x 5 min
5	ddH <sub>2</sub> O	by choice

After rehydration, peroxidase was blocked with H<sub>2</sub>O<sub>2</sub> for 10 min, and sections were washed several times first in distilled water and then in PBS. Sections were demasked with proteinase K (1µl/1ml) digestion for 5 min, and subsequently washed with distilled water and PBS.

## **Material and Methods**

---

Antibodies (see the section 3.1.7) were diluted in the Sample Diluent (Dako, Glostrup, Denmark) with 1:100 or 1:200 dilution for anti-Gr1 and 1:50 for anti-F4/80 over night at 4°C. After incubation with biotinylated polyclonal rabbit anti-rat antibody (Dako, Glostrup, Denmark) and EnVision-HRP (Dako, Glostrup, Denmark), the signal was developed with AEC Substrate (Dako, Glostrup, Denmark). Samples were counterstained with Shandon Gill3 Hematoxylin.

**PCNA staining** - Cut sections were treated the same way as described in the section 3.2.15 to the step of staining with the primary antibody. Antibody was diluted in the Sample Diluent (Dako, Glostrup, Denmark) with 1:100 dilution over night at 4°C. After incubation with biotinylated polyclonal rabbit anti-rat antibody (Dako, Glostrup, Denmark) and EnVision-HRP (Dako, Glostrup, Denmark), the signal was developed with AEC Substrate (Dako, Glostrup, Denmark). Samples were counterstained with Shandon Gill3 Hematoxylin.

### **3.2.16 Proteome Profiler™ – Mouse Cytokine Array**

To determine the relative expression levels of multiple cytokines from tissue homogenates, Mouse Cytokine Array Panel A was used (see the section 3.1.8). Capture Antibodies for different cytokines were spotted in duplicate on nitrocellulose membranes. 200µg of sample was diluted and mixed with the cocktail of biotinylated detection antibodies. The sample/antibody mixture was then incubated with the Mouse Cytokine Array membranes over night at 4°C. To remove the excess of unbound material, membranes were washed in the Washing solution (provided by manufacturer), incubated with the Streptavidin-HRP and chemiluminescent detection reagents. The signal was detected with the CCD camera Fuji LAS1000. The quantification was determined with the program ImageJ version 1.47.

### **3.2.17 Proteome Profiler™ – Mouse Phospho-RTK Array**

Proteome Profiler Phospho-RTK antibody Array (RTK Array) is a tool which enables to detect changes in phosphorylation of receptor tyrosine kinases between different samples. Capture antibodies for different phosphorylated receptors were spotted in duplicate on nitrocellulose membranes. Recombinant tyrosine phosphorylated proteins were used to choose capture antibodies. 200µg of lung tissue lysate was diluted and prepared according to manufacture's recommendation, and incubated with the RTK Array

## **Material and Methods**

---

membranes over night at 4°C. To remove the excess of unbound material, membranes were washed in the Washing solution (provided by manufacturer), incubated with the Streptavidin-HRP and chemiluminescent detection reagents. The signal was detected with the CCD camera Fuji LAS1000. The quantification was determined with the program ImageJ version 1.47.

## 4 Results

### 4.1 ADAM17<sup>ex/ex</sup> mice are protected in a model of experimental metastasis

In order to study the role of ADAM17 in the metastatic niche, we used a murine metastasis model. Hereby, syngeneic tumor cells were injected i.v. into the tail vein of wild type or ADAM17<sup>ex/ex</sup> mice. Animals were sacrificed at different time points post injection at 20h, 7, 14 and 21 days (Figure 4.1.1).

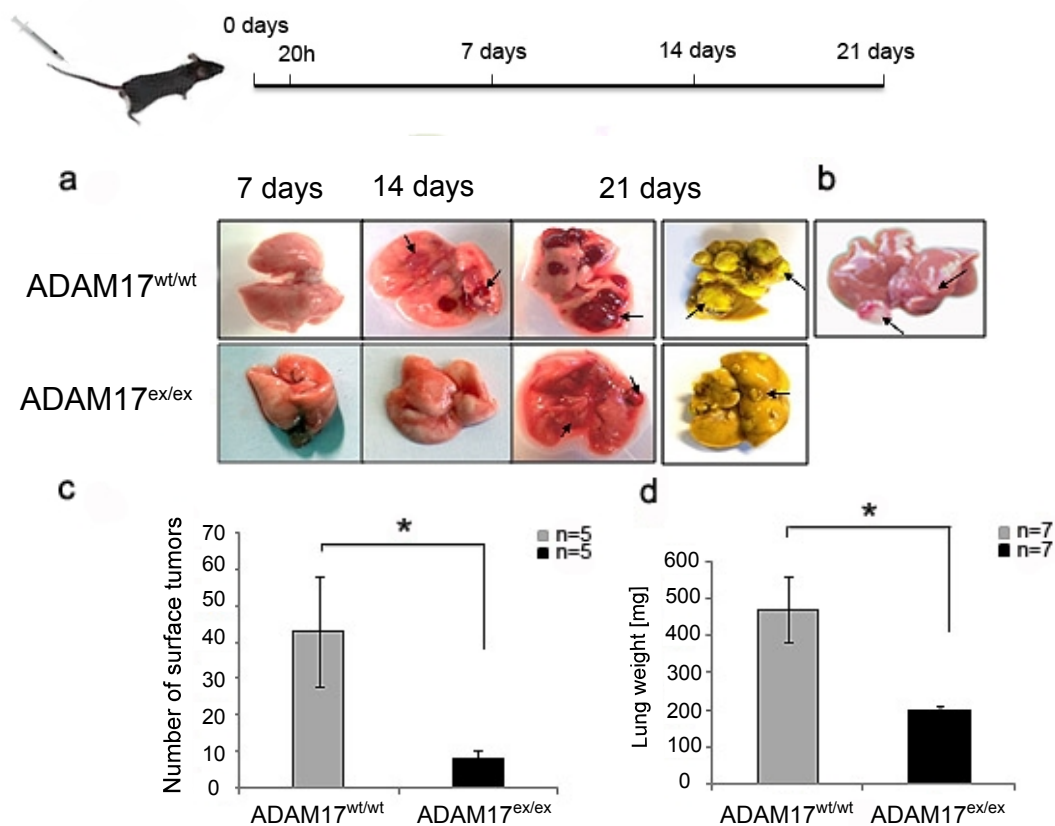


**Figure 4.1.1 Metastasis to the lungs and liver after LLC inoculation.** **a** Lungs of ADAM17<sup>wt/wt</sup> and ADAM17<sup>ex/ex</sup> mice 7, 14 and 21 days after inoculation with  $5 \times 10^5$  LLC cells per mouse (tumors are indicated by black arrows; for the ease of detection, lungs were stained with Bouin's solution (right panel, 21 days, lungs colored in yellow), **b** Liver of ADAM17<sup>wt/wt</sup> mice 21 days after LLC inoculation (tumors are marked by black arrows), **c** Number of surface tumors in the lungs and **d** lung weight of ADAM17<sup>wt/wt</sup> and ADAM17<sup>ex/ex</sup> mice 21 days after LLC inoculation. Data are represented as means  $\pm$  s.e.m. \* p<0.05.

We were not able to detect any macroscopic differences in the lungs between ADAM17<sup>wt/wt</sup> and ADAM17<sup>ex/ex</sup> mice as early as 20h and 7 days post LLC injection. First macroscopic differences appeared 14 days after tumor cells injection (Figure 4.1.1 a). ADAM17<sup>wt/wt</sup> animals had several small visible tumors, while the lungs of ADAM17<sup>ex/ex</sup> animals revealed



## Results

normal lung morphology. 21 days after LLC inoculation, we detected a significant difference in the number of microscopical tumors in the lungs (Figure 4.1.1 c). Wild type mice developed five times more tumor lesions in the lungs than ADAM17<sup>ex/ex</sup> mice. This was also reflected in a significant difference in total lung weight (Figure 4.1.1 d). While ADAM17<sup>ex/ex</sup> animals had normal lung weight, the weight of ADAM17<sup>wt/wt</sup> lungs was 2.5 times higher. Metastasis to the liver, while less frequent, appeared only in ADAM17<sup>wt/wt</sup> mice (Figure 4.1.1 b).

In order to determine if the observed effects were restricted to lung carcinoma cells or the observed effects were the consequence of reduced ADAM17 expression in the host, we injected B16F1 melanoma cells i.v. into ADAM17<sup>wt/wt</sup> and ADAM17<sup>ex/ex</sup> mice. Metastasis was analyzed 21 days post B16F1 injection. We were able to detect metastatic lesions in the lungs and livers in both animal groups (Figure 4.1.2 a), with higher incidence in ADAM17<sup>wt/wt</sup> than in ADAM17<sup>ex/ex</sup> mice (Figure 4.1.2 b). Metastasis to the kidneys appeared only in ADAM17<sup>wt/wt</sup> mice (Figure 4.1.2 c).

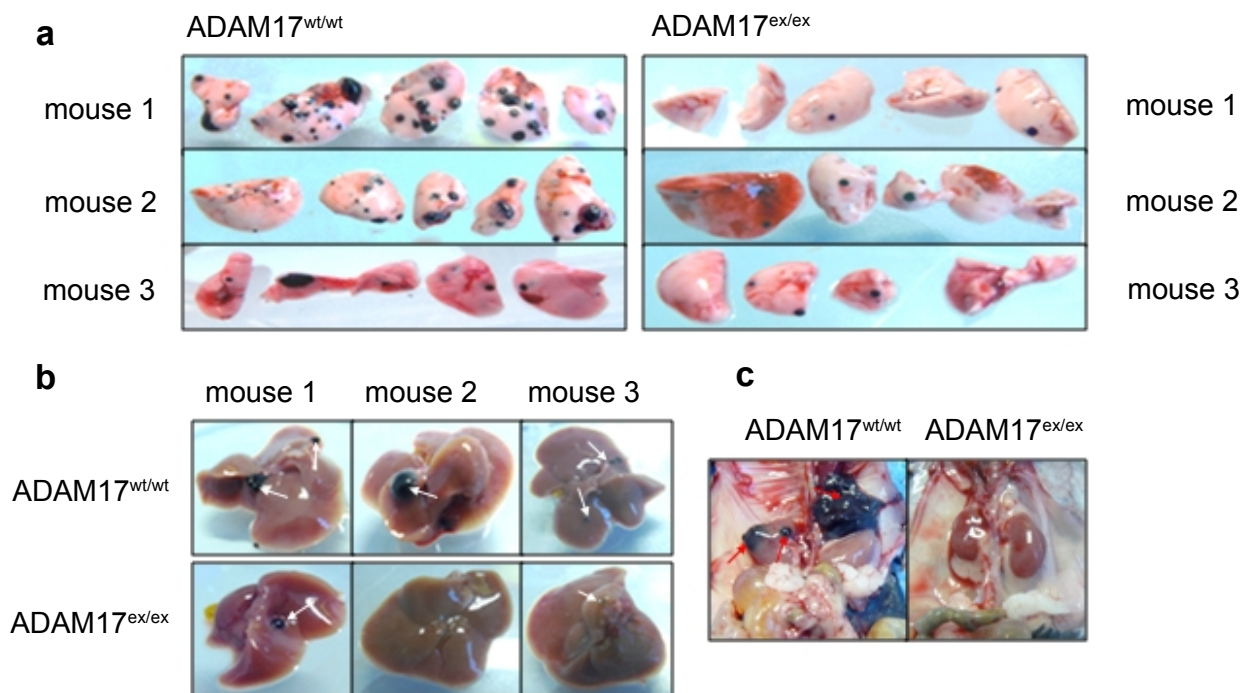


**Figure 4.1.2 Metastasis to the lungs, liver and kidneys 21 days after B16F1 inoculation.** **a** Lobes of the lung of ADAM17<sup>wt/wt</sup> (n=3) and ADAM17<sup>ex/ex</sup> (n=3) mice were dissected for better tumor visibility. Tumor lesions are visible in black, as a consequence of melanin production by B16F1 melanoma cells, **b** Livers of 3 different ADAM17<sup>wt/wt</sup> and ADAM17<sup>ex/ex</sup> mice 21 days after inoculation with  $5 \times 10^5$  B16F1 cells per mouse (liver metastasis are indicated by white arrows), **c** kidneys of ADAM17<sup>wt/wt</sup> and ADAM17<sup>ex/ex</sup> mice 21 days post B16F1 injection (metastasis is indicated by red arrows).

## Results

The number of microscopical tumors in the lungs of ADAM17<sup>wt/wt</sup> mice was ten times higher compared to ADAM17<sup>ex/ex</sup> mice (Figure 4.1.3). Differences in lung weight were not significant between these two groups, although lung weight of wild type animals was increased compared to the lung weight of hypomorphic animals.

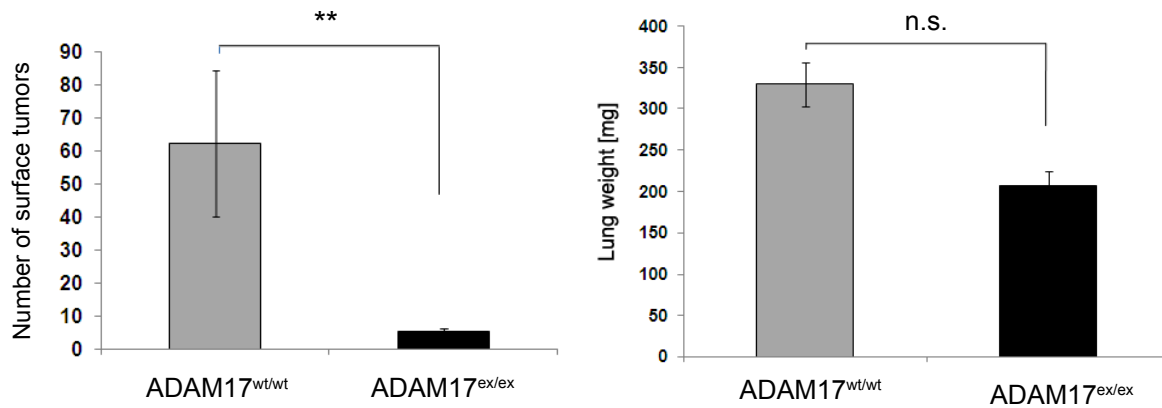


**Figure 4.1.3 Quantification of tumor burden in B16F1 injected animals.** Number of surface lung tumors and lung weight of ADAM17<sup>wt/wt</sup> (n=3) and ADAM17<sup>ex/ex</sup> (n=3) mice 21 days after injection with  $5 \times 10^5$  B16F1 cells per mouse. *n.s.* - not significant Data are represented as means  $\pm$  s.e.m. \*\*  $p < 0.005$ .

Survival of ADAM17<sup>ex/ex</sup> mice was dramatically increased in comparison to wild type mice after LLC injection. The survival rate of 50% for ADAM17<sup>wt/wt</sup> animals was observed 24 days post LLC cell injection (Figure 4.1.4), whereas ADAM17<sup>ex/ex</sup> mice were completely protected from metastasis induced death within observed time.

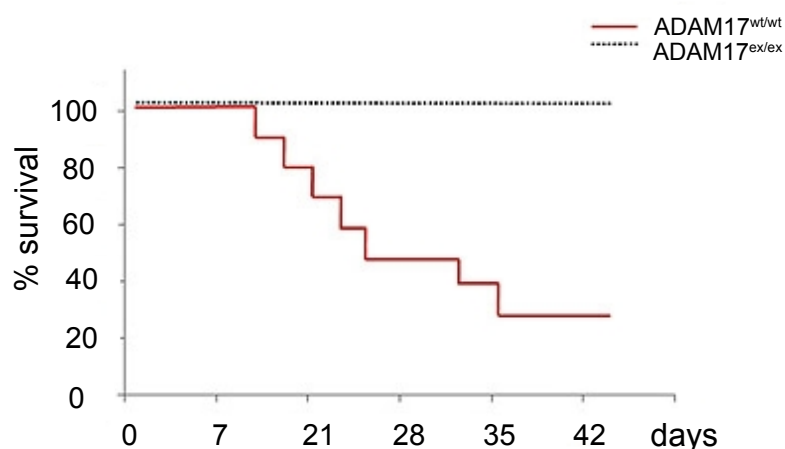


**Figure 4.1.4 Survival rate of LLC injected animals.** Survival of ADAM17<sup>wt/wt</sup> (n = 11) and Adam17<sup>ex/ex</sup> (n = 7) mice injected with  $5 \times 10^5$  LLC cells in a time course of 43 days.

#### 4.2 ADAM17 in the metastatic niche supports metastatic progression

We analyzed inflammatory infiltrations in tumor bearing lungs of ADAM17<sup>wt/wt</sup> and ADAM17<sup>ex/ex</sup> mice by immunohistochemistry. Tumor lesions in the lungs were readily detectable in HE staining 3 weeks after injection, in both LLC and B16F1 injected mice (Figure 4.2.1). ADAM17<sup>wt/wt</sup> animals displayed a 5 fold increased number of Ly6G/Gr1<sup>+</sup> myeloid cell infiltrations compared to ADAM17<sup>ex/ex</sup> hypomorphic animals (Figure 4.2.2). Ly6G/Gr1<sup>+</sup> cells were detectable mainly in the tumorous part of the lung tissue.

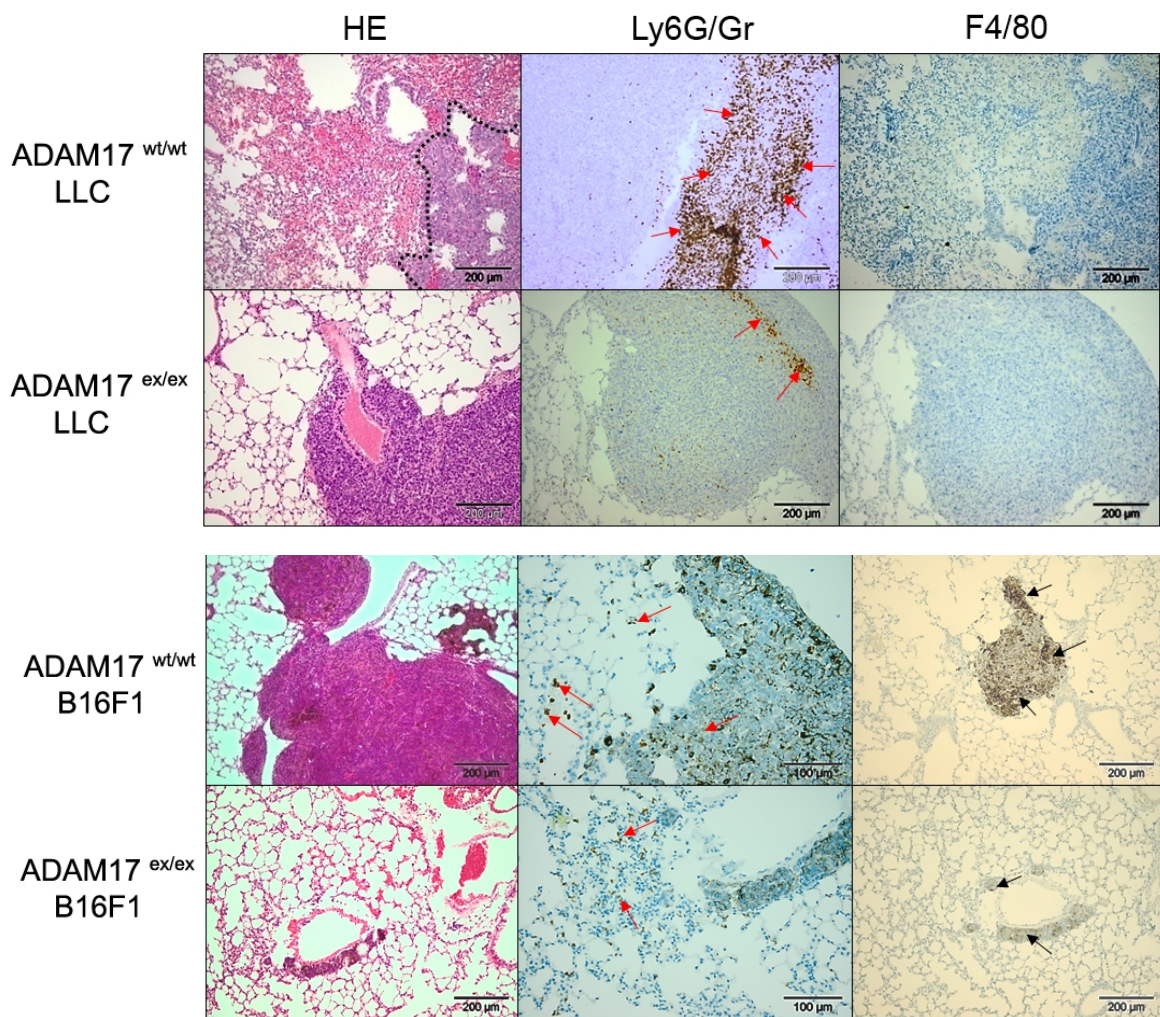


**Figure 4.2.1 Infiltration of Gr1<sup>+</sup> myeloid cells depends on ADAM17 in the metastatic niche.** Immunohistochemical stainings of tumor bearing lungs 21 days post tumor cell injection ( $5 \times 10^5$  per mouse); **HE** - Hematoxylin and eosin staining, **Gr1/Ly6G** – granulocyte staining, **F4/80** - macrophage staining, **ADAM17<sup>wt/wt</sup> LLC** - wild type mice injected with LLC cells, **ADAM17<sup>wt/wt</sup> B16F1** – wild type mice injected with B16F1 cells, **ADAM17<sup>ex/ex</sup> LLC** – hypomorphic mice injected with LLC cells, **ADAM17<sup>ex/ex</sup> B16F1** – hypomorphic mice injected with B16F1 cells; (black dot-line represents the boundary between tumorous and non-tumorous tissue, red arrows indicate the presence of Ly6G/Gr1<sup>+</sup> cells, black arrows indicate B16F1 tumor cells).

## Results

F4/80 immunohistochemistry performed on lung tissue from tumor bearing mice on 21 days post-tumor cells injection revealed the absence of these cells in the lungs in both ADAM17<sup>wt/wt</sup> and ADAM17<sup>ex/ex</sup> mice (Figure 4.2.1). Interestingly, this was the case in both, LLC and B16F1 injected mice.

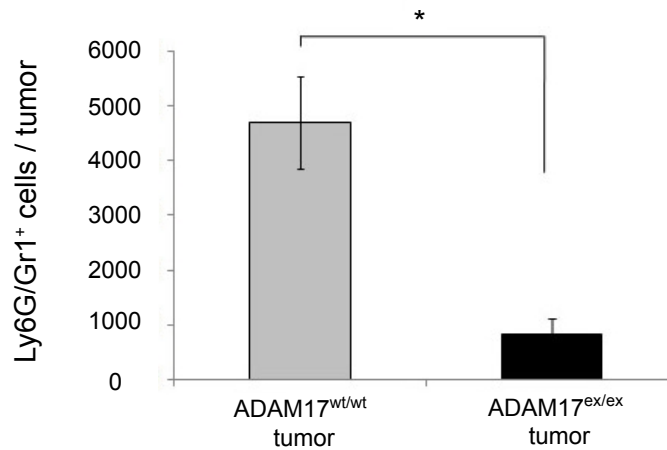


**Figure 4.2.2 ADAM17<sup>wt/wt</sup> tumor bearing lungs reveal increased infiltration of Ly6G/Gr1<sup>+</sup> myeloid cells.** Quantification of Ly6G/Gr1<sup>+</sup> cells from 3 different tumorous areas of each ADAM17<sup>wt/wt</sup> and ADAM17<sup>ex/ex</sup> mice 21 days after LLC inoculation analyzed from immunohistological sections. Data are represented as means  $\pm$  s.e.m. \*  $p < 0.05$ .

We attempted to quantify the number of Ly6G/Gr1<sup>+</sup> and F4/80<sup>+</sup> cells in lung tissue sections of ADAM17<sup>wt/wt</sup> and ADAM17<sup>ex/ex</sup> mice inoculated with B16F1 cells, but unfortunately we were not successful. B16F1 cells express a substantial amount of melanin, thus displaying a black color in the sections. Ly6G/Gr1<sup>+</sup> and F4/80<sup>+</sup> cells after staining are recognized by dark brown color, therefore making the identification impossible due to mutual overlapping. Since we did not reveal F4/80<sup>+</sup> cells in the non-tumorous areas, we concluded that these myeloid cells did not infiltrate into the lung tissue.

Using FACS analysis of tumor bearing lungs from ADAM17<sup>wt/wt</sup> and ADAM17<sup>ex/ex</sup> mice 21 days after LLC cells injection, we determined the precise phenotype of Ly6G/Gr1<sup>+</sup> myeloid cells. We could identify Ly6G/Gr1<sup>+</sup> myeloid cells as CD11b<sup>+</sup>CD11c<sup>-</sup>Ly6G/Gr1<sup>+</sup>F4/80<sup>-</sup> cells (Figure 4.2.3). This phenotype of myeloid cells correlated to a specific subset of MDSCs called granulocytic MDSCs. Interestingly, the granulocytic subset of MDSCs was already described in several mouse tumor models and it strongly correlated with poor prognosis (Movahedi et al., 2008).



## Results

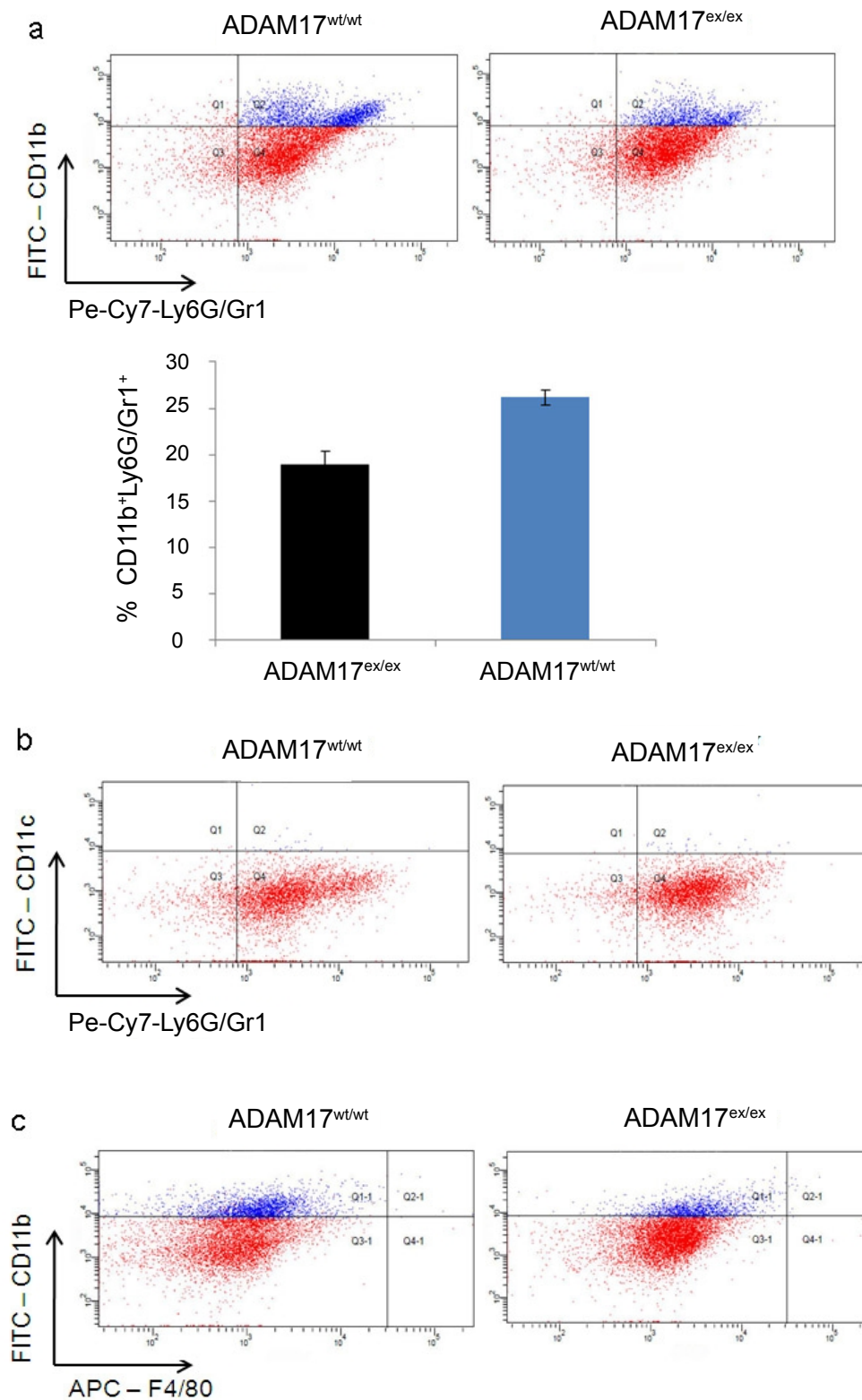


**Figure 4.2.3 ADAM17<sup>wt/wt</sup> tumor bearing lungs display stronger infiltration of MDSCs.** Representative FACS analysis of single cell suspensions from whole lung tissue of ADAM17<sup>wt/wt</sup> (n=3) and ADAM17<sup>ex/ex</sup> (n=3) mice 21 days after LLC cells inoculation ( $5 \times 10^5$  cells per mouse) **a** CD11b<sup>+</sup>Ly6G/Gr1<sup>+</sup> MDSCs, **b** CD11c<sup>+</sup>Ly6G/Gr1<sup>+</sup> MDSCs, **c** CD11b<sup>+</sup>F4/80<sup>+</sup> MDSCs. Data are represented as means  $\pm$  s.e.m.

## Results

### 4.3 Early phase of metastasis is marked with accumulation of Ly6G/Gr1<sup>+</sup> but not F4/80<sup>+</sup> cells

To better understand if reduced tumor growth in ADAM17<sup>ex/ex</sup> animals was due to decreased MDSCs recruitment, we analyzed earlier time points post LLC cell injection for MDSCs infiltration. Mice were sacrificed 7 and 14 days after LLC cell injection. Although we were unable to detect tumor nodules in the lungs of one week injected mice, we could see an increased thickening of the inter-alveolar septae in immunohistochemical stainings in ADAM17<sup>wt/wt</sup> but not in ADAM17<sup>ex/ex</sup> tumor bearing lungs (Figure 4.3.1).

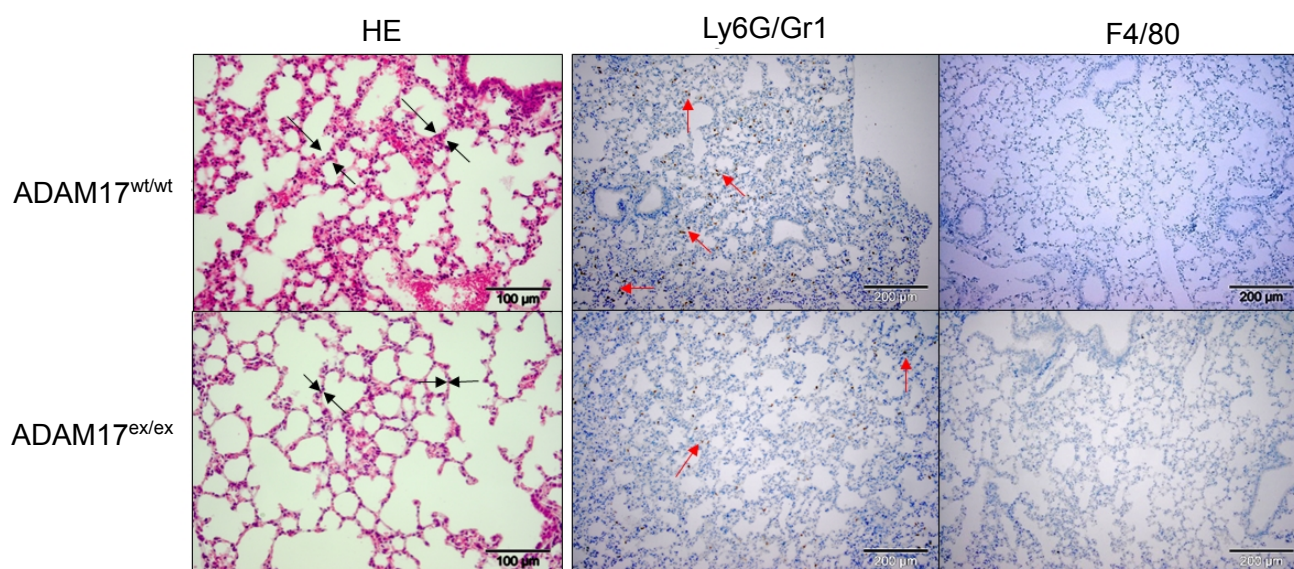


**Figure 4.3.1 Myeloid infiltrations in the lungs of ADAM17<sup>wt/wt</sup> and ADAM17<sup>ex/ex</sup> mice 7 days after LLC cells injection.** ADAM17<sup>wt/wt</sup> and DAM17<sup>ex/ex</sup> mice were injected with  $5 \times 10^5$  LLC cells per mouse. After 7 days, lungs were excised and analyzed by immunohistochemistry; **a** Hematoxylin and eosin (HE) staining of lung tissue one week post LLC inoculation (black arrows indicate for different thickness of inter-alveolar septae), **b** Immunohistochemical stainings for Ly6G/Gr1<sup>+</sup> and F4/80<sup>+</sup> immune cells (red arrows indicate Ly6G/Gr1<sup>+</sup> cells in the lungs).

One of the causes for thickening of inter-alveolar septae could be the infiltration of immune cells into the interstitium. We could detect an increased infiltration of Ly6G/Gr1<sup>+</sup> cells as early as one week after injection. However, we were unable to detect infiltration of F4/80<sup>+</sup> cells (Figure 4.3.1). Macroscopically visible tumors in the lungs of ADAM17<sup>wt/wt</sup> but not ADAM17<sup>ex/ex</sup> mice, appeared as early as 14 days after LLC cell inoculation. The increase in thickening of inter-alveolar septae in wild type animals was even more evident 14 days after LLC cell inoculation (Figure 4.3.2). However, it was absent in hypomorphic mice. The amount of Ly6G/Gr1<sup>+</sup> cell infiltrations was markedly increased in ADAM17<sup>wt/wt</sup> animals,

## Results

whereas it was barely detectable in ADAM17<sup>ex/ex</sup> animals. We could not detect F4/80<sup>+</sup> cells in both mice groups (Figure 4.3.2).

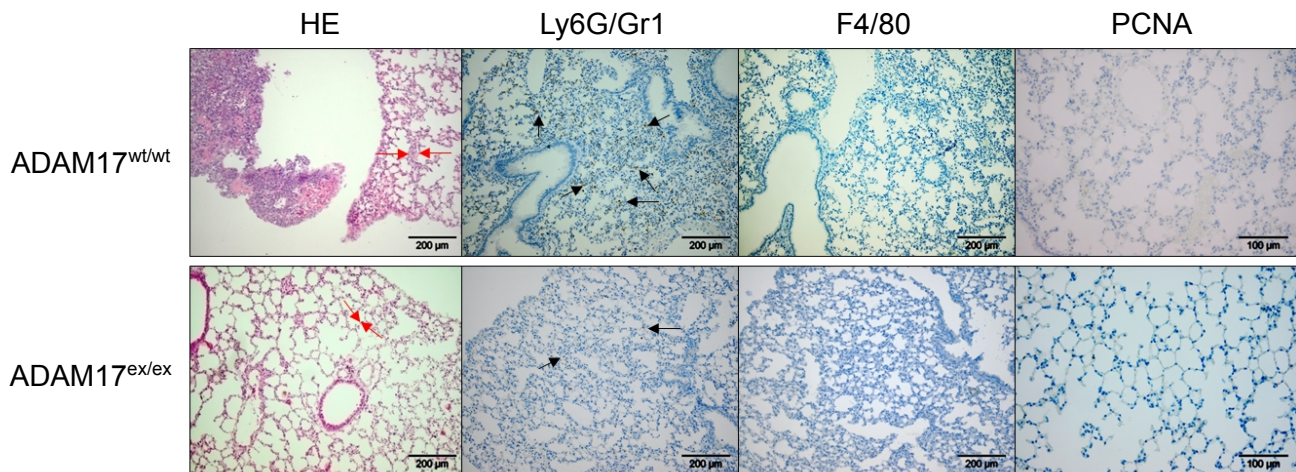


**Figure 4.3.2 ADAM17<sup>wt/wt</sup> mice show increased myeloid infiltration 14 days after LLC cells injection.** ADAM17<sup>wt/wt</sup> and DAM17<sup>ex/ex</sup> mice were injected with  $5 \times 10^5$  LLC cells per mouse. After 14 days, lungs were excised and analyzed by immunohistochemistry; Hematoxylin and eosin (**HE**) staining, immunohistochemical staining for **Ly6G/Gr1** and **F4/80** myeloid cells and proliferating cell nuclear antigen (**PCNA**) 14 days after LLC cells injection from paraffin embedded tissue samples (red arrows indicate stronger thickening of inter-alveolar septae in wilde type mice than one week after LLC inoculation, black arrows indicate Ly6G/Gr1<sup>+</sup> cell staining).

Taken together, these data demonstrate a correlation of tumor progression in wild type animals with Ly6G/Gr1<sup>+</sup> MDSCs recruitment. Therefore, we concluded that reduced tumor growth in ADAM17<sup>ex/ex</sup> animals was due to decreased recruitment of MDSCs infiltration.

### 4.4 Tumor-bearing lungs of ADAM17<sup>ex/ex</sup> mice produce less factors implicated in MDSCs expansion and survival

We sought to analyze inflammatory cytokine and chemokine production in different time points post LLC cells injection. We took advantage of the Proteome Profile Murine cytokine antibody array (see the section 3.2.16) using lung tumor tissue lysates from ADAM17<sup>wt/wt</sup> and ADAM17<sup>ex/ex</sup> animals 21 days after LLC cells injection (Figure 4.4.1). We could detect significant differences in protein expression for several cytokines and chemokines between wild type and hypomorphic animals. The strongest difference was detectable in levels of CCL2/MCP-1. Interestingly, in previous studies, CCL2/MCP-1 has been linked to the recruitment and expansion of MDSCs at the tumor site (Sawanobori et al., 2008).



## Results

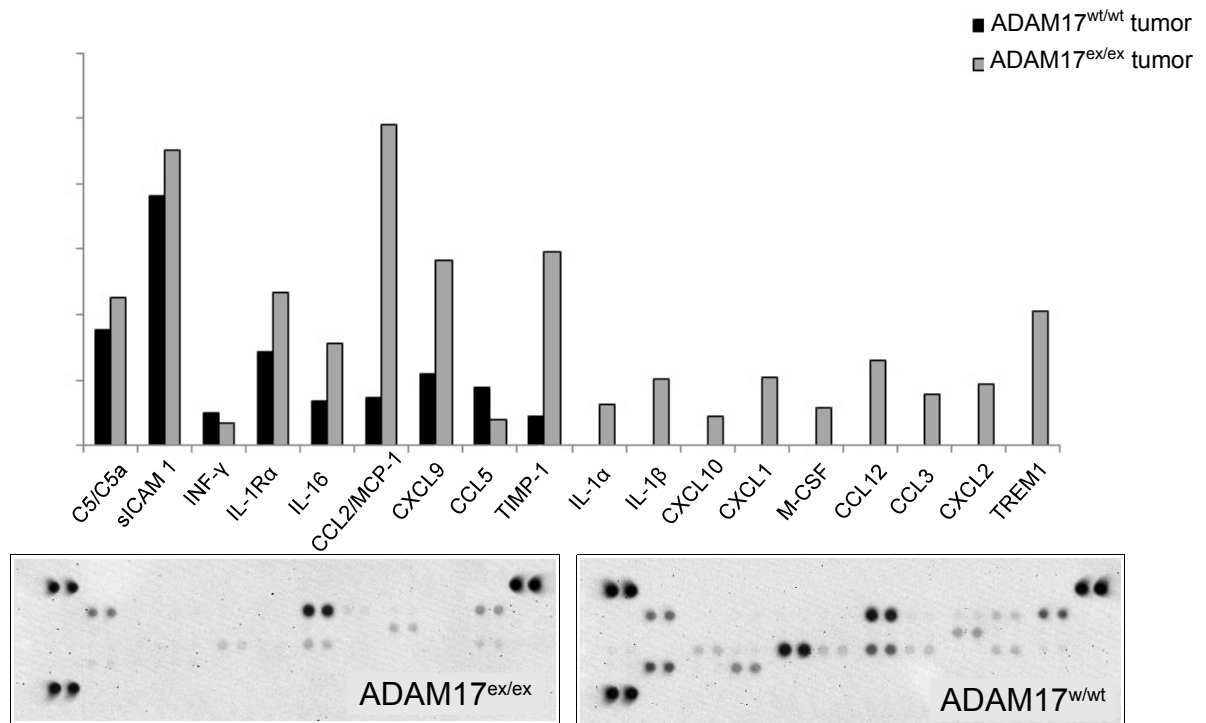


**Figure 4.4.1 Tumors of ADAM17<sup>wt/wt</sup> mice display increased production of inflammatory cytokines and chemokines.** Tumorous and non-tumorous parts of the lung tissue 21 days after LLC cell inoculation from ADAM17<sup>wt/wt</sup> and ADAM17<sup>ex/ex</sup> mice were dissected, lysed (see the sections 3.1.4 and 3.2.6) and 200 µg of protein lysate from tumorous part of the tissue was used for the Cytokine Array. Black and gray bars represent densitometric analysis; **C5/C5a** - complement component 5, **sICAM1** - soluble Intercellular Adhesion Molecule 1, **INF-γ** - interferon gamma, **IL-1Ralpha** - interleukin 1 receptor alpha, **IL-16** - interleukin 16, **CCL2/MCP1** - chemokine (C-C) motif 2/monocyte chemotactic protein1, **CXCL9** - chemokine C-X-C motif ligand 9, **CCL5** - chemokine (C-C) motif ligand 5, **TIMP-1** - tissue inhibitor of metalloproteases 1, **IL-1alpha** - interleukin 1 alpha, **IL-1beta** - interleukin 1 beta, **CXCL10** - chemokine (C-X-C) motif ligand 10, **KC/CXCL1** - chemokine (C-X-C) motif ligand 1, **M-CSF** - macrophage colony stimulating factor, **CCL12/MCP5** - chemokine (C-C) motif ligand 12/monocyte chemotactic protein 5, **MIP-1a/CCL3** - macrophage inflammatory protein 1 alpha/ chemokine (C-C) motif ligand 3, **CXCL2** - chemokine (C-X-C) motif ligand 2, **TREM 1** - triggering receptor expressed on myeloid cells 1.

We hypothesized that tumor cells could be the source of CCL2/MCP-1, thus contributing to strong infiltration of CD11b<sup>+</sup>Ly6G/Gr1<sup>+</sup>Ly6C<sup>+</sup>F4/80<sup>-</sup> MDSCs. To test this hypothesis, we analyzed the cell culture medium of wtLLC and kdADAM17-LLC cells (see the section 4.9) for the production of CCL2/MCP-1. We were able to show that this chemokine derived from tumor cells (Figure 4.4.2). Furthermore, we were able to validate the finding from Proteome Profile Murine cytokine antibody array for the protein expression of CCL2/MCP-1 in tumor bearing lungs of ADAM17<sup>wt/wt</sup> and ADAM17<sup>ex/ex</sup> mice by ELISA.



## Results

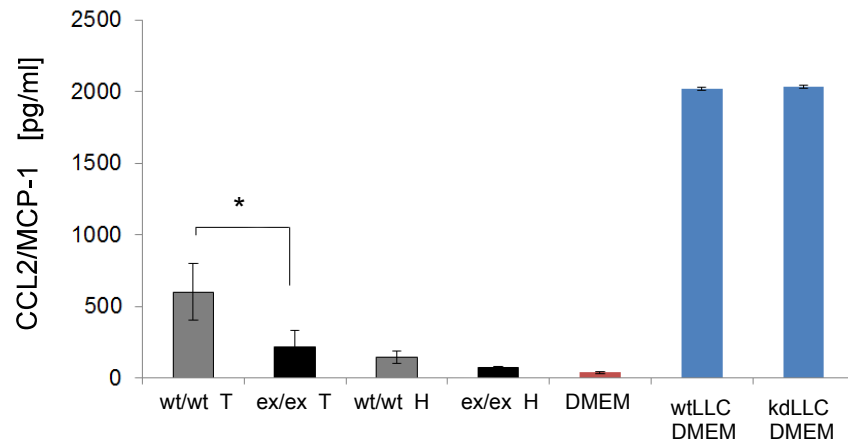


**Figure 4.4.2 CCL2/MCP-1 is predominantly produced by tumor cells.** CCL2/MCP-1 concentration in 200 µg of protein tissue lysates from ADAM17<sup>wt/wt</sup> (n=3) and ADAM17<sup>ex/ex</sup> (n=3) tumor-bearing lungs 21 days after LLC cell inoculation measured by ELISA; **ex/ex T**- tumorous part of the lung tissue from ADAM17<sup>ex/ex</sup> mice, **wt/wt T**- tumorous part of the lung tissue from ADAM17<sup>wt/wt</sup> mice, **wt/wt H**- non-tumorous part of the lung tissue from ADAM17<sup>wt/wt</sup> mice, **ex/ex H**- non-tumorous part of the lung tissue from ADAM17<sup>ex/ex</sup> mice, **wtLLC DMEM**- filtered cell culture medium from wtLLC cells, **kdLLC DMEM**- filtered cell culture medium from kdADAM17-LLC cells, **DMEM** was used as a control. Data are represented as means ± s.e.m. \* p<0.05.

We were also able to detect CCL2/MCP-1 mRNA expression by qRT-PCR (Figure 4.4.3). Significant differences in the expression of CCL2/MCP-1 between ADAM17<sup>wt/wt</sup> and ADAM17<sup>ex/ex</sup> mice appeared at early stages of metastasis. Only 7 days post LLC injection, with peaking after 14 days and sustaining until the final stage of metastasis in ADAM17<sup>wt/wt</sup> mice. The expression of CCL2/MCP-1 mRNA was slightly increase over time in ADAM17<sup>ex/ex</sup> mice.

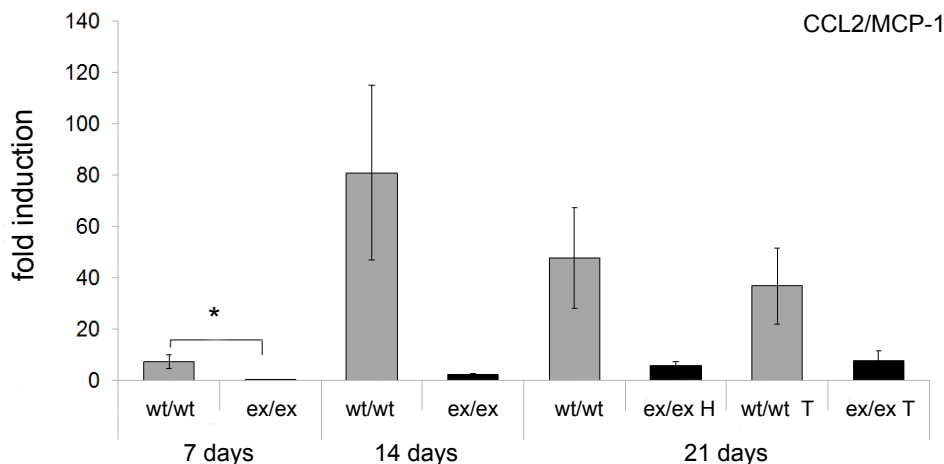


**Figure 4.4.3 Tumor bearing lungs of ADAM17<sup>wt/wt</sup> mice reveal high mRNA expression of CCL2/MCP-1.** RNA was extracted from the lungs of ADAM17<sup>wt/wt</sup> (n=3) and ADAM17<sup>ex/ex</sup> (n=3) mice at indicated time points after LLC inoculation ( 5x10<sup>5</sup> cells per mouse). Quantitative RT-PCR was performed and mRNA was quantified as above, the amounts in non-inoculated lungs from ADAM17<sup>wt/wt</sup> and ADAM17<sup>ex/ex</sup> mice were set to value of 1.0; **H** - healthy/non-tumorous part of the tissue, **T** - tumorous part of the tissue. Data are represented as means ± s.e.m. \* p<0.05.

## Results

To better understand the mechanism behind such a strong difference in myeloid infiltration between ADAM17<sup>wt/wt</sup> and ADAM17<sup>ex/ex</sup> mice, the whole lung tissue, from different time points post LLC cells injection, was analyzed for the expression of genes implicated in the infiltration of granulocytic MDSCs.

Expression of CXCL2/MIP-2 has been previously correlated with infiltration of Ly6G/Gr1<sup>+</sup> myeloid cell (Belperio et al., 2002). We could observe that mRNA levels of the inflammatory chemokine CXCL2/MIP-2 was induced in earlier time points, reaching the maximum of its expression 14 days after LLC inoculation and persisting with insignificant decrease through metastasis progression in ADAM17<sup>wt/wt</sup> mice (Figure 4.4.4). mRNA expression for CXCL2/MIP-2 remained unchanged through all time points in ADAM17<sup>ex/ex</sup> mice.

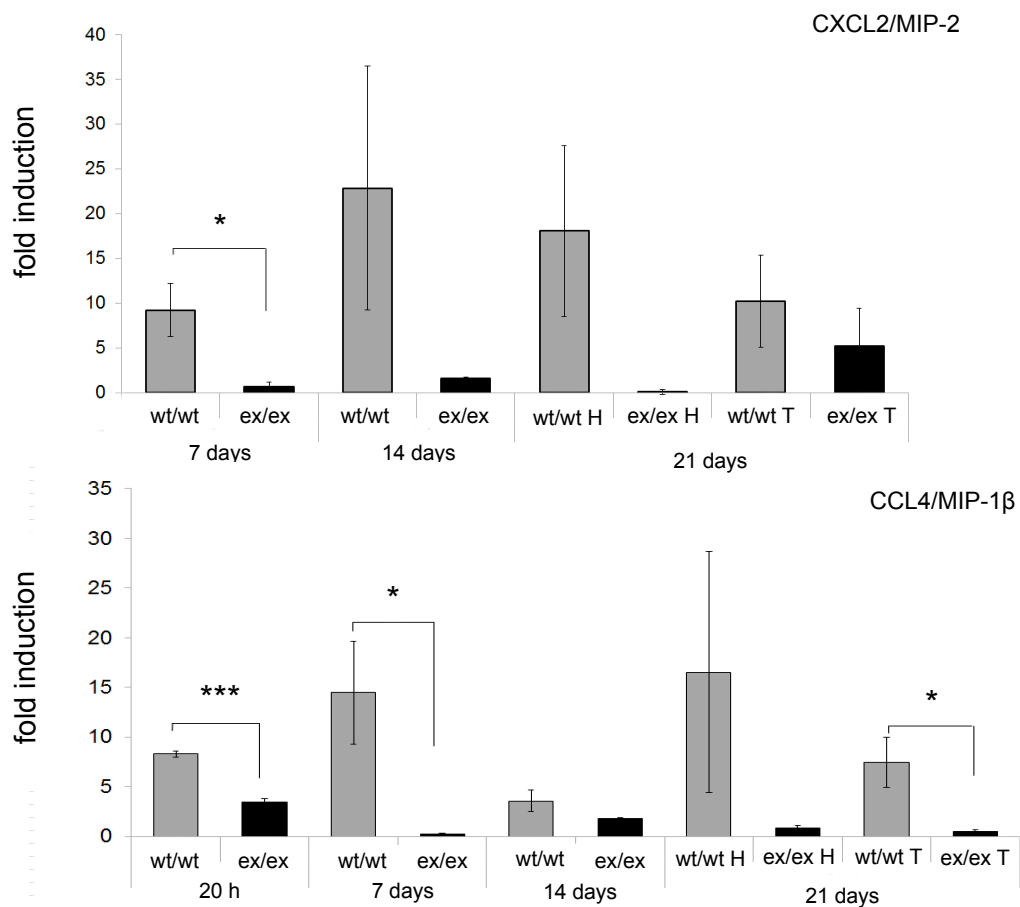


**Figure 4.4.4 Early phase of metastasis is characterized by an increased transcription of inflammatory chemokines.** RNA was extracted from the lungs of ADAM17<sup>wt/wt</sup> (n=3) and ADAM17<sup>ex/ex</sup> (n=3) mice at the indicated time points after LLC inoculation (  $5 \times 10^5$  cells per mouse). mRNA was quantified as above and the amounts in non-inoculated lungs from ADAM17<sup>wt/wt</sup> and ADAM17<sup>ex/ex</sup> mice were set to 1.0 - basal level; *H* - healthy/non-tumorous part of the tissue, *T* - tumorous part of the tissue. Data are represented as means  $\pm$  s.e.m. \*p<0.05, \*\*\*p<0.001.

## Results

Furthermore, we observed that the inflammatory chemokine CCL4/MIP-1 $\beta$  mRNA was induced only 20h after LLC inoculation (Figure 4.4.4) in both ADAM17<sup>wt/wt</sup> and ADAM17<sup>ex/ex</sup> mice, peaking 7 days post injection with a slight decrease in a late stage in ADAM17<sup>wt/wt</sup> animals. In ADAM17<sup>ex/ex</sup> animals the expression of CCL4/MIP-1 $\beta$  mRNA was insignificantly decreased over time.

### 4.5 TNF- $\alpha$ is released from the surface of Ly6G/Gr1<sup>+</sup> cells in the early phase of metastasis

We were able to see a significant upregulation of gene expression of the pro-inflammatory cytokines TNF- $\alpha$  and IL-1 $\beta$  predominantly at early phases of metastasis in ADAM17<sup>wt/wt</sup> but not in ADAM17<sup>ex/ex</sup> tumor bearing lungs (Figure 4.5.1).

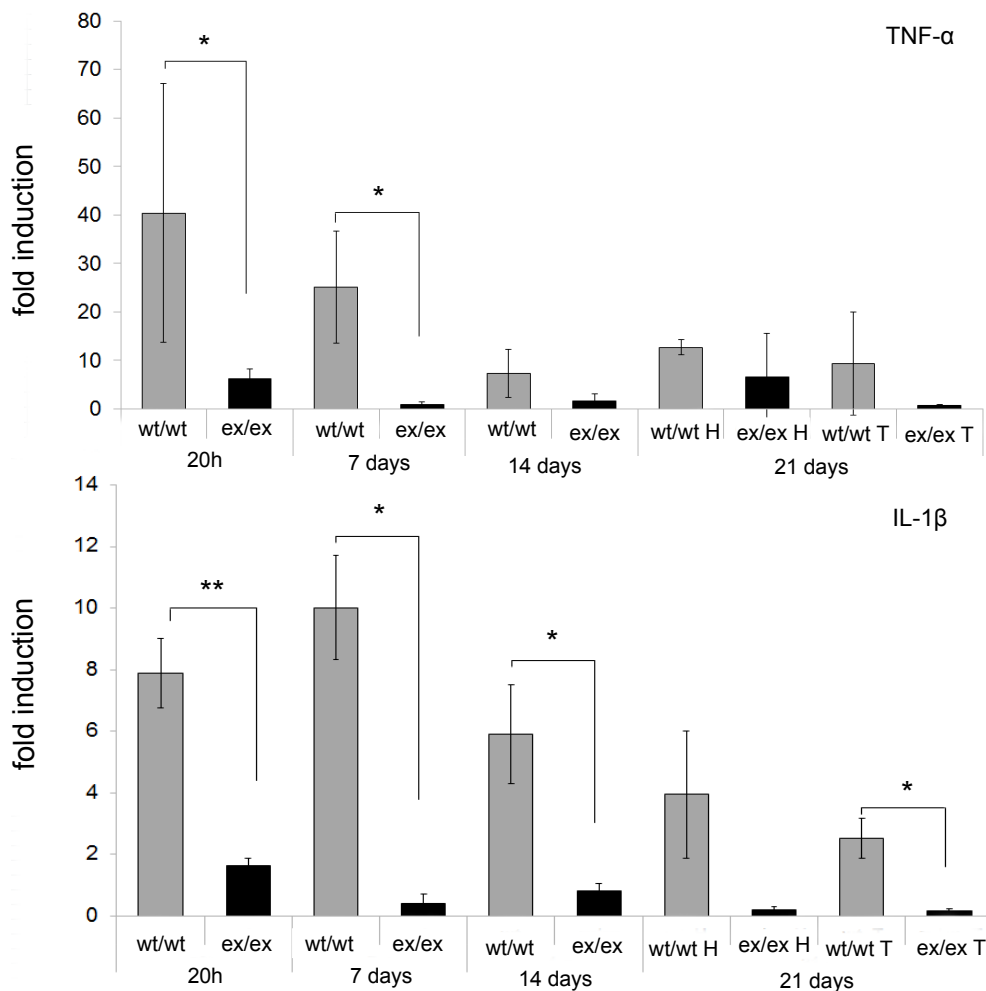


**Figure 4.5.1 TNF- $\alpha$  and IL-1 $\beta$  are upregulated at early time points of metastasis.** RNA was extracted from the lungs of ADAM17<sup>wt/wt</sup> (n=3) and ADAM17<sup>ex/ex</sup> (n=3) mice at the indicated time points after LLC inoculation (  $5 \times 10^5$  per mouse). mRNAs were quantified as above and the amounts in non-inoculated lungs from ADAM17<sup>wt/wt</sup> and ADAM17<sup>ex/ex</sup> mice was set to 1; *H* - healthy/non-tumorous part of the tissue, *T* - tumorous part of the tissue. Data are represented as means  $\pm$  s.e.m. \*  $p < 0.05$ , \*\* $p < 0.005$ .

## Results

Since we could observe stronger accumulation of Ly6G/Gr1<sup>+</sup>, but not of F4/80<sup>+</sup> cells in immunohistological stainings of tumor bearing lungs (section 4.3) in ADAM17<sup>wt/wt</sup> mice at early stage of lung metastasis, we speculated that infiltrated myeloid cells could be the source of the pro-inflammatory cytokines TNF- $\alpha$  and IL-1 $\beta$ . In order to confirm this hypothesis, bone marrow cells were isolated from ADAM17<sup>wt/wt</sup> and ADAM17<sup>ex/ex</sup> mice, and differentiated to neutrophils and macrophages with rm G-CSF or rm M-CSF, respectively (see the sections 3.2.9 and 3.2.10). Successful differentiation was verified by FACS analysis for the presence of Ly6G/Gr1, CD11b and F4/80 antigens (data not shown). Differentiated cells were stimulated with conditioned medium of LLC cells. Interestingly, we could detect TNF- $\alpha$  in the supernatant of wild type bone marrow derived macrophages (BMDM) and bone marrow derived neutrophils (BMDN). However, as expected, in supernatants of BMDMs and BMDNs derived from hypomorphic mice, the amount of TNF- $\alpha$  was strongly reduced (Figure 4.5.2). To confirm that ADAM17 is the main sheddase responsible for the cleavage of TNF- $\alpha$  from the surface of BMDNs upon stimulation with LLC conditioned medium, two hydroxamate-based ADAM17 inhibitors, GI and GW, were tested. The inhibitor GW280264X (GW) has the ability to potently block the activity of ADAM10 and ADAM17, whereas GI254023X (GI) has the ability to block ADAM10 100-fold better than ADAM17 (Ludwig et al., 2005).

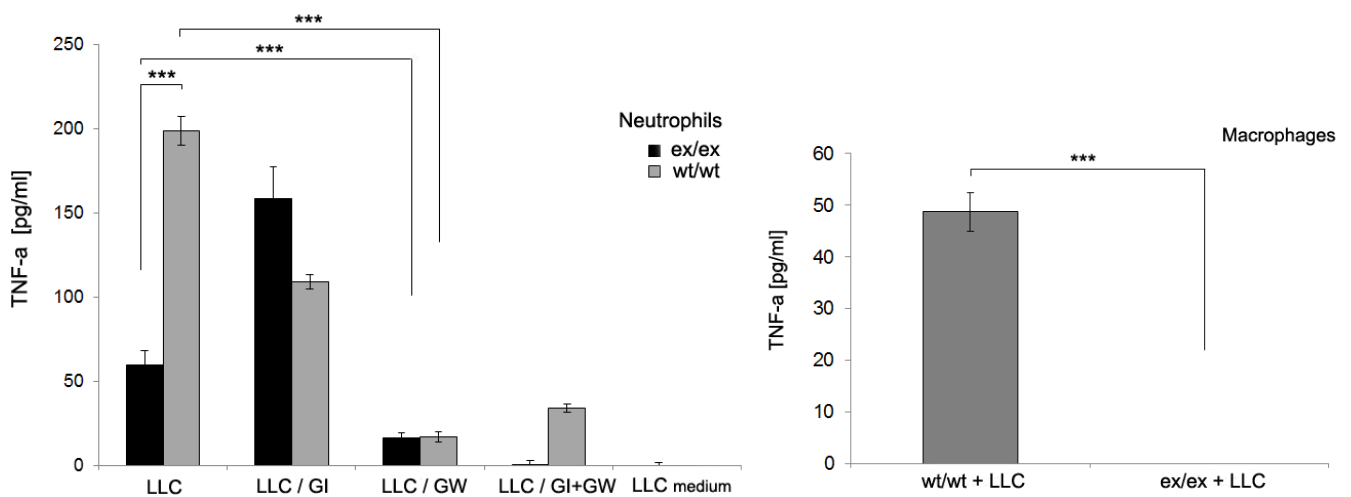


**Figure 4.5.2 BMDNs and BMDMs produce TNF- $\alpha$  upon stimulation with LLC cell supernatant.** BMDNs and BMDMs were cultured with conditioned medium of LLC cells for 24h. BMDNs were cultured in presence or absence of 3 $\mu$ M GI or GW, and production of TNF- $\alpha$  was measured by ELISA; **ex/ex** - bone marrow cells from ADAM17<sup>ex/ex</sup> mice. **wt/wt** - bone marrow cells from ADAM17<sup>wt/wt</sup> mice. Data are represented as means  $\pm$  s.e.m. \*\*\*p<0.001.

## Results

As shown in Figure 4.5.2, GI reduced shedding of TNF- $\alpha$  for 35% while GW reduced shedding of TNF- $\alpha$  for 90% from the surface of wild type BMDNs. These data indicate that ADAM17 is responsible for supernatant-induced release of TNF- $\alpha$  from the surface of myeloid cells.

Taken together, we can conclude that factors secreted by LLC cells stimulate infiltrated myeloid cells to release TNF- $\alpha$  in an ADAM17 dependent manner.

### 4.6 ADAM17 generates proliferatory signals during lung metastasis

Proliferating Cell Nuclear Antigen (PCNA) is a nuclear protein that is a cofactor of DNA polymerase delta. PCNA acts as a homotrimer and helps to increase the processivity of leading strand synthesis during DNA replication. Frequently, it is used as marker for cell proliferation.

We performed PCNA immunohistological staining of paraffin sections from lung tissue of ADAM17<sup>wt/wt</sup> and ADAM17<sup>ex/ex</sup> mice 21 days after LLC cell injection (Figure 4.6.1). Interestingly, in the tumorous part of wild type mice we detected 3.5 times more PCNA<sup>+</sup> cells than in lung sections of hypomorphic mice.

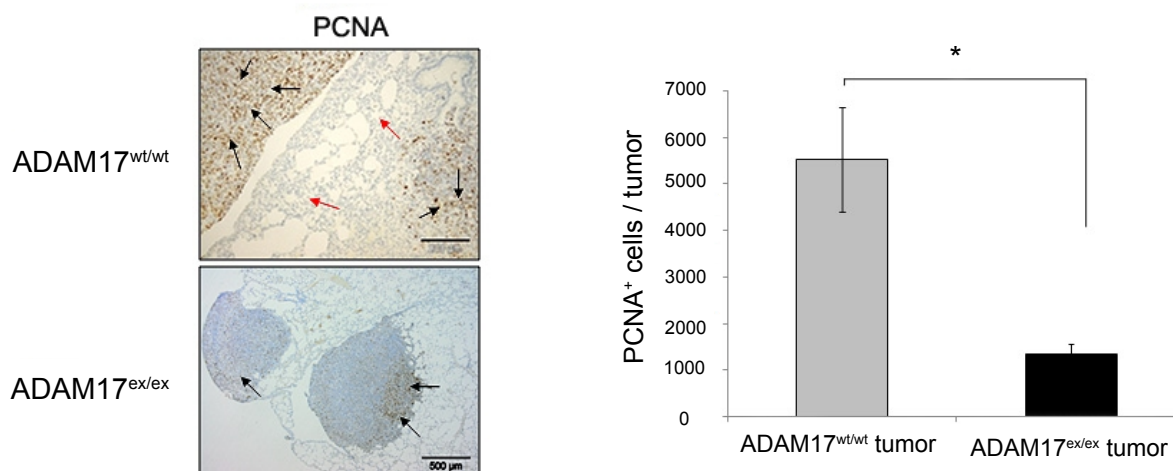


**Figure 4.6.1 ADAM17 in the host contributes to cell proliferation.** Immunohistological staining and number of PCNA<sup>+</sup> cells from 3 different tumorous tissue areas of ADAM17<sup>wt/wt</sup> and ADAM17<sup>ex/ex</sup> mice 21 days after LLC inoculation; black arrows indicate PCNA<sup>+</sup> cells in the tumorous part of the tissue, red arrows indicate PCNA<sup>+</sup> cells in the non-tumorous part of the tissue; **PCNA** - proliferating cell nuclear antigen. Data are represented as means  $\pm$  s.e.m. \*  $p < 0.05$ .

In recent publication, Rivas and colleagues demonstrated that TNF- $\alpha$  can induce the proliferation of murine mammary tumor cells C4HD *in vitro* and *in vivo* (Rivas et al., 2008).

## Results

They demonstrated that through the activation of p42/p44 MAPK, JNK, PI3-K/Akt pathways and NF- $\kappa$ B transcriptional activation, TNF- $\alpha$  induces proliferation of C4HD tumor cells. Interestingly, they showed that blockage of TNFR1 or TNFR2, with specific antibodies, was enough to impair TNF- $\alpha$  signaling. Furthermore, Rivas and colleagues demonstrated that administration of TNF- $\alpha$  *in vivo* supported C4HD tumor growth. Injection of a NF- $\kappa$ B selective inhibitor, Bay 11-7082, in mice resulted in regression of TNF- $\alpha$  promoted tumor growth.

We hypothesized that LLC cells can proliferate upon TNF- $\alpha$  stimulation. Therefore, we stimulated LLC cells for 120h with different concentrations of rm TNF- $\alpha$  (Figure 4.6.2).

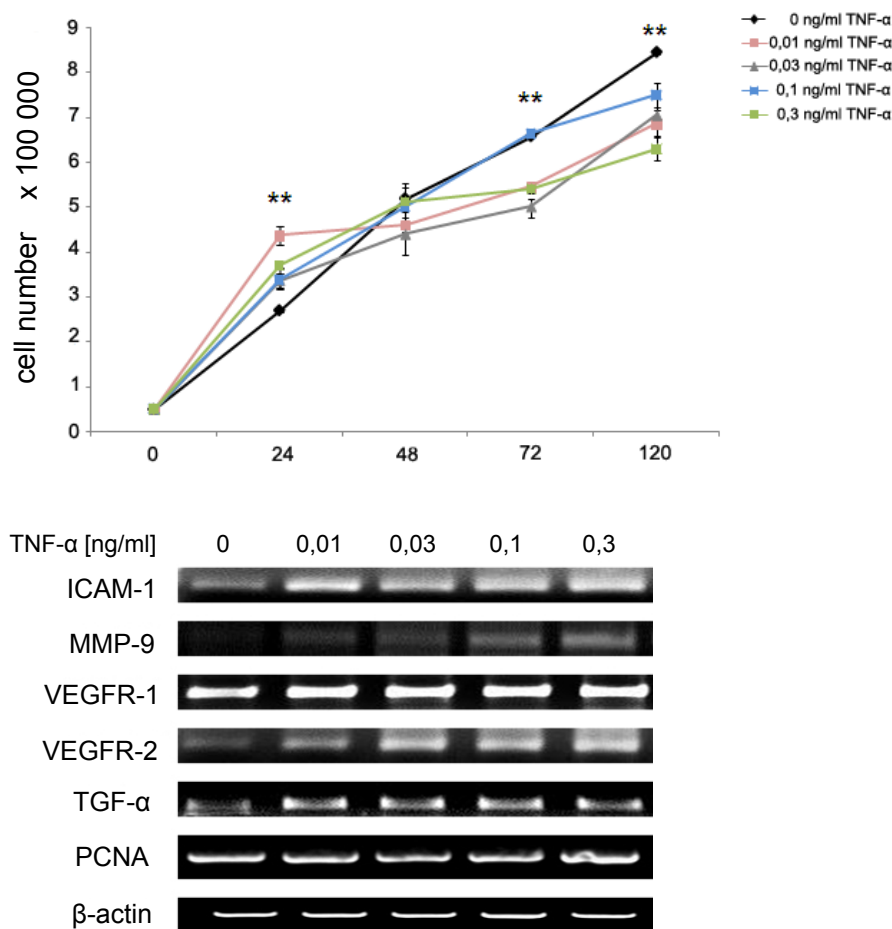


**Figure 4.6.2 TNF- $\alpha$  increases proliferation of wild type LLC cells at early time points.**  $5 \times 10^5$  cells per well were seeded into 6 well plates; cells were cultured in DMEM supplemented with 0,5% FCS for 120h in the presence or absence of rmTNF- $\alpha$ ; cells were counted after 24, 48, 72 and 120h. RNA was isolated from the cells stimulated for 24h with different concentrations of rmTNF- $\alpha$  and gene expression for ICAM-1, MMP-9, VEGFR-1 and 2, TGF- $\alpha$  and PCNA was analyzed by semiquantitative RT-PCR; **ICAM-1** – intercellular adhesion molecule 1, **MMP-9** – matrix metalloprotease 9, **VEGFR-1/-2** – vascular endothelial growth factor receptor transcript variants 1 and 2, **TGF- $\alpha$**  – transforming growth factor alpha, **PCNA**- proliferating cell nuclear antigen. Data are represented as means  $\pm$  s.e.m. \*\*  $p < 0.005$ .

## Results

Interestingly, preliminary data suggest that 24h after TNF- $\alpha$  stimulation, all stimulated LLC cells had a significantly higher proliferation rate than TNF- $\alpha$  unstimulated cells. Furthermore, in the first 24h of stimulation, we could detect a TNF- $\alpha$  concentration dependent mRNA upregulation of intercellular adhesion molecule 1 (ICAM-1), matrix metalloprotease 9 (MMP-9) and vascular endothelial growth factor receptor 2 (VEGFR-2). Furthermore, 48h after stimulation, proliferation rate of TNF- $\alpha$  stimulated and non-stimulated cells equalized. At later time points proliferation of all TNF- $\alpha$  stimulated cells was significantly reduced compared to unstimulated cells.

Taken into account that TNF- $\alpha$  was upregulated in the lungs shortly after LLC injection, we concluded that TNF- $\alpha$  can be a proliferatory stimulus for cancer cells at early stages of metastasis.

Receptor tyrosine kinases (RTKs) are high-affinity cell surface receptors for many polypeptide growth factors, cytokines and hormones. Receptor tyrosine kinases have been shown not only to be the key regulators of normal cellular processes but also to have a critical role in the development and progression of many types of cancer (Zwick et al., 2001). Ser/Thr kinase extracellular-signal-regulated kinase (ERK) is activated downstream of several RTKs.

To investigate proliferatory signals in ADAM17<sup>wt/wt</sup> and ADAM17<sup>ex/ex</sup> tumor bearing lungs, we analyzed ERK phosphorylation by Immuno blot analysis (Figure 4.6.3).

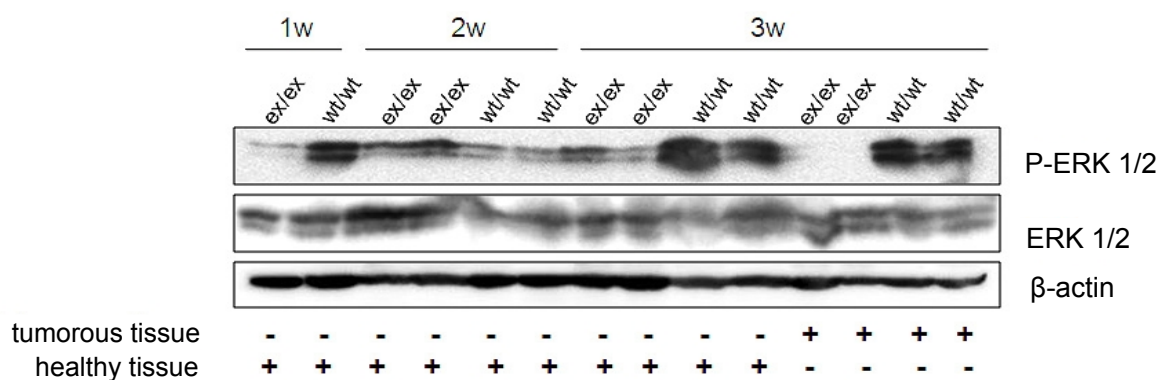


**Figure 4.6.3 Tumor bearing lungs of ADAM17<sup>wt/wt</sup> mice show activation of ERK kinase.** 200  $\mu$ g of protein lysate from the lung tissue from 7, 14 and 21 days after LLC cells injection in ADAM17<sup>wt/wt</sup> and ADAM17<sup>ex/ex</sup> mice was used for Immuno blot analysis. Antibodies against P-ERK1/2 and ERK1/2 were used (see the section 3.1.8) for Immunoblot analysis; **1w** -1 week, **2w** -2 weeks, **3w** -3 weeks, **ex/ex** -protein lysates from ADAM17<sup>ex/ex</sup> mice, **wt/wt** -protein lysates from ADAM17<sup>wt/wt</sup> mice, **ERK1/2** - extracellular-signal-regulated kinase, **P-ERK1/2** - phosphorylated extracellular-signal-regulated kinase.



## Results

Interestingly, tumorous parts of the lung tissue from wild type animals 21 days post LLC cells injection, revealed increased ERK phosphorylation, in wild type animals compared to hypomorphic animals.

To better understand which receptor tyrosine kinase was implicated in ERK activation, we performed a phospho-RTK antibody array (RTK array) (see the section 3.2.17).

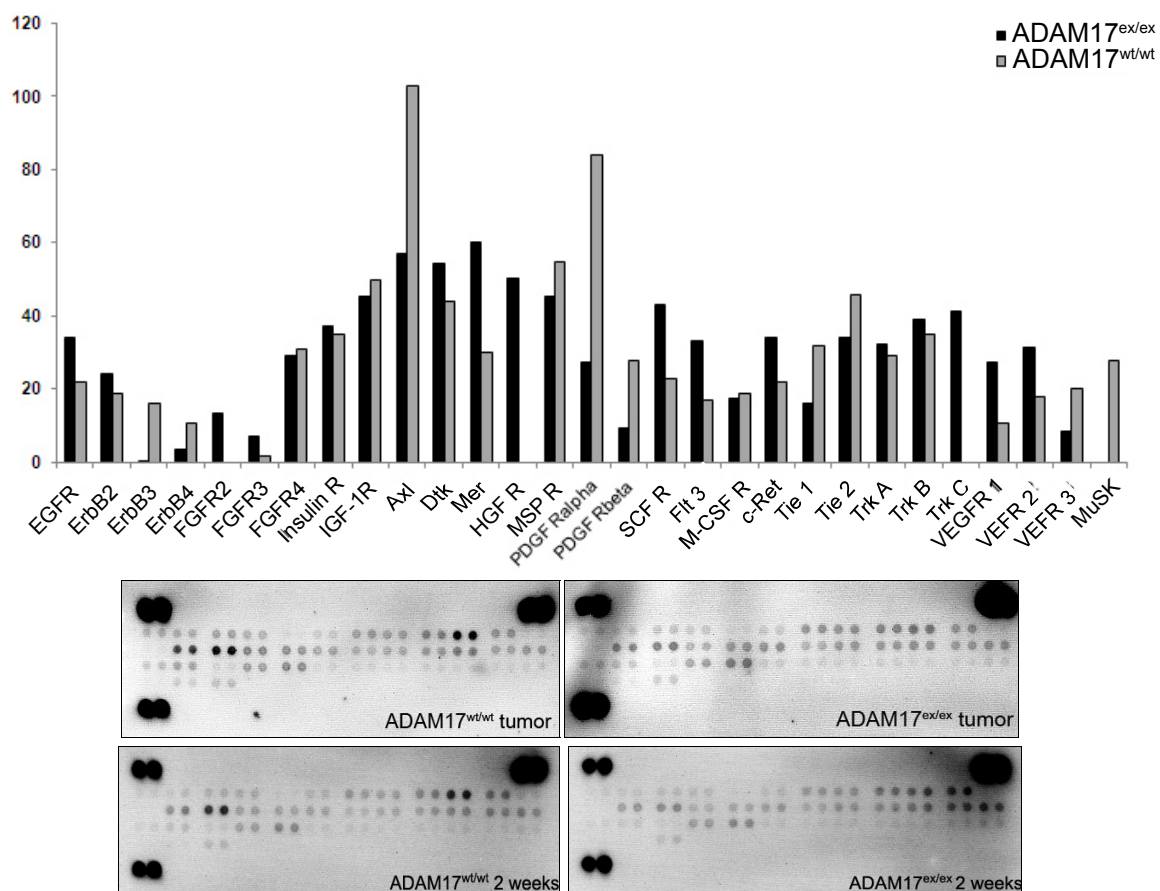


**Figure 4.6.4 Phospho-RTK antibody array from lung tissue of ADAM17<sup>wt/wt</sup> and ADAM17<sup>ex/ex</sup> mice 2 and 3 weeks post LLC cell injection.** 200µg of protein lysate was used for the Phospho-RTK array; quantification of receptor phosphorylation in the tumor lysates 3 weeks after LLC inoculation was measured by densitometry. (Quantification of receptor phosphorylation in the lysates 2 weeks after LLC inoculation not shown); **EGFR** - epidermal growth factor receptor, **FGFR 2** - fibroblast growth factor receptor 2, **FGFR 3** - fibroblast growth factor receptor 3, **Insulin R** - insulin receptor, **IGF-1R** - insulin-like growth factor receptor 1, **Axl** - Axl receptor tyrosine kinase, **Mer** - Proto-oncogene tyrosine-protein kinase MER, **HGF R** - hepatocyte growth factor receptor, **MSP R** - macrophage stimulating protein receptor, **PDGFR alpha** - platelet-derived growth factor receptor alpha, **PDGFR beta** - platelet-derived growth factor receptor beta, **SCFR** - stem cell factor receptor, **Flt3** - Fms-like tyrosine kinase 3, **M-CSF R** - macrophage colony stimulating factor receptor, **Tie1** - Tyrosine kinase with immunoglobulin-like and EGF-like domains 1, **Tie 2** - Tyrosine kinase with immunoglobulin-like and EGF-like domains 2, **Trk A** - neurotrophic tyrosine kinase receptor type 1, **Trk B** - neurotrophic tyrosine kinase receptor type 2, **Trk C** - neurotrophic tyrosine kinase receptor type 3, **VEGFR1** - vascular endothelial growth factor receptor 1, **VEGFR2** - vascular endothelial growth factor receptor 2, **VEGFR3** - vascular endothelial growth factor receptor 3, **MusK** - Muscle-Specific Kinase.



## Results

We used tumor lysates from animals 14 and 21 days post LLC injection for the phospho-RTK antibody array (Figure 4.6.4). We detected slight difference in the phosphorylation of ErbB3 and ErbB4, which belong to the EGFR family. However, the most striking differences in the phosphorylation of RTKs between ADAM17<sup>wt/wt</sup> and ADAM17<sup>ex/ex</sup> tumor bearing lungs were seen in PDGFR $\alpha$  and Axl. Phosphorylation of both RTKs was detectable 2 and 3 weeks post LLC injection.

Taken together, these data indicate that ADAM17 expression in the host tissue correlates with Axl, PDGFR- $\alpha$  and ErbB3/4 activation.

### 4.7 ADAM17 is required for Notch activation at early phases of metastasis

ADAM17 has been implicated in the shedding of Notch receptor ligand Jagged-1 (Lu et al, 2013). As soluble Jagged-1 can induce cancer stem cell (CSC) phenotype in disseminated cancer cells, we analyzed Notch activation in tumor bearing lungs of ADAM17<sup>wt/wt</sup> and ADAM17<sup>ex/ex</sup> mice at different time points. We were unable to detect Notch-1 ICD by Immunoblotting and immunohistochemistry (data not shown). However, we could see an upregulation of the Notch-target genes Hes1 and Hey1 20h and 7 days after LLC cell injection (Figures 4.7.1 and 4.7.2).

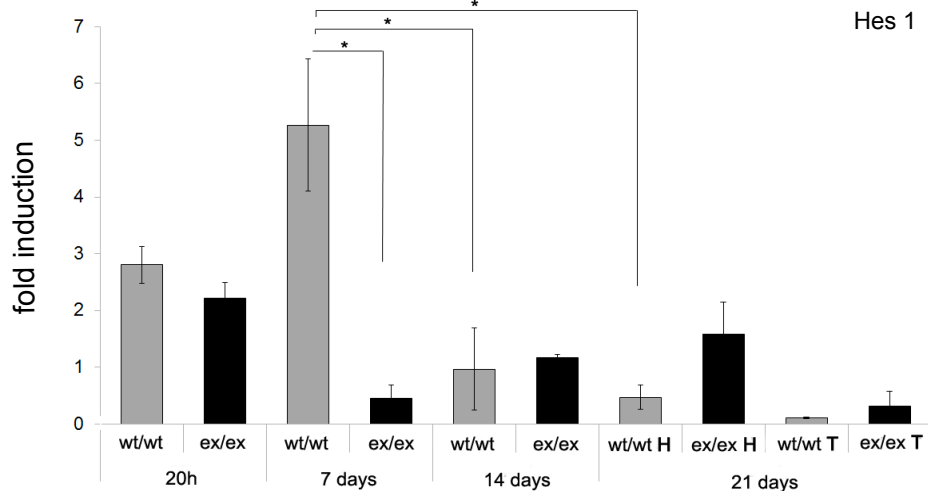


**Figure 4.7.1 ADAM17<sup>ex/ex</sup> mice show decreased activation of Notch signaling in an early phase of metastasis.** RNA was extracted from the lungs of ADAM17<sup>wt/wt</sup> (n=3) and ADAM17<sup>ex/ex</sup> (n=3) mice at indicated time points after LLC inoculation ( $5 \times 10^5$  cells per mouse). Real time PCR was performed and mRNA was quantified as above, the amounts in non-inoculated lungs from ADAM17<sup>wt/wt</sup> and ADAM17<sup>ex/ex</sup> mice were given value of 1.0 - basal level; **H** - healthy/non-tumorous part of the tissue, **T** - tumorous part of the tissue) **Hey 1** - Hairy/enhancer-of-split related YRPW motif like protein 1, Hes 1 - Hairy/Enhancer and Split 1. Data are represented as means  $\pm$  s.e.m. \*  $p < 0.05$ .

## Results

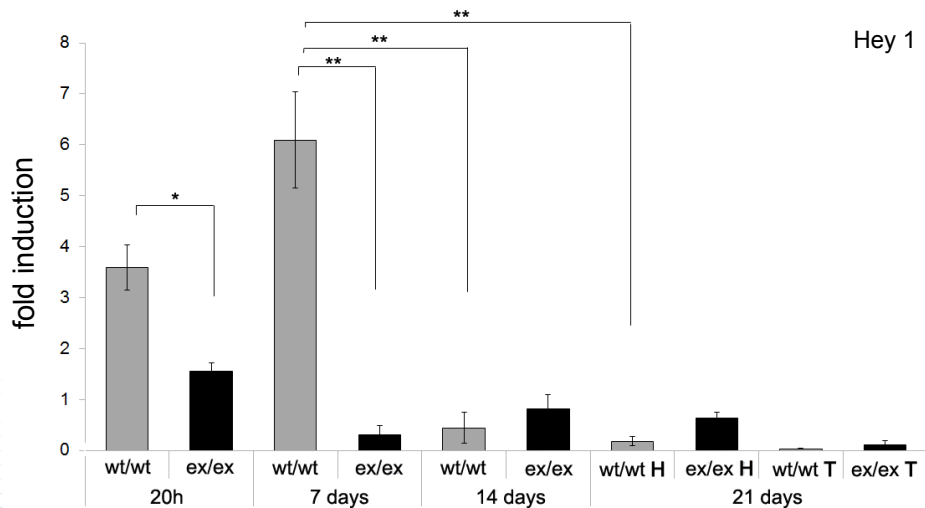


**Figure 4.7.2 ADAM17<sup>ex/ex</sup> mice show decreased activation of Notch signaling at early phase of metastasis.** RNA was extracted from the lungs of ADAM17<sup>wt/wt</sup> (n=3) and ADAM17<sup>ex/ex</sup> (n=3) mice at indicated time points after LLC inoculation (5x10<sup>5</sup> cells per mouse). Real time PCR was performed and mRNA was quantified as above, the amounts in non-inoculated lungs from ADAM17<sup>wt/wt</sup> and ADAM17<sup>ex/ex</sup> mice were given value of 1.0 - basal level; **H** - healthy/non-tumorous part of the tissue, **T** - tumorous part of the tissue) **Hey 1** - Hairy/enhancer-of-split related YRPW motif like protein 1, Hes 1 - Hairy/Enhancer and Split 1. Data are represented as means  $\pm$  s.e.m. \* p<0.05, \*\* p<0.005.

### 4.8 IL-6 trans-signaling does not promote lung metastasis

IL-6 can act via IL-6 classic and IL-6 trans-signaling. Binding of IL-6 to the membrane bound IL-6 receptor induces the recruitment of two gp130 molecules and downstream activation of intracellular signaling cascades. This process is marked IL-6 classic signaling. Binding of IL-6 to soluble IL-6R (sIL-6R) induces formation of IL-6/sIL-6R complex which can interact with gp130 molecule and induce its dimerization and downstream activation of intracellular signaling cascades. This process is marked IL-6 trans-signaling.

Interestingly, gp130 molecule exists in a soluble form (sgp130). sgp130 molecule is predominantly generated by alternative splicing. It can associate with the IL-6/sIL-6R complex and inhibit signaling via membrane bound gp130 (Montero-Julian, 2001; Mueller-Newen et al., 1998). Jostock and colleagues postulated that sgp130 molecule acts as a natural inhibitor of IL-6 trans-signaling (Jostock et al., 2001). Therefore, a designer protein, was generated by fusion of the Fc part of a human IgG to extracellular portion of gp130 molecule. The resulting protein, termed sgp130Fc, is a preformed homodimer and strongly resembles the endogenous receptor on the living cell. Interestingly, Becker and colleagues demonstrated that administration of sgp130Fc has tumor suppressor activity in colon cancer (Becker et al., 2004). Furthermore, Zhang and colleagues were able to show

## Results

that during severe acute pancreatitis (SAP) IL-6 trans-signaling promotes acute lung injury (ALI), as secondary effect of SAP (Zhang et al., 2013). They were able to reduce SAP induced ALI by administration of sgp130Fc protein. Symptoms of ALI very much resembled to symptoms of strong lung inflammation characteristic for initial phases of lung metastasis.

We hypothesized that inhibition of IL-6 trans-signaling could decrease the inflammatory response and delay metastasis progression in LLC model of experimental metastasis. To test this hypothesis, we used sgp130Fc transgenic mice, which express sgp130Fc under the control of the liver-specific PEPCK (phosphoenolpyruvate carboxykinase) promoter. However, sgp130Fc protein is distributed via the bloodstream to all organs except the brain (Rabe et al, 2008). Lung metastasis was induced via i.v. injection of LLC cells in sgp130Fc and control, C57Bl6/N mice. Lung and liver tissues were analyzed 21 days post LLC injection (Figure 4.8.1).

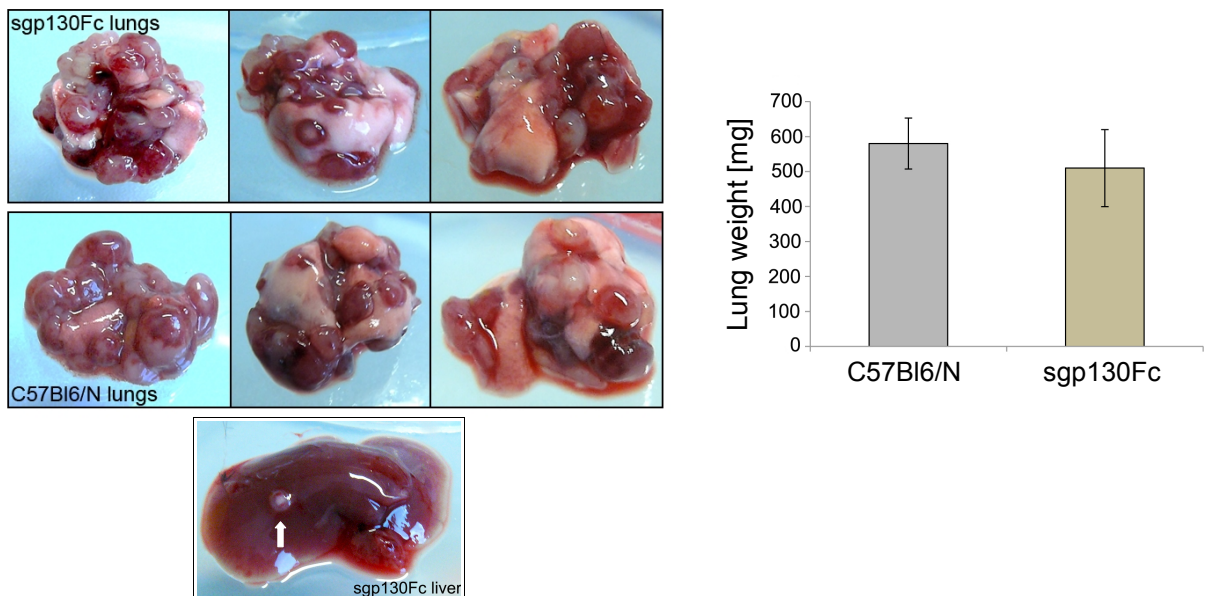


**Figure 4.8.1 Experimental metastasis with LLC cells in sgp130Fc and C57Bl6/N mice.** Lungs of sgp130Fc (n=3) and C57Bl6/N (n=3) mice 21 days after LLC inoculation with  $5 \times 10^5$  LLC cells per mouse. Liver metastasis in one sgp130Fc mouse is indicated with white arrow. Data are represented as means  $\pm$  s.e.m.

21 days after LLC cells inoculation, we did not detect any difference in lung appearance and tumor burden in sgp130Fc and C57Bl6/N mice. Total lung weight was 3 times above the average lung weight, with no significant difference between sgp130Fc and C57Bl6/N

## Results

mice. Metastasis to the liver appeared only in one sgp130Fc mouse (Figure 4.8.2 – sgp130Fc liver).

We performed immunohistochemical stainings from tumor bearing lungs of sgp130Fc and C57Bl6/N mice (Figure 4.8.2).

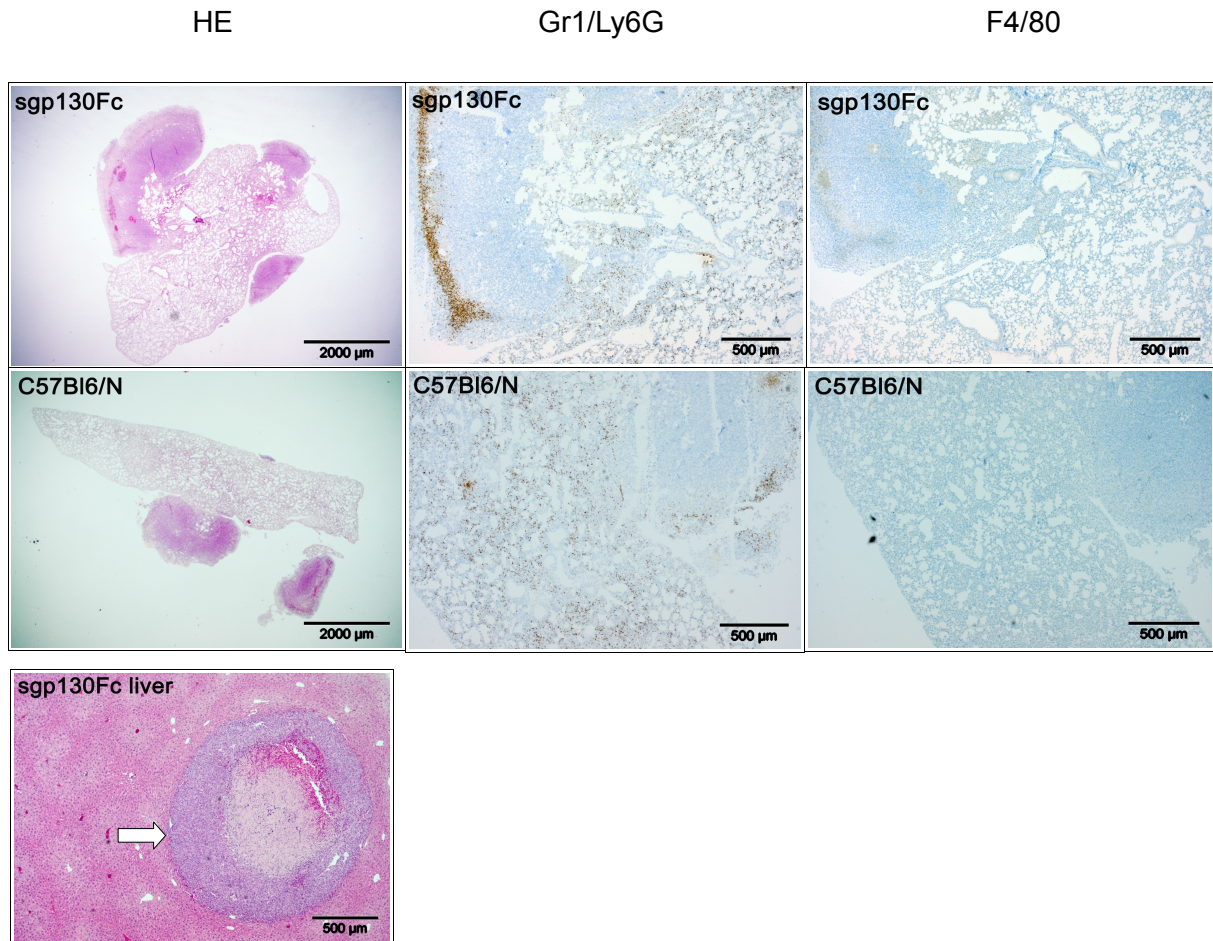


**Figure 4.8.2 sgp130Fc and C57Bl6/N mice show same tumor burden.** Immunohistological stainings of lung tissue from sgp130Fc and C57Bl6/N tumor bearing lungs 21 days after LLC inoculation; **HE** - haematoxylin and eosin staining, **Ly6G** - staining for granulocytes, **F4/80** - staining for macrophages white arrow indicate liver tumor of sgp130Fc mice; **sgp130Fc liver** - HE stainings of liver metastasis in sgp130Fc mice.

From immunohistochemical stainings we concluded that there was no difference in the level of lung damage between sgp130Fc and control mice. We were able to detect strong infiltration of Ly6G/Gr1<sup>+</sup> myeloid cells in both sgp130Fc and C57Bl6/N lung tissue. We could not detect F4/80<sup>+</sup> cells in both mice groups.

According to these data we can conclude that sgp130Fc does not play a protective role in lung metastasis.



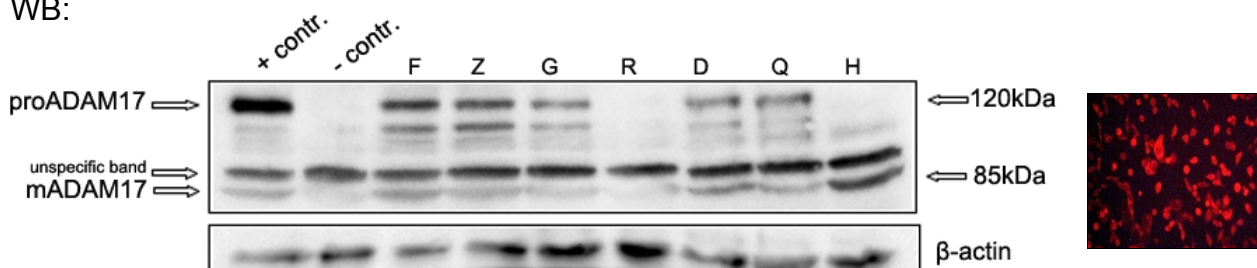
## Results

### 4.9 ADAM17 in tumor cells contributes to tumor cell growth *in vitro* and metastatic growth *in vivo*

In the model of experimental metastasis with LLC cells we could demonstrate the importance of ADAM17 in the stroma for metastatic progression and spread. Next, we were interested whether ADAM17 in the tumor cells was equally important for metastatic growth. To test this assumption, we generated LLC cells with a stable ADAM17 knock down (kdADAM17-LLC) by lentiviral transduction (see the sections 3.2.2 and 3.2.3). The lentiviral vector, termed sh17-pLeGO-C/BSD, contained, as well, a cassette coding for the fluorescent protein mCherry (the 'm' in the name denotes its monomer configuration). mCherry is a monomeric fluorescent protein with peak absorption/emission at 587 nm and 610 nm, respectively. It matures quickly, within 15 minutes, allowing it to be visualized soon after translation.

After LLC cell transduction, we selected single cell clones, positive for mCherry expression, expanded and tested them for ADAM17 protein and mRNA expression by Immunoblotting (WB) and RT-PCR, respectively (Figures 4.9.1).

WB:



RT-PCR:

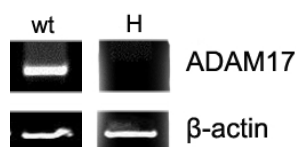


**Figure 4.9.1 ADAM17 protein and mRNA expression in different kdADAM17-LLC clones.**  $10^6$  kdADAM17LLC cells were seeded into 6 well plates in DMEM supplemented with 10% FCS. After 24h mCherry protein expression was observed and photographed under fluorescent microscope (red cells in the upper right picture panel) and cells were lysed. After 24h RNA from kdADAM17-LLC cells, clone H, was isolated and RT-PCR for ADAM17 and  $\beta$ -actin was performed. SDS-polyacrylamide gel electrophoresis from the cell lysates was performed on 8% gel. Immuno-blot was performed with anti-ADAM17 antibody; **+ contr.** - lysate of  $10^6$  ADAM17 wild type cells used as a positive control, **- contr.** - lysate of  $10^6$  ADAM17 knock down colon cancer cells (kdADAM17-CMT93) used as a negative control, **proADAM17** - ADAM17 with pro-domain, **mADAM17** - mature ADAM17, **wt** - wild type LLC cells, **F, Z, R, D, Q, H, G** - different clones of kdADAM17-LLCs.

## Results

From the Immunoblot analysis we could conclude that clones R and H did not express pro-ADAM17, while only clone H, but not clone R, expressed mature ADAM17. Both kdADAM17-LLC cell clones had significantly reduced proliferation rate compared to wild type LLC cells (data not presented for the clone R). Interestingly, clone R grew less efficiently than clone H. Therefore, we decided to use the clone H for further experiments.

Proliferation of unstimulated kdADAM17-LLC cells was significantly reduced compared to unstimulated wild type LLC cells (wtLLC). Proliferation rates were significantly different already in the first 24h (Figure 4.9.3). We observed that the difference in proliferation was increasing over time. From this experiment we could conclude that ADAM17 in the tumor cells is necessary for tumor cell growth.

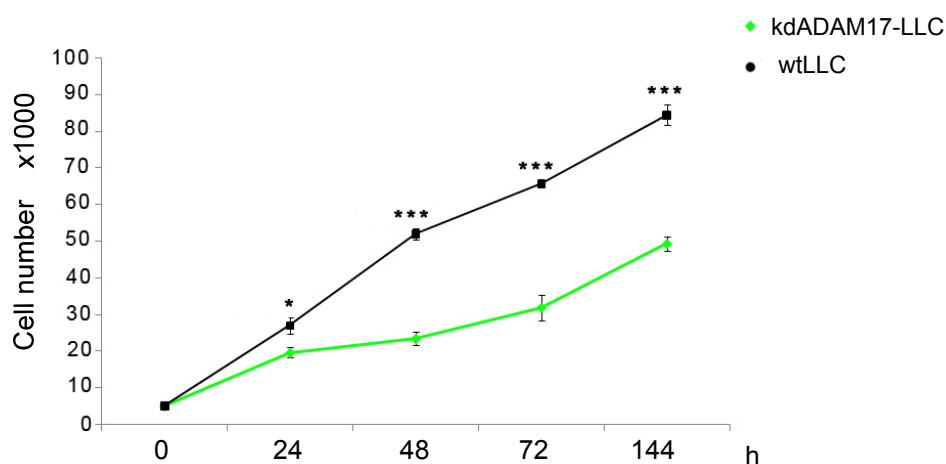


**Figure 4.9.2 kdADAM17-LLC cells grow significantly slower than wild type LLC cells.**  $5 \times 10^5$  cells per well were seeded into 6 well plates in DMEM supplemented with 10% FCS and P/S; cells were cultured for 144h; number of cells was analyzed 24h, 48h, 72h and 144h after seeded. Each measurement was performed in triplicate. Data are represented as means  $\pm$  s.e.m. \*  $p < 0.05$ , \*\*\*  $p < 0.001$ .

In preliminary experiments, we analyzed the potential of kdADAM17-LLC cell to induce lung metastasis *in vivo*. kdADAM17-LLC cells were injected i.v. via tail vein into C57Bl6/N mice and the lung tissue was analyzed 21 days post injection (Figure 4.9.4). As a control for successful i.v. injection, we injected wtLLC cells into C57Bl6/N mice.

## Results

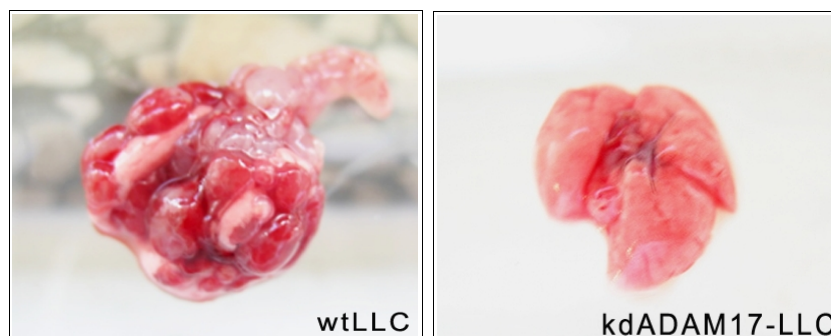


**Figure 4.9.3 ADAM17 in tumor cells is necessary for metastatic growth *in vivo*.**  $5 \times 10^5$  kdADAM17-LLC or wtLLC cells per mouse were injected in C57NI6/N mice; 3 mice per each group were used; lungs were excised and photographed 21 days after cells inoculation; mice within the same group displayed an equal effect in lung metastases, therefore from each group, lung picture from a single mouse is presented here; **wtLLC** – C57BI6/N mice injected with wild type LLC cells, **kdADAM17-LLC** – C57BI6.N mice injected with kdADAM17-LLC cells.

We could show that lacking of ADAM17 in the tumor cells resulted in null development of lung metastasis. This was reflected in a significant difference in a total lung weight (Table 4.9.1) between C57BI6/N mice injected with wtLLC and kdADAM17-LLC cells (clone H).

Mouse	Lung weight [mg]
C57BI6/N 1 with kdADAM17-LLC	180
C57BI6/N 2 with kdADAM17-LLC	200
C57BI6/N 3 with kdADAM17-LLC	190
C57BI6/N 1 with wtLLC	480
C57BI6/N 2 with wtLLC	520
C57BI6/N 3 with wtLLC	570

**Table 4.9.1 Lung weight of C57BI6/N mice 3 weeks after injection of wild type or kdADAM17-LLC cells.**  $5 \times 10^5$  cells were injected via the tail vein into C57BI6/N mice. 21 days post tumor cells injection lungs were excised and measured.

We were able to detect the presence of kdADAM17-LLC cells in the tumor bearing lungs, performing RT-PCR for the expression of mCherry mRNA (Figure 4.9.4).

## Results

---

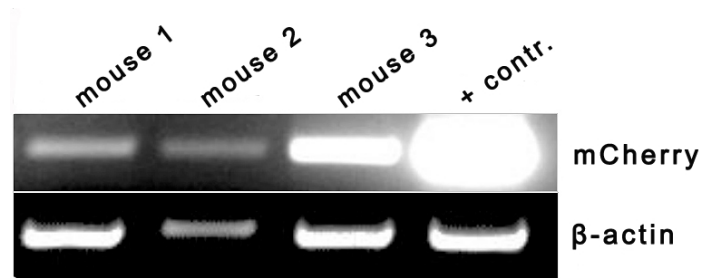


**Figure 4.9.4 mRNA expression of mCherry in the lungs of C57Bl6/N mice injected with kdADAM17-LLC cells.** RNA was extracted from the whole lung tissue of 3 different C57Bl6/N mice (mouse 1, 2, 3) injected with kdADAM17-LLC cells 21 days post injection. Semiquantitative RT-PCR was performed for the expression of mCherry protein; **+ *contr.*** - RNA from kdADAM17-LLC cells.



### 5 Discussion

#### 5.1 ADAM17 in model of experimental metastasis

In the present study we used a murine model of experimental metastasis to investigate the role of ADAM17 in metastatic progression. We used ADAM17 hypomorphic mice (ADAM17<sup>ex/ex</sup>) which express barely detectable level of ADAM17 protein (Chalaris et al., 2010), thus mimicking the condition where ADAM17 is inhibited in the host. To induce lung metastasis we injected LLC lung carcinoma or B16F1 melanoma cells through the tail vein.

We were able to show that three weeks after inoculation with LLC or B16F1 cells, ADAM17<sup>wt/wt</sup> animals displayed a significantly higher number of macroscopical tumors in the lungs than ADAM17<sup>ex/ex</sup> animals, independent of the tumor entity. Furthermore, lung weight of control mice was significantly increased while the lung weight of ADAM17<sup>ex/ex</sup> hypomorphic mice was in the normal range of 200±50 mg. In the case of B16F1 injection, all control animals had multiple liver and kidney metastasis, while 67% of hypomorphic animals had single liver and no kidney metastasis.

A remarkable difference was seen in the survival rate of ADAM17<sup>ex/ex</sup> mice compared to ADAM17<sup>wt/wt</sup> mice within an observed time of 43 days after LLC cell inoculation. All ADAM17<sup>ex/ex</sup> mice were alive, while 80% of wild type mice died in this time period.

Our results indicate that ADAM17 in the metastatic niche plays an important role for metastatic progression via proliferatory, inflammatory and immunosuppressive stimuli (Figure 5.1).

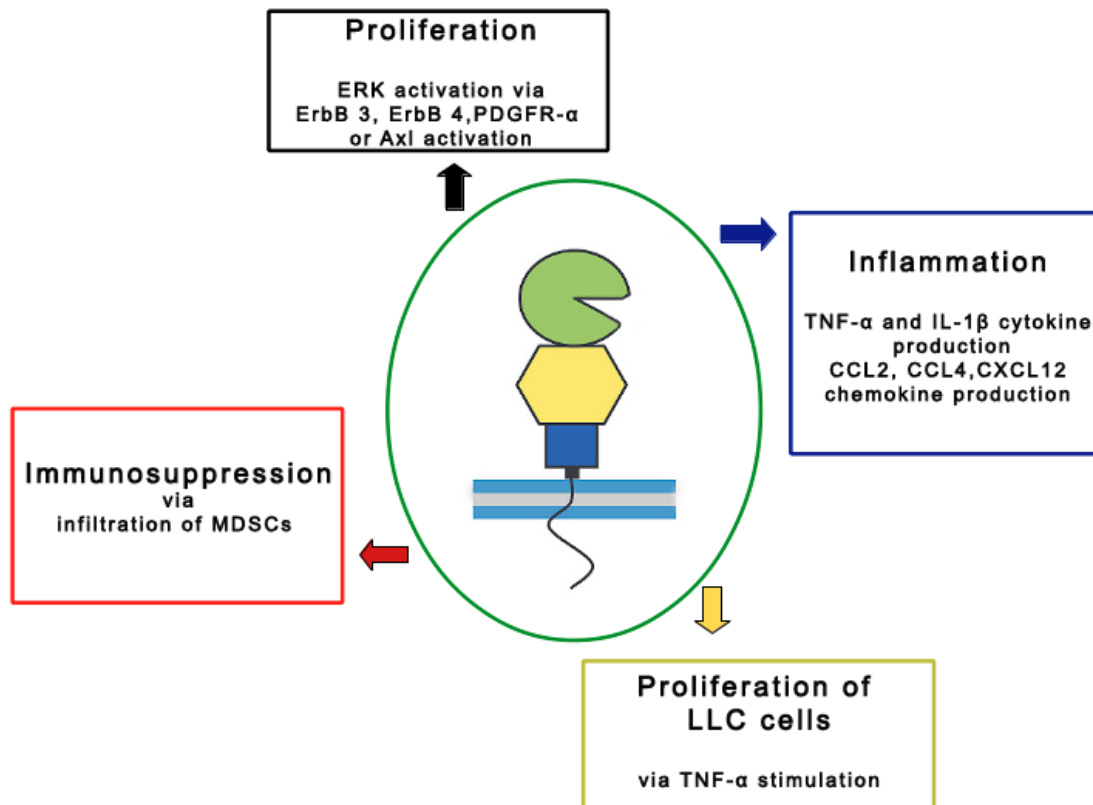


**Figure 5.1 ADAM17 contribution to lung metastasis.** ADAM17 in the metastatic niche plays a crucial role for progression of lung metastasis. It influences inflammatory and proliferatory signals via shedding of different substrates. Shedding of TNF- $\alpha$  induces early inflammatory response and transcription of chemokines necessary for myeloid cell infiltration. At early phases of lung metastasis increased amount of TNF- $\alpha$  can influence LLC cell proliferation, as well. Infiltration of myeloid cells (MDSCs) leads to immunosuppression. ADAM17 sheds growth factors implicated in RTK EGF family activation, thus contributing to cell proliferation and survival. Cartoon of ADAM17 was taken from Scheller et al., 2011.

## 5.2. ADAM17 in the metastatic niche is important for inflammatory signals

We were able to demonstrate by quantitative real time PCR from whole lung tissue that TNF- $\alpha$  and IL-1 $\beta$  are the major inflammatory mediators responsible for the induction of lung damage in early stages of metastasis. qRT-PCR analysis of genes implicated in inflammatory response clearly demonstrated significant upregulation, even up to 10 times, of TNF- $\alpha$  and IL-1 $\beta$  in ADAM17<sup>wt/wt</sup> compared to ADAM17<sup>ex/ex</sup> mice. The strongest difference in TNF- $\alpha$  mRNA expression was 20h and 7 days post LLC cell injection, with tendency to decrease almost to a basal level in later time points. Interestingly, we could demonstrate that soluble TNF- $\alpha$  (sTNF- $\alpha$ ) derives from myeloid cells *in vitro*.

## Discussion

---

Bone marrow derived macrophages (BMDM) produced TNF- $\alpha$  upon stimulation with conditioned medium of LLC cells. BMDMs from ADAM17<sup>wt/wt</sup> mice produced 50 times more sTNF- $\alpha$  than BMDMs from ADAM17<sup>ex/ex</sup> mice. However, we were not able to detect macrophages stained against F4/80 antigen in lung tissue sections in all four time points. Surprisingly, we could detect cells positive for Ly6G/Gr1 antigen in immunohistological analysis from all time points.

Thus, we hypothesized, that bone marrow derived granulocytes/neutrophils (BMDN) might be the source of TNF- $\alpha$  in tumor bearing lungs. Stimulation of BMDNs with LLC conditioned medium resulted in the production of TNF- $\alpha$ . Interestingly, BMDNs from ADAM17<sup>wt/wt</sup> mice produced 4 times more sTNF- $\alpha$  than BMDMs when stimulated with the same conditioned medium. At the same time, BMDNs from ADAM17<sup>wt/wt</sup> mice produced 4 times more sTNF- $\alpha$  than BMDNs from ADAM17<sup>ex/ex</sup> mice. Our data demonstrated that the generation of sTNF- $\alpha$  by ADAM17 from the surface of wild type BMDNs was efficiently blocked (~90%) by combined ADAM10 and ADAM17 inhibitor, GW280264X, while the ADAM10 specific inhibitor, GI254023X, was not as efficient in blocking of TNF- $\alpha$  shedding (~30%).

Interestingly, the group of M. Karin identified TNF- $\alpha$  as a major inducer of metastasis progression in a model of experimental metastasis with LLC cells (Kim et al., 2009). They could show that TNF- $\alpha$ <sup>-/-</sup> mice had increased survival rate, less tumors and reduced infiltration of myeloid cells into the lungs. However, ADAM17<sup>ex/ex</sup> mice display even higher protection rate than TNF- $\alpha$ <sup>-/-</sup> mice. Nevertheless, they excluded IL-6, as inducer of inflammation and proliferation in metastasis in this model. Using IL-6<sup>-/-</sup> mice they demonstrated that metastasis progression was not delayed or reduced, but it was the same like in control mice. As well, they demonstrated that LLC cells, among several types of cancer cells, were the most potent activators of macrophages for TNF- $\alpha$  and IL-6 production.

Our results indicate that sTNF- $\alpha$  in our metastasis model was mainly generated by infiltrated myeloid cells. We hypothesized that abrogation of TNF- $\alpha$  shedding from the surface of myeloid cells by ADAM17 would lead to reduced inflammation and subsequently reduced metastasis progression. To validate this hypothesis, we will use a model of experimental metastasis with LLC cells in ADAM17-LysM-Cre conditional knock out mice,

## Discussion

---

which lack ADAM17 in myeloid cells.

During tumor development, myeloid cells are recruited and can be converted into potent immunosuppressive cells. Immature myeloid cells with the same phenotype as immunosuppressive cells are generated in the bone marrow of healthy individuals and differentiated into mature myeloid cells without causing any kind of immunosuppression. However, in a cancerous state, myeloid cells are differentiated into pathological myeloid derived suppressor cells (MDSCs) which can suppress the host anti-tumor immune response. Human granulocytic MDSCs isolated from peripheral blood of patients suffering from breast, colon or lung cancer were indicators of poor prognosis (Greten et al., 2011).

Following tumor progression through 14 and 21 days post LLC cell inoculation, we were able to detect an increase in the number of Ly6G/Gr1<sup>+</sup> cells in immunohistological staining from tumor bearing lungs of both ADAM17<sup>wt/wt</sup> and ADAM17<sup>ex/ex</sup> animals. We were able to see the same effect in Ly6G/Gr1<sup>+</sup> cell infiltration in the tumor bearing lungs of ADAM17<sup>wt/wt</sup> and ADAM17<sup>ex/ex</sup> animals 21 days after inoculation with B16F1 melanoma cells. Tumor bearing lungs of ADAM17<sup>wt/wt</sup> mice had stronger infiltration of granulocytic MDSCs characterized with CD11b<sup>+</sup>Ly6G/Gr1<sup>+</sup>F4/80<sup>-</sup>CD11c<sup>-</sup> phenotype (Youn et al., 2008), than tumor bearing lungs of ADAM17<sup>ex/ex</sup> mice.

ADAM17 has been shown to have an important role in immunosuppression of T-cells by MDSCs. Namely, ADAM17 on the surface of MDSCs can cleave L-selectin (CD62L) on the surface of naïve CD4<sup>+</sup> and CD8<sup>+</sup> T-cells in the tumor (Hanson, 2009). Shedding of L-selectin from the surface of naïve CD4<sup>+</sup> and CD8<sup>+</sup> T-cells disables recirculation of T cells to the lymph nodes, thus reducing host immune response against the tumor. Unfortunately, until now we did not determine the presence of CD4<sup>+</sup> and CD8<sup>+</sup> T-cells in the tumor bearing lungs of ADAM17<sup>wt/wt</sup> and ADAM17<sup>ex/ex</sup> mice. We hypothesized that immunosuppression is much stronger in tumor bearing lungs of ADAM17<sup>wt/wt</sup> than in ADAM17<sup>ex/ex</sup> mice. Therefore, we assume that hypomorphic mice should have significantly higher number of CD4<sup>+</sup> and CD8<sup>+</sup> T-cells in tumor bearing lungs than wild type mice.

To better understand the mechanism of myeloid cells attraction into tumor bearing lungs, we performed quantitative real time PCR for mRNA expression of different chemokines

## Discussion

---

at all time points post LLC cell injection. We found increased transcription of the inflammatory chemokine CCL4/MIP-1 $\beta$  only 20h after LLC inoculation in whole lung tissue from ADAM17<sup>wt/wt</sup> mice. Expression of CCL4/MIP-1 $\beta$  in ADAM17<sup>ex/ex</sup> lung tissue was on a basal level through all four time points. Interestingly, our data correlated with previously published data that over-expression of IL-1 $\beta$  can induce production of CCL4/MIP-1 $\beta$  (Zhang et al., 2003). We could demonstrate that IL-1 $\beta$  mRNA expression was significantly upregulated in tumor bearing lungs of ADAM17<sup>wt/wt</sup> mice in all time points peaking 7 days post injection. Interestingly, IL-1 $\beta$  can be induced by TNF- $\alpha$ . We were able to detect an increased expression of TNF- $\alpha$  as early as 20h after LLC cell injection in wild type animals. We can hypothesize that sTNF- $\alpha$ , generated by ADAM17 shedding, induces IL-1 $\beta$  expression thus indirectly contributing to CCL4/MIP-1 $\beta$  production. CCL4/MIP-1 $\beta$  chemokine is important for T-cell infiltration.

It is possible that secretion of TNF- $\alpha$  and IL-1 $\beta$  early after tumor cell extravasation induces expression of CXCL2/MIP-2 resulting in attraction of myeloid cells to the lungs. CXCL2/MIP-2 is a very potent neutrophil chemoattractant, and it has been correlated with infiltration of neutrophils before, in a model of acute lung injury induced by LPS (Gupta et al., 1996).

One of the factors implicated in attraction, expansion and activation of MDSCs in cancer is CCL2/MCP-1. Isolating RNA from the whole lung tissue of ADAM17<sup>wt/wt</sup> and ADAM17<sup>ex/ex</sup> mice from all time points post injection, we were able to demonstrate an upregulation of CCL2/MCP-1 gene expression in control mice. Significant differences in the expression of CCL2/MCP-1 gene in ADAM17<sup>wt/wt</sup> and ADAM17<sup>ex/ex</sup> mice appeared 20h post LLC injection, peaking after 14 days and sustaining until the final stage of metastasis. The expression of CCL2/MCP-1 remained unchanged through all time points in ADAM17<sup>ex/ex</sup> mice. 20h post LLC cell injection CCL2/MCP-1 was 15 times more expressed in tumor bearing lungs than in the untreated lungs of ADAM17<sup>wt/wt</sup> mice. Finally, we wanted to ascertain that upregulation of CCL2/MCP-1 gene expression lead to increased CCL2/MCP-1 protein production. We were able to confirm that protein expression from whole lung tissue of ADAM17<sup>wt/wt</sup> mice was significantly increased compared to ADAM17<sup>ex/ex</sup> mice in the final stage of metastasis. Furthermore, we were able to show that produced CCL2/MCP-1 mainly derived from tumor cells. This finding supported already published data

## Discussion

---

(Sawanobori et al., 2008).

High CCL2/MCP-1 serum levels in breast cancer patients correlated with disease progression and poor prognosis (Soria et al., 2008). Soria and colleagues demonstrated that MDSCs are recruited to the tumor via CCL2/CCR2 pathway (Huang et al., 2007). They isolated cancerous tissue from patients suffering from breast, ovarian or gastric cancer and demonstrated that migration of MDSCs was depended of CCL2/CCR2 pathway. Namely, they used a transwell apparatus where they placed tumor samples from patients in a lower chamber, and MDSCs isolated from the same patients blood in upper chamber. They could show significant reduction in transmigration of MDSCs towards tumorous tissue when anti-CCL2 or anti-CCR2 antibody was used. Interestingly, production of CCL2/MCP-1 was already recognized in murine tumor models where LLC and B16F1 cells were used (Gabrilovich et al., 2009).

Our data demonstrate that ADAM17 plays an important role for the infiltration of immunosuppressive myeloid cells to tumor bearing lungs initially via CXCL2/MIP-2 and in later stages via CCL2/MCP-1 chemokine production. This supports already published data that CCL2/MCP-1, which derives from the tumor cells, has implication in MDSC infiltration in later stages of cancer development (Huang et al., 2007).

Since CCL2/MCP-1 mainly derived from cancer cells, we hypothesize that the difference in CCL2/MCP-1 expression between ADAM17<sup>wt/wt</sup> and ADAM17<sup>ex/ex</sup> mice correlates with the different number of tumor cells in the lungs. The difference in tumor cell number could be explained by a different ability of tumor cells to extravasate into the lung tissue. In endothelial and epithelial cell junctions, a variety of proteins are involved. JAM-A is located at tight endothelial and epithelial junctions and it has been shown to be a substrate of ADAM17 (Dreymueller et al., 2012). When it is shed, like in ADAM17<sup>wt/wt</sup> animals, the extravasation of tumor cells can be unimpeded and when JAM-A is not shed, potentially like in ADAM17<sup>ex/ex</sup> animals, extravasation of tumor cells can be reduced. To validate this hypothesis, we will use a model of experimental metastasis with mCherry-LLC cells. mCherry-LLC cells are LLC cells stably transduced with an empty vector containing a cassette coding for the fluorescent protein mCherry. Since we were successful in tracing the mCherry labeled kdADAM17-LLC cells via RT-PCR (section 4.9), we want to use this

method to investigate is tumor cells extravasation altered in ADAM17<sup>ex/ex</sup> mice.

### 5.3 ADAM17 enhances metastatic progression via proliferatory stimuli

We were able to detect significantly higher number of PCNA<sup>+</sup> cells in tumor bearing lungs of ADAM17<sup>wt/wt</sup> than ADAM17<sup>ex/ex</sup> animals. PCNA<sup>+</sup> areas in the lung tissue were mainly tumorous areas, while the surrounding tissue was less proliferating. In the line of these findings, we could detect an increased phosphorylation of ERK1/2 kinase 21 days after injection. Impressive difference in activation of ERK1/2 kinase between ADAM17<sup>wt/wt</sup> and ADAM17<sup>ex/ex</sup> mice was mainly in the tumorous part of the lung tissue. Interestingly, we were not able to detect any phosphorylation of ERK1/2 kinase in tumor lysates from hypomorphic mice. To better understand from which signaling pathway such significant difference derived, we tested tumor lysates from 2 and 3 weeks injected mice for phosphorylation of different receptor tyrosine kinases using a Phospho-RTK antibody array. We could detect increased phosphorylation of PDGFR- $\alpha$  and Axl in tumor samples of ADAM17<sup>wt/wt</sup> compared to ADAM17<sup>ex/ex</sup> mice.

PDGFR- $\alpha$  and PDGFR- $\beta$  are receptor tyrosine kinases highly implicated in tumor development and metastasis. They have been implicated in lymphangiogenesis, alteration in tumor vasculature and interactions between metastatic microenvironment and malignant cells (Oestman et al., 2007). In a recent study Rikova and colleagues identified PDGFR- $\alpha$  to be highly activated in NSCLC (Rikova et al., 2007). The group of C. Blobel could demonstrate that activation of the PDGFR- $\beta$  induced ADAM17 activity and increased shedding of TNF- $\alpha$  and TGF- $\alpha$  from the cell surface (Mendelson et al., 2010).

Axl belongs to the **TAM** family (**T**yro3, **A**xl and **M**ertk) of receptor tyrosine kinases. It is a transmembrane protein, which is activated upon interaction with its ligand - growth arrest-specific protein 6 (Gas6). It regulates cell survival, growth and migration thus influencing tumorigenesis (Linger et al., 2008). Interestingly, Axl can influence proliferation via activation of Ras/MAPK pathway upon Gas6 stimulation (Fridell et al., 1996) or expression of anti-apoptotic factors Bcl-XL and Bcl-2 via NF- $\kappa$ B activation (Demarchi et al., 2001). Namely, Gas6 stimulation can increase I $\kappa$ B degradation, thus releasing NF- $\kappa$ B and allowing its translocation to the nucleus where it act as a transcription factor. Increase of Axl activity and its over-expression is common in many pathological conditions,

## Discussion

---

mainly in cancer (Linger et al., 2010). Inhibition of Axl signaling downregulates expression of pro-inflammatory cytokines, which are important mediators of tumor metastasis (Holland et al., 2010).

Taking into consideration that tumors of ADAM17<sup>wt/wt</sup> mice have sustained inflammatory status which is reflected in TNF- $\alpha$  production and NF- $\kappa$ B activation, we can hypothesize that synergistic effect of Axl and TNF- $\alpha$  in activation of NF- $\kappa$ B in tumors of ADAM17<sup>wt/wt</sup> mice can lead to stronger inflammatory stimuli, thus to increased infiltration of myeloid cells and poor prognosis.

A strong correlation between high EGFR activity and high ADAM17 levels in breast tumors was reported (Borrell-Pages et al., 2003). Interestingly, we did not see expected significant difference in phosphorylation of EGFR between ADAM17<sup>wt/wt</sup> and ADAM17<sup>ex/ex</sup> mice. However, we could notice a slight difference in phosphorylation of ErbB3 and ErbB4 in tumor lysates of 3 weeks injected mice by Phospho-RTK antibody array.

Performing quantitative real time PCR, we were able to show that target genes of Notch signaling, Hes 1 and Hey 1, were upregulated in the whole lung tissue as early as 20h post LLC injection, peaking 7 days and at later time points decreasing to a basal level. We noticed a significant difference in the expression of these genes in tumor bearing lungs between ADAM17<sup>wt/wt</sup> and ADAM17<sup>ex/ex</sup> animals. Hypomorphic mice displayed an upregulation of transcription of Notch target genes only at the earliest time point, and just 2 times higher than the basal level with relapse to normal at later time points. Control mice had 3-4 times higher expression of both genes compared to untreated mice (basal level) 20h after LLC inoculation. Maximum of the Hes 1 and Hey 1 expression was measured 7 days post injection with relapse to basal level at later time points. This implied that ADAM17 was implicated in Notch activation shortly after tumor cell injection. We assume that Notch is activated within the cancer cells. Because of the lack of ADAM17 activity in hypomorphic mice, endothelial cells might be incapable to release a soluble Jagged-1, therefore impairing cancer stem cell formation. However, analysis of cancer stem cells in our model is still ongoing.



## Discussion

---

It is known that Notch signaling has a multiple role in lung development, repair and cancer. Notch promotes proximal cell fate in early lung development, it coordinates alveolar formation via cell fate specification and cell differentiation in the parenchyma and vascular compartments. Knock-out studies for Notch-1, Notch-2, and the Notch ligands Jagged-1 and DLL-1 clearly demonstrate how important Notch signaling is for embryonic development, since these mutants die in an early embryonic stage. During development and progression of lung cancer, Notch signaling has a prominent role. In 30% of human lung cancers expression of the Notch inhibitor Numb is reduced, which was linked to a poor prognosis (Westhoff et al., 2009). Also, Notch receptor signaling was analyzed in different lung cancer cell lines under hypoxic conditions, thus mimicking the surrounding in tumors. It was found that Notch-1 signaling was increased under hypoxic conditions and that it was imperative for cancer cell survival (Chen et al., 2007). Interestingly, under conditions of severe hypoxia, ADAM17 expression and activation was upregulated (Ryzmski et al., 2012). Ryzmski and colleagues could demonstrate that hypoxia inducible factor-1 alpha (HIF-1 $\alpha$ ) was important to maintain basal levels of ADAM17 mRNA under hypoxic conditions. Additionally, proteolytic release of Jagged-1 from endothelial cells by ADAM17 has been shown to be important for the transformation of colorectal cancer cells into cancer stem cells (Lu et al., 2013). Collectively, these findings point out the complexity and significance of Notch signaling, both for the host and for cancer cells, and the possible implication of ADAM17 in Notch activation.

Interestingly, in some cases activation of NF- $\kappa$ B signaling can support proliferatory signals. Therefore, we tested the influence of TNF- $\alpha$  on proliferation of LLC cells. Wild type LLC cells were treated for 144h with different concentrations of rm TNF- $\alpha$ . 24h after TNF- $\alpha$  stimulation, all stimulated LLC cells had a significantly higher proliferation rate than unstimulated cells. 48h after TNF- $\alpha$  stimulation, there was no difference in the proliferation rate between TNF- $\alpha$  stimulated and unstimulated LLC cells.

From these data we can conclude that TNF- $\alpha$  can be a proliferatory stimulus for cancer cells at very early stages of metastasis.

### **5.4 IL-6 trans-signaling does not play a protective role in LLC induced lung metastasis**

In previous publications IL-6 classic and trans-signaling have been correlated with

tumorigenesis (Bollrath et al., 2009). Elevated level of IL-6 in patients suffering from lung and breast cancer, was strongly correlated with a poor prognosis (Qu et al., 2009). Interestingly, patients who suffer from severe acute pancreatitis (SAP) as a secondary effect of disease develop acute lung injury (ALI) which much resembles the inflammatory state in lung cancer. Zhang and colleagues, using sgp130Fc transgenic mice, could determine the underlying molecular mechanism in ALI development (Zhang et al., 2013). They demonstrated that blocking IL-6 trans-signaling increased survival rate via reduction of ALI in a mouse model of SAP. Using IL-6<sup>-/-</sup> mice, in a situation where IL-6 signaling is completely blocked, progression of disease was even enhanced. These data suggested that protective signals derive from classic IL-6 pathway, while disease stimulatory signals derived from IL-6 trans-signaling.

Using sgp130Fc mice in our model of experimental metastasis with LLC cells we were able to show that blocking IL-6 trans-signaling did not have a beneficial effect on tumor metastasis. Both mice groups displayed same the tumor development and lung damage. Total lung weight was increased 3 times more than normal in both mice groups compared to untreated mice. We were able to detect one liver metastasis in sgp130Fc mice and none in control mice. Immunohistological analysis revealed the same immune response in the lungs of sgp130Fc mice like in C57Bl6/N control mice. Tumor bearing lungs of sgp130Fc mice displayed strong infiltration of Ly6G/Gr1<sup>+</sup> cells but not of F4/80<sup>+</sup> cells.

### **5.5 ADAM17 in tumor cells is necessary for tumor cell growth *in vitro* and *in vivo***

In order to investigate the importance of ADAM17 in tumor cells for tumor cell growth *in vitro* and *in vivo*, we generated LLC cells with stable ADAM17 knock down (kdADAM17-LLC). We were able to demonstrate that proliferation of kdADAM17-LLC cells was significantly reduced already in the first 24h. As compared to wtLLC cells, we observed that the difference in proliferation rate was increasing with time progression.

In preliminary experiments, we could see that lack of ADAM17 in tumor cells influences tumor growth *in vivo*. We performed i.v. injection of kdADAM17-LLC cells into C57Bl6/N mice. We were able to see that lack of ADAM17 in the tumor cells resulted in null tumor formation in the lungs. 21 days after kdADAM17-LLC cell inoculation there were no visible tumors in the lungs, compared to control mice injected with wild type LLC cells. To

## **Discussion**

---

investigate the presence of kdADAM17-LLC cells in the lungs of injected mice, we isolated RNA from the whole lung tissue, and performed semiquantitative RT-PCR for gene expression of mCherry. Confirming the expression of mCherry in the lungs of kdADAM17-LLC injected mice, we were able to confirm the presence of kdADAM17-LLC cells in the whole lung tissue.

Our data demonstrate that expression and activity of ADAM17 in the metastatic niche significantly contributes to the growth of metastatic tumors. Targeting ADAM17 in the tumor stroma seem to be very promising as the tumor stroma is not prone to mutations (Junttila et al., 2013).

### 6 Summary

Most cancer deaths are not the result of primary cancer development, but rather the result of its spread, a process called metastasis. Metastasis is a complex process where cancer cells leave the original tumor site, intravasate into the bloodstream, migrate to a distant organs and initiate invasive growth. Numerous studies have contributed to better understanding the underlying cellular and molecular processes of metastasis.

In the present study we could show that ADAM17 plays a crucial role in the tumor cell growth in the metastatic niche of lung metastasis.

In a murine metastasis model using the LLC and B16F1 tumor cell lines we could see that ADAM17<sup>ex/ex</sup> animals, that express low levels of ADAM17, had a much reduced tumor burden. The reduced metastatic growth was accompanied with reduced expression of inflammatory chemokines like e.g. MCP-1 and MIP-2.

Consequently, we observed a reduced infiltration of inflammatory cells, in particular Ly6G/Gr1<sup>+</sup>CD11b<sup>+</sup> myeloid derived suppressor cells in ADAM17<sup>ex/ex</sup> mice.

Furthermore, ADAM17 seems to influence metastatic growth through the activation of the receptor tyrosine kinases PDGFR- $\alpha$  and Axl, as well as the activation of the transmembrane protein Notch.

Taken together, ADAM17 represents a promising drug target for the inhibition of metastasizing process.

### 6 Zusammenfassung

Mortalität bei Tumorerkrankungen ist meistens nicht auf das Wachstum des Primärtumors zurückzuführen, sondern vielmehr auf seine maligne Streuung, der Metastasierung. Metastasierung ist ein komplexer Prozess, bei dem Tumorzellen den Primärtumor verlassen, in die Blutzirkulation eintreten, zu entfernten Organen wandern und dort invasiv wachsen. Zahlreiche Studien haben bereits dazu beigetragen, die zugrundeliegenden zellulären und molekularen Prozesse besser zu verstehen und dem Schritt einer kausalen Therapie metastasierender Erkrankungen näher zu kommen.

In der vorliegenden Studie können wir zeigen, dass ADAM17 in metastasierenden Tumorzellen, aber vor allem auch in Zellen der Metastasennische eine unverzichtbare Rolle für das Wachstum von Lungenmetastasen spielt.

In einem tierexperimentellen Metastasierungsmodell mit murinen LLC und B16F1 Tumorzellen konnten wir sehen, dass ADAM17<sup>ex/ex</sup> Mäuse, die nahezu kein ADAM17 mehr exprimieren, eine deutlich reduzierte Tumorlast aufwiesen. Das reduzierte Metastasenwachstum ging einher mit einer verminderten Expression entzündlicher Zytokine, wie TNF $\alpha$  und IL1 $\beta$  und einer verminderten Expression an entzündlichen Chemokinen wie z.B. MCP-1 und MIP-2. Als Resultat konnten wir in ADAM17<sup>ex/ex</sup> Tieren eine reduzierte Infiltration entzündlicher Zellen, insbesondere sg. Ly6G/Gr1+CD11b+ myeloider Immunsupressorzellen feststellen.

ADAM17 scheint darüberhinaus das Metastasenwachstum durch die Aktivierung der Rezeptortyrosinkinasen PDGFR- $\alpha$  und Axl, sowie dem Transmembranprotein Notch maßgeblich zu beeinflussen.

Zusammengefasst stellt ADAM17 ein vielversprechendes drug target für die Hemmung metastasierender Prozesse dar.

### 7 References

Albina, J.E., M. Caldwell, W.L. Henry and C.D. Mills. 1989. Regulation of macrophage function by L-arginine. *J. Exp. Med.* 169, 1021-1029.

Baud, V. and Karin, M. 2009. Is NF- $\kappa$ B good target for cancer therapy? Hopes and pitfalls. *Nat. Rev. Drug Discovery* 8, 33-40.

Baumgart, A., S. Seidl, P. Vlachou, L. Michel, N. Mitova, N. Schatz, K. Specht, I. Koch, T. Schuster, R. Grundler, M. Kremer, F. Fend, J.T. Siveke, C. , Peschel, J. Duyster and T. Dechow. 2010. ADAM17 regulates Epidermal Growth Factor Receptor expression through the activation of Notch1 in Non–small cell lung cancer. *Cancer Res.* 70, 5368-5378.

Becker, C., M.C. Fantini, C. Schramm, H.A. Lehr, S. Wirtz, A. Nikolaev, J. Burg, S. Strand, R. Kiesslich, S. Huber, H. Ito, N. Nishimoto, K. Yoshizaki, T. Kishimoto, P.R. Galle, M. Blessing, S. Rose-John and M.F. Neurath. 2004. TGF-beta suppresses tumor progression in colon cancer by inhibition of IL-6 trans-signaling. *Immunity* 21, 491-501.

Belperio, J.A., M.P. Keane, M.D. Burdick, V. Londhe, Y.Y. Xue, K. Li, R.J. Phillips and R.M. Strieter. 2002. Critical role for CXCR2 and CXCR2 ligands during the pathogenesis of ventilation-induced lung injury. *J. Clin. Invest.* 110, 1703-1716.

Black, R. A., and J. M. White. 1998. ADAMs: focus on the protease domain. *Curr. Opin. Cell Biol.* 10, 654-659.

Blanschot-Jossic, F., A. Jarry, D. Masson, K., Bach-Ngohou, J. Paineau, M.G. Denis, C.L. Laboisie and J.F. Mosnier. 2005. Up-regulated expression of ADAM17 in human colon carcinoma: co-expression with EGFR in neoplastic and endothelial cells. *J. Pathol.* 207, 156-163.

Blobel, C. P. 1997. Metalloprotease-disintegrins: links to cell adhesion and cleavage of TNF alpha and Notch. *Cell* 90, 589-592.

## References

---

Borrell-Pages, M., F. Rojo, J. Albanell, J. Baselga and J. Arribas. 2003. TACE is required for the activation of the EGFR by TGF- $\alpha$  in tumors. *EMBO J.* 22, 1114-1124.

Bollrath, J., T.J. Phesse, V.A. Von Burstin, T. Putoczki, M. Bennecke, T. Bateman, T. Nebelsiek, T. Lundgren-May, O. Canli, S. Schwitalla, V. Matthewa, R.M. Schmid, T. Kirchner, M.C. Arkan, M. Ernst and F.R. Greten. 2009. gp130-mediated Stat3 activation in enterocytes regulates cell survival and cell-cycle progression during colitis-associated tumorigenesis. *Cancer Cell* 15, 91–102.

Nijkamp, F.P. And M.J. Parnham. Principles of Immunopharmacology: 3<sup>rd</sup> revised and extended edition. 10.1007/978-3-0346-0136-8\_2. Springer, Basel, 2011.

Brou, C., F. Logeat, N. Gupta, C. Bessia, O. LeBail, J.R. Doedens, A. Cumano, P. Roux, R.A. Black and A. Israeel. 2000. A novel proteolytic cleavage involved in Notch Signaling: The role of the disintegrin-metalloprotease TACE. *Mol. Cell* 5, 207-216.

Bozkulak, E. and Weinmaster, G. 2009. Selective use of ADAM10 and ADAM17 in activation of Notch1 signaling. *Mol. Cell. Biol.* 29, 5679-5695.

Carswell, E.A., L.J. Old, R.L. Kassel, S. Green, N. Fiore and B. Williamson. 1975. An endotoxin-induced serum factor that causes necrosis of tumors. *Proc. Natl. Acad. Sci.* 72, 3666–3670.

Catlett-Falcone, R., T.H. Landowski, M.M. Oshiro, J. Turkson, A. Levitzki, R. Savino, G. Ciliberto, L. Moscinski, J.L. Fernandez-Luna, G. Nunez, W.S. Dalton and R. Jove. 1999. Constitutive activation of Stat3 signaling confers resistance to apoptosis in human U266 myeloma cells. *Immunity* 10, 105-115.

Chalaris, A., N. Adam, C. Sina, P. Rosenstiel, J. Lehmann-Koch, P. Schirmacher, D. Hartmann, J. Cichy, O. Gavrilova, S. Schreiber, T. Josrock, V. Matthews, R. Häslar, C. Becker, M.F. Neurath, K. Reiss, P. Saftig, J. Scheller and S. Rose-John. 2010. Critical role of the disintegrin metalloprotease ADAM17 for intestinal inflammation and regeneration in mice. *J. Exp. Med.* 207, 1617-1624.

## References

---

- Chen, Y., M.A. De Marco, I. Graziani, A.F. Gazdar, P.R. Strack, L. Miele and M. Bocchetta. 2007. Oxygen concentration determines the biological effects of NOTCH-1 signaling in adenocarcinoma of the lung. *Cancer Res.* 67, 7954-7959.
- Demarchi, F., R. Verardo, B. Varnum, C. Brancolini and C. Schneider. 2001. Gas6 anti-apoptotic signaling requires NF- $\kappa$ B activation. *J. Biol. Chem.* 276, 31738-31744.
- Diep, B.A., L. Chan, P. Tattevin, O. Kajikawa, T.R. Martin, L. Basuino, T.T Mai, H. Marbach, K. Braughton, A.R. Whitney, D.J. Gardner, X. Fan, C.W. Tseng, G.Y. Liu, C. Badiou, J. Etienne, G. Lina, M.A. Matthay, F.R. DeLeo and H.F. Chambers. 2010. Polymorphonuclear leukocytes mediate *Staphylococcus aureus* Panton-Valentine leukocidin-induced lung inflammation and injury. *Proc. Natl. Acad. Sci.* 12, 5587–5592.
- Ding, X., L.Y. Yang, G.W. Huang, W. Wang and W.Q. Lu. 2004. ADAM17 mRNA expression and pathological features of hepatocellular carcinoma. *World J. Gastroenterol.* 10, 2735-2739.
- Dreymueller, D., C. Martin, T. Kogel, J. Pruessmeyer, F.M. Hess, K. Horiuchi, S. Uhlig and A. Ludwig. 2012. Lung endothelial ADAM17 regulates the acute inflammatory response to lipopolysaccharide. *EMBO Mol. Med.* 4, 412-423.
- Fridell, Y.W.C., Y. Jin, L.A. Quilliam, A. Burchert, P. McCloskey, G. Spizz, B. Varnum, C. Der and E.T. Liu. 1996. Differential activation of the Ras/extracellular-signal-regulated protein kinase pathway is responsible for the biological consequences induced by the Axl receptor tyrosine kinase. *Mol. Cell. Biol.* 16, 135-145.
- Fidler, I. J. 2003. The pathogenesis of cancer metastasis: the „seed and soil“ hypothesis revisited. *Nat. Rev. Cancer* 3, 453-458.
- Fu, S., N. Zhang, A.C. Yopp, D. Chen, M. Mao, D. Chen, H. Zhang, Y. Ding and J.S. Bromberg. 2004. TGF- $\beta$  induces Focp3<sup>+</sup> T-regulatory cells from CD4+CD25 precursors. *Am. J. Transplant.* 4, 1614-1627.



## References

---

- Gabrilovich, D. and Nagaraj, S. 2009. Myeloid-derived suppressor cells as regulators of the immune system. *Nature* 9, 162-174.
- Grell, M., E. Douni, H. Wajant, M. Loehden, M. Clauss, B. Mazeiner, S. Georgopoulos, W. Lesslauer, G. Kollias, K. Pfizenmaier and P. Scheurich. (1995). The transmembrane form of tumor necrosis factor is the prime activating ligand of the 80 kDa tumor necrosis factor receptor. *Cell* 83, 793–802.
- Greten, T.F., M.P. Manns and F. Korangy. 2011. Myeloid derived suppressor cells in human diseases. *Int. Immunopharmacol.* 11, 802-807.
- Gupta, S., L. Feng, T. Yoshimura, J. Redick, S.M. Fu and C.E.Jr. Rose. 2006. Intra-alveolar macrophage-inflammatory peptide 2 induces rapid neutrophil localization in the lung. *Am. J. Respir. Cell. Mol. Biol.* 15, 656-63.
- Hanahan, D. and Weinberg, R.A. 2000. The hallmarks of Cancer. *Cell* 100, 57-70.
- Hanahan, D. and Weinberg, R.A. 2011. Hallmarks of Cancer: The Next Generation. *Cell* 144, 646-674.
- Hanson, E.M., V.K. Clements, P. Sinha, D. Ilkovitch and S. Ostrand-Rosenberg. 2009. Myeloid-derived suppressor cells down-regulate L-selectin expression on CD4<sup>+</sup> and CD8<sup>+</sup> T cells. *J. Immunol.* 183, 937-944.
- Harrari, O. and J.L. Liao. 2004. Inhibition of MHC II gene transcription by nitric oxide and antioxidants. *Curr. Pharm. Des.* 10, 893-898.
- Holland, S.J., A. Pan, C. Franci, Y. Hu, B. Chang, W. Li, M. Duan, A. Torneros, J. Yu, T.J. Heckrodt, J. Zhang, P. Ding, A. Apatira, J. Chua, R. Brandt, P. Pine, D. Goff, R. Singh, D.G. Payan and Y. Hitoshi. 2010. R428, a selective small molecule inhibitor of Axl kinase, blocks tumor spread and prolongs survival in models of metastatic breast cancer. *Cancer Res.* 70, 1544–1554.

## References

---

Huang, B., P.-J. Pan, Q. Li, A.I. Sato, D.E. Levy, J.Bromberg, C.M. Divino and S.-H. Chen. 2006. Gr1+CD115+ Immature myeloid suppressor cells mediate the development of tumor-induced T regulatory cells and T-cell anergy in tumor-bearing host. *Cancer Res.* 66, 1123-1131.

Huang, B., Z. Lei, J. Zhao, W. Gong, J. Liu, Z. Chen, Y. Liu, D. Li, Y. Yuan, G.M. Zhang, and Z.H. Feng. 2007. CCL2/CCR2 pathway mediates recruitment of myeloid suppressor cells to cancers. *Cancer Lett.* 252, 86-92.

Huang M.T., Y.S. Dai, Y.B. Chou, Y.H. Juan, C.C Wang and B.L. Chiang. 2009. Regulatory T-cells negatively regulate neovasculature of airway remodeling via DLL4-Notch signaling. *J. Immunol.* 183, 4745-4754.

Isogai, Z., T. Shinomura, N. Yamakawa, J. Takeuchi, T. Tsuji, D. Heinegard and K. Kimata. 1996. 2B1 antigen characteristically expressed on extracellular matrices of human malignant tumors is a large chondroitin sulfate proteoglycan, PG-M/versican. *Cancer Res.* 56, 3902-3908.

Jinushi, M., H. Yagita, H. Yoshiyama and H. Tahara. 2013. Putting the brakes on anticancer therapies: suppression of innate immune pathways by tumor-associated myeloid cells. *Trends Mol. Med.* 19, 536-545.

Jostock, T., J. Muellberg, S. Ozbek, R. Atreya, G. Blinn, N. Volyz, M. Fischer, M.F. Neurath and S. Rose-John. 2001. Soluble gp130 is the natural inhibitor of soluble interleukin-6 receptor transsignaling responses. *Eur. J. Biochem.* 268, 160-167.

Joyce, J.A. and Pollard, J.W. 2009. Microenvironmental regulation of metastasis. *Nat. Rev. Cancer* 9, 239-52.

Junttila, M.R. and de Sauvage, F. 2013. Influence of tumor microenvironment heterogeneity in therapeutic response. *Nature* 501, 346-354.

Kaplan, R.N., R.D. Riba, S. Zacharoulis, A.H. Bramley, L. Vincent, C. Costa, D.D. Mac

## References

---

- Donald, D.K. Jin, K. Shido, S.A. Kerns, Z. Zhu, D. Hicklin, Y. Wu, J.L. Port, N. Altorki, E.R. Port, D. Ruggero, S.V. Shmelkov, K.K. Jensen, S. Rafii and D. Lyden. 2005. VEGFR1-positive haematopoietic bone marrow progenitors initiate the pre-metastatic niche. *Nature* 438, 820-827.
- Kawai, T. and Akira, S. 2007. Signaling to NF- $\kappa$ B by Toll-like receptors. *Trends Mol. Med.* 13, 460-469.
- Kim, S., H. Takahashi, W.W. Lin, P. Descargues, S. Grivnenkov, Y. Kim, J.L. Luo and M. Karin. 2009. Carcinoma-produced factors activate myeloid cells through TLR2 to stimulate metastasis. *Nature* 457, 102-107.
- Kishimoto, T., S. Akira, M. Narazaki, and T. Taga. 1995. Interleukin-6 family of cytokines and gp130. *Blood* 86, 1243-1254.
- Kopan, M. and M.X.G. Liagan. 2009. The Canonical Notch Signaling Pathway: Unfolding the Activation Mechanism. *Cell* 137, 216-233.
- Kusmartsev, S., Y. Nefedova, D. Yoder and D. Gabrilovich. 2004. Antigen-specific inhibition of CD8<sup>+</sup> T cell response by immature myeloid cells in cancer is mediated by reactive oxygen species. *J. Immunol.* 172, 989-999.
- Linger, R.M., A.K. Keating, H.S. Earp and D.K. Graham. 2008. TAM receptor tyrosine kinases: biologic functions, signaling, and potential therapeutic targeting in human cancer. *Adv. Cancer Res.* 100, 35–83.
- Linger, R.M., A.K. Keating, H.S. Earp and D.K. Graham. 2010. Taking aim at Mer and Axl receptor tyrosine kinases as novel therapeutic targets in solid tumors. *Expert Opin. Ther. Targets* 14, 1073–1090.
- Lu, J., X. Ye, F. Fan, L. Xia, R. Bhattacharya, S. Bellister, F. Tozzi, E. Sceusi, Y. Zhou, I. Tachibana, D.M. Maru, D.H. Hawke, J. Rak, S.A. Mani, P. Zweidler-McKay and L.M. Ellis. 2013. Endothelial cells promote the Colorectal Cancer Stem Cell phenotype through a soluble form of Jagged-1. *Cancer Cell* 23, 171-185.

## References

---

Ludwig, A., C. Hundhausen, M. H. Lambert, N. Broadway, R. C. Andrews, D. M. Bickett, M. A. Leesnitzer, and J. D. Becherer. 2005. Metalloproteinase inhibitors for the disintegrin-like metalloproteinases ADAM10 and ADAM17 that differentially block constitutive and phorbol ester-inducible shedding of cell surface molecules. *Comb. Chem. High Throughput Screen* 8, 161-171.

Luo, J.L., S. Maeda, L.C. Hsu, H. Yagita and M. Karin. 2004. Inhibition of NF- $\kappa$ B in cancer cells converts inflammation-induced tumor growth mediated by TNF- $\alpha$  to TRAIL-mediated tumor regression. *Cancer Cell* 6, 297-305.

Mackay, H.J. and Twelves, C.J. 2007. Targeting the protein kinase C family: are we there yet? *Nat. Rev. Cancer* 7, 554-562.

Männel, D.N., P. Orosz, M. Hafner and W. Falk. 1994. Mechanisms involved in metastasis enhanced by inflammatory mediators. *Circ. Shock*. 44, 9-13.

Matthews, V., B. Schuster, S. Schütze, I. Bussmeyer, A. Ludwig, C. Hundhausen, T. Sadowski, P. Saftig, D. Hartmann, K. J. Kallen, and S. Rose-John. 2003. Cholesterol depletion of the plasma membrane triggers shedding of the human interleukin-6 receptor by TACE and independently of PKC. *J. Biol. Chem.* 278, 38829- 38839.

Mendelson, K., S. Swendeman, P. Saftig and C.P. Blobel. 2010. Stimulation of Platelet-derived Growth Factor Receptor (PDGFR) Activates ADAM17 and Promotes Metalloproteinase-dependent cross-talk between the PDGFR and Epidermal Growth Factor Receptor (EGFR) signaling pathways. *J. Biol. Chem.* 285, 25024-25032.

Minn, A.J., G.P. Gupta, P.M. Siegel, P.D. Bos, W. Shu, D.D. Giri, A. Vial, A., Olshen, W.L. Gerald and J. Massague. 2005. Genes that mediate breast cancer metastasis to lung. *Nature* 436, 518-524.

Monter-Julian, F.A. 2001. The soluble IL-6 receptors: serum levels and biological function. *Cell Mol. Biol. (Noisy-le-grand)* 47, 583-597.

## References

---

- Movahedi, K., M. Guilliams, J. Van den Bossche, C. Gysemans, A. Beschin, P. De Baetselier and J.A. Van Ginderachter. 2008. Identification of a discrete tumor-induced myeloid-derived suppressor cell subpopulations with distinct T-cell suppressive activity. *Blood* 111, 4233-4244.
- Mueller-Newen, G.A., A. Kuster, U. Hammann, R. Kuel, U. Horsten, A. Martens, L. Graeve, J. Wijdenes and P.C. Heinrich. 1998. Soluble IL-6 receptor potentiates the antagonistic activity of soluble gp130 on IL-6 responses. *J. Immunol.* 161, 6347-6355.
- Muraguchi, A., T. Hirano, B. Tang, T. Matsuda, Y. Horii, K. Nakajima and T. Kishimoto. 1988. The essential role of B cell stimulatory factor 2 (BSF-2/IL-6) for the terminal differentiation of B cells. *J. Exp. Med.* 167, 332-344.
- Ni, S.S., J. Zhang, W.L. Zhao, X.C. Dong and J.L. Wang. 2013. ADAM17 is over-expressed in Non-small cell lung cancer and its expression correlates with poor patient survival. *Tumor Biol.* 34, 1813-1818.
- Olayioye, M.A., R.M. Neve, H.A. Lane and N.E. Hynes. 2000. The erbB signaling network: heterodimerization in development and cancer. *EMBO J.* 19, 3159-3167.
- Palladino, M.A., F.R. Bahjat, E.A. Theodorakis and L.L. Moldawer. 2003. Anti-TNF- $\alpha$  therapies: the next generation. *Nat. Rev. Drug Discov.* 2, 736-746.
- Pannuti, A., K. Foreman, P. Rizzo, C. Osipo, T. Golde, B. Osborn and I. Miele. 2010. Targeting Notch to target cancer stem cells. *Clin. Cancer Res.* 16, 3141-3152.
- Peschon, J.J., J.L. Slack, P. Reddy, K.L. Stocking, S.W. Sunnarborg, D.C. Lee, W.E. Russell, B.J. Castner, R.S. Johnson, J.N. Fitzner, R.W. Boyce, N. Nelson, C.J. Kozlosky, M.F. Wolfson, C.T. Rauch, D.P. Cerretti, R.J. Paxton, C.J. March and R.A. Black. 1998. An essential role for ectodomain shedding in mammalian development. *Science* 282, 1281-1284.
- Pirinen, R., T. Leinonen, J. Boehm, R. Johansson, K. Ropponen, E. Kumpulainen and V.M.

## References

---

Kosma. 2005. Versican in non-small cell lung cancer: relation to hyaluronan, clinicopathologic factors, and prognosis. *Hum. Pathol.* 36, 44-50.

Rabe, B., A.Chalaris, U. May, G.H. Waetzig, D. Seegert, A.S. Williams, S.A. Jones, S. Rose-John and J. Scheller. 2008. Transgenic blockade of interleukin 6 transsignaling abrogates inflammation. *Blood* 111, 1021-1028.

Ranganathan, P., K.L. Weaver and A.J. Capobianco. 2011. Notch signaling in solid tumors: a little bit of everything but not all the time. *Nature* 11, 338-351.

Richards, F.M., C.J. Tape, D.I. Jodrell and G. Murphy. 2012. Anti-tumour effects of a specific anti-ADAM17 antibody in an ovarian cancer model in vivo. *PLoS One* 7, 1-10.

Rikova, K., A. Guo, Q. Zeng, A. Possemato, J. Yu, H. Haack, J. Nardone, K. Lee, C. Reeves, Y. Li, Y. Hu, Z. Tan, M. Stokes, L. Sullivan, J. Mitchell, R. Wetzel, J. Macneill, J.M. Ren, J. Yuan, C.E. Bakalarski, J. Villen, J.M. Kornhauser, B. Smith, D. Li, X. Zhou, S.P. Gygi, T.L. Gu, R.D. Polakiewicz, J. Rush and M.J. Comb. 2007. Global survey of phosphotyrosine signaling identifies oncogenic kinases in lung cancer. *Cell* 131, 1190-11203.

Rivas, M.A., R.P. Carnevale, C.J. Proietti, C. Rosembliit, W. Beguelin, M. Salatino, E.H. Charreau, I. Frahm, S. Sapia, P. Brouckaert, P.V. Elizalde and R. Schillaci. 2008. TNF $\alpha$  acting on TNFR1 promotes breast cancer growth via p42/P44 MAPK, JNK, Akt and NF- $\kappa$ B-dependent pathways. *Exp. Cell Res.* 314, 509-519.

Rivoltini, L., M. Carrabba, V. Huber, C. Castelli, L. Novellino, P. Dalebra, R. Mortarini, G. Arancia, A. Anichini, S. Fais and G. Parmiani. 2002. Immunity to cancer: attack and escape in T-lymphocyte-tumor cell interaction. *Immunol. Rev.* 188, 97-113.

Rodriguez, P.C. A.R. Zea, K.S. Culotta, J. Zabaleta, J.B. Ochoa and A.C.Ochoa. 2002. Regulation of T-cell receptor CD3 $\zeta$  chain expression by L-arginine. *J. Biol. Chem.* 277, 21123-21129.

## References

---

- Rodriguez, P.C., D.G. Quiceno and A.C. Ochoa. 2007. L-arginine availability regulates T-lymphocyte cell-cycle progression. *Blood* 109, 1568-1573.
- Romashkova, J.A. and Makarov, S.S. 1999. NF-kappaB is a target of AKT in anti-apoptotic PDGF signalling. *Nature* 401, 89-90.
- Rose-John, S. 2012. IL-6 Trans-Signaling via the Soluble IL-6 Receptor: Importance for the Pro-Inflammatory Activities of IL-6. *Int. J. Biol. Sci.* 8, 1237-1247.
- Rose-John, S., Waetzig, G.H., Scheller, J., Groetzinger, J. and Seegert, D. 2007. The IL6/sIL-6R complex as a novel target for therapeutic approaches. *Expert Opin. Ther. Targets* 11, 613-624.
- Ryzmski, T., A. Petry, D. Kracun, F. Reiss, L. Pike, A.L. Harris and A. Goerlach. 2012. The unfolded protein response controls induction and activation of ADAM17/TACE by severe hypoxia and ER stress. *Oncogene* 31, 3621-3634.
- Sahin, U., G. Weskamp, K. Kelly, H.M. Zhou, S. Higashiyama, J. Peschon, D. Hartmann, P. Saftig. and Blobel. 2004. Distinct roles for ADAM10 and ADAM17 in ectodomain shedding of six EGFR ligands. *J. Cell Biol.* 164, 769-779.
- Santiago-Josefat, B., C. Esselens, J.J. Bech-Serra and J. Arribas. 2007. Post-transcriptional up-regulation of ADAM17 upon Epidermal Growth Factor Receptor activation and in breast tumors. *J. Biol. Chem.* 282, 8325-8331.
- Sawanobori, Y., S. Ueha, M. Kurachi, T. Shimaoka, J.E. Talmadge, J. Abe, Y. Shono, M. Kitabatake, K. Kakimi, N. Mukaida and K. Matsushima. 2008. Chemokine-mediated rapid turnover of myeloid-derived suppressor cells in tumor bearing mice. *Blood* 111, 5457-5466.
- Scheller, J., A. Chalaris, C. Garbers and S. Rose-John. 2011. ADAM17-molecular switch to control inflammation and tissue regeneration. *Trends Immunol.* 32, 380-387.
- Schloendorff, J., J.D. Becherer and C.P. Blobel. 2000. Intracellular maturation and

## References

---

localization of the tumor necrosis factor  $\alpha$  convertase (TACE). *Biochem. J.* 347, 131-138.

Schmielau, J. and O.J. Finn. 2001. Activated granulocytes and granulocyte-derived hydrogen peroxide are the underlying mechanism of suppression of T-cell function in advanced cancer patients. *Cancer Res.* 61, 4756-4760.

Seo, N., S. Nayakawa, M. Takigawa and Y. Tokura. 2001. Interleukin-10 expression at early tumor sites induces subsequent generation of CD(4+) T-regulatory cells and systemic collapse of antitumor immunity. *Immunology* 103, 449-457.

Shackleton, M., E. Quintana, E.R. Fearon and S. Morrison. 2009. Heterogeneity in cancer: cancer stem cells versus clonal evolution. *Cell* 138, 822-829.

Smalley, D.M. And K. Ley. 2005. L-selectin: mechanisms and physiological significance of ectodomain cleavage. *J. Cell. Mol. Med.* 9, 255-266.

Soria, G. and A. Ben-Baruch. 2008. The inflammatory chemokines CCL2 and CCL5 in breast cancer. *Cancer Lett.* 267, 271-285.

Srivastava, M.K., P. Sinha, V.K. Clements, P. Rodriguez and S. Ostrand-Rosenberg. 2010. Myeloid derived suppressor cells inhibit T-cell activation by depleting cystin and cystein. *Cancer Res.* 70, 68-77.

Stöcker, W., F. Grams, U. Baumann, P. Reinemer, F. X. Gomis-Ruth, D. B. McKay, and W. Bode. 1995. The metzincins-topological and sequential relations between the astacins, adamalysins, serralysins, and matrixins (collagenases) define a superfamily of zinc-peptidases. *Protein Sci.* 4, 823-840.

Tabaries, S., Z. Dong, M.G. Annis, A. Omeroglu, F. Pepin, V. Ouellet, C. Russo, M. Hassanain, P. Metrakos, Z. Diaz, M. Basik, N. Bertos, M. Park, C. Guettier, R. Aam, M. Hallett and P.M. Siegel. 2011. Claudin-2 is selectively enriched in and promotes the formation of breast cancer liver metastases through engagement of integrin complexes. *Oncogene* 30, 1318-28.



## References

---

- Tarin, D. 2008. Comparisons of metastases in different organs: biological and clinical implications. *Clin. Cancer Res.* 14, 1923-1925.
- Valastyan, S. and R.A. Weinberg. 2011. Tumor metastasis: Molecular Insights and Evolving Paradigms. *Cell* 147, 275-292.
- Vickers, S.M., L.A. MacMillan-Crow, M Green, C. Ellis and J.A. Thompson. 1999. Association of increased immunostaining for inducible nitric oxide synthase and nitrotyrosine with fibroblast growth factor transformation in pancreatic cancer. *Arch. Surg.* 134, 245-251.
- Wanf, Y., A.C. Zhang, Z. Ni, A. Herrera and B. Walcheck. 2010. ADAM17 activity and other mechanisms of soluble L-selectin production during death receptor-induced leukocyte apoptosis. *J. Immunol.* 184, 444744-54.
- Westhoff, B., I.N. Colaluca, G. D'Ario, M. Donzelli, D. Tosoni, S. Volorio, G. Pelosi, L. Spaggiari, G. Mazzarol, G. Viele, S. Pece and P.P. Di Fiore. 2009. Alterations of the Notch pathway in lung cancer. *Proc. Natl. Acad. Sci.* 106, 22293-22298.
- Waetzig, G.H. and Rose-John, S. 2012. Hitting a complex target: an update on interleukin-6 trans-signalling. *Expert Opin. Ther. Targets* 16, 225-36.
- Yan, H.H., M. Pickup, Y. Pang, A.E. Gorska, Z. Li, A. Chytil, Y. Geng, J.W. Gray, H.L. Moses and L. Yang. 2010. Gr1+CD11b+ Myeloid cells tip the balance of Immune protection tumor promotion in the premetastatic lung. *Cancer Res.* 70, 6139-6149.
- Yi, H., H.J. Cho, S.M. Cho, K. Jo, J.A. Park, N.H. Kim, G.L. Amidon, J.S. Kim and H.C. Shin. 2012. Blockade of interleukin-6 receptor suppresses the proliferation of H460 lung cancer stem cells. *Int. J. Oncol.* 41, 310-316.
- Young, J. I., S. Nagaraj, M. Collazo and D.I. Gabrilovich. 2008. Subsets of myeloid-derived suppressor cells in tumor-bearing mice. *J. Immunol.* 181, 5791-5802.

## References

---

Zhang, H., P. Neuhofer, L. Song, B. Rabe, M. Lesina, M.U. Kurkowski, M. Treber, T. Wartmann, S. Regner, H. Thorlacius, D. Saur, G. Weirich, A. Yashimura, W. Halangk, J.P. Mizgerd, R.M. Schmidt, S. Rose-John and H. Algül. 2013. IL-6 trans-signaling promotes pancreatitis associated lung injury and lethality. *J. Clin. Invest.* 123, 1019-1031.

Zhang, T., C.J. Guo, Y. Li, S.D. Douglas, X.X. Qi, L. Song and W.Z. Ho. 2003. Interleukin-1beta induces macrophage inflammatory protein-1beta expression in human hepatocytes. *Cell Immunol.* 226, 45-53.

Zhou, B.B., M. Peyton, B. He, C. Liu, L. Girard, E. Caudler, Y. Lo, F. Baribaud, I. Mikami, N. Reguart, G. Yang, Y. Li, W. Yao, K. Vaddi, A.F. Gazdar, S.M. Friedman, D.M. Jablons, R.C. Newton, J.S. Fridman, J.D. Minna and P.A. Scherle. 2006. Targeting ADAM-mediated ligand cleavage to inhibit HER3 and EGFR pathways in non-small cell lung cancer. *Cancer Cell* 10, 39-50.

Zwick, E., J. Bange and A. Ullrich. 2008. Receptor tyrosine kinase signaling as a target for cancer intervention strategies. *Endocr. Relat. Cancer* 8, 161-173.

### 8 Abbreviations

ADAM17	A Disintegrin and Metalloprotease 17
AR	Amphiregulin
APS	Amonium- persulphat
B16F1	Murine melanoma cell line
BCD	Blasticidin
BMDC	Bone Marrow Derived Cells
BMDM	Bone Marrow Derived Macrophages
BMDN	Bone Marrow Derived Neutrophils
BSA	Bovine Serum Albumin
Br	Bromine
bp	base pair
°C	degrees of Celsius
C5/C5a	Complement component 5
CaCl <sub>2</sub>	Calcium (II) - chloride
(Ca) <sub>3</sub> (PO <sub>4</sub> ) <sub>2</sub>	Calcium (II) - phosphate
CCL2	Chemokine (C-C motif) ligand 2
CCL3	Chemokine (C-C motif) ligand 3
CCL4	Chemokine (C-C motif) ligand 4
CCL5	Chemokine (C-C motif) ligand 5
CCL12	Chemokine (C-C motif) ligand 12
CD	Cluster of Differentiation
CDK2	Cyclin-dependent kinase 2
Co-R	Transcriptional co-repressors
CSF-1	Macrophage colony-stimulating factor 1

## Appendix

---

CSF1R	Macrophage colony-stimulating factor 1 Receptor
CSL	DNA-binding protein
CXCR4	C-X-C chemokine receptor type 4
CXCL12	C-X-C motif chemokine 12 (also known as SDF-1)
CXCL1	C-X-C motif chemokine 1 (also known as KC)
CXCL2	C-X-C motif chemokine 2 (also known as MIP-2 $\alpha$ )
CXCL8	C-X-C motif chemokine 8
CXCL9	C-X-C motif chemokine 9
CXCL10	C-X-C motif chemokine 10
DD	Death Domain
ddH <sub>2</sub> O	Double-distilled water
DMEM	Dulbecco's Modified Eagle Medium
DNA	Deoxyribonucleic Acid
dNTP	Deoxy-nucleoside triphosphate
EDTA	Ethylenediaminetetraacetic acid
EGF	Epidermal Growth Factor
EGFR	Epidermal Growth Factor Receptor
ELISA	Enzyme-Linked Immunosorbent Array
EMT	Epithelial-Mesenchymale Transition
ER	Endoplasmic Reticulum
Erk1/2	extracellular-signal-regulated kinases 1/2
FACS	Fluorescence-activated cell sorting
FCS	Fetal Calf Serum
FGFR 2	Fibroblast growth factor receptor 2
FGFR 3	Fibroblast growth factor receptor 3

## Appendix

---

g	gram
G-CSF	Granulocyte Colony-stimulating Factor
GI	GI254023X – hydroxamate inhibitor of the ADAM10
Glc	Glucose
Gln	L-glutamine
gp130	Glycoprotein 130
Gr1	Granulocyte marker
GW	GW280264X – hydroxamate inhibitor of the ADAM17 and ADAM10
HB-EGF	Heparin Binding – Epidermal Growth Factor
HBS	Hepes Buffered Saline
HE	Hematoxylin/Eosine
HEK293T	Human Embryonic Kidney 293 cells
HEPES	4-(2-hydroxyethyl)-1-piperazineethanesulfonic acid
Hes	Hairy and enhancer of split-1
Hey	Hairy/enhancer-of-split related with YRPW motif protein 1
HRP	Horseradish-peroxidase
H <sub>2</sub> SO <sub>4</sub>	Sulfuric acid
ICAM-1	Intercellular Adhesion Molecule 1
IGF-1R	Insulin-like growth factor 1 receptor
INF- $\gamma$	Interferon gamma
I $\kappa$ B	Inhibitor of NF- $\kappa$ B
IKK	I $\kappa$ B kinase
IL-1 $\beta$	Interleukin 1 beta
IL-1R	Interleukin 1 receptor

## Appendix

---

IL-6	Interleukin 6
IL-6R	Interleukin 6 Receptor
IL-8	Interleukin 8
IL-16	Interleukin 16
iNOS	Inducible nitric oxide synthase
KCl	Potassium (I) - Chloride
kDa	kiloDalton
KHCO <sub>3</sub>	Potassium-hydrogen carbonate
L	liter
LLC	Lewis Lung Carcinoma
LPS	Lyopolisaccharide
MAM	Mastermind - co-activator
MAPK	Mitogen activated protein kinase
MCP-1	Monocyte chemotactic protein-1
M-CSF	Macrophage-Colony stimulating factor
MDSC	Myelod Derived Suppressor Cells
MEM	Minimum Essential Medium
MEKK 1	Mitogen-activated protein kinase kinase kinase 1
min	minute
MIP-1 $\beta$	Macrophage Inflammatory protein – 1 beta
MIP-2	Macrophage Inflammatory protein - 2
mg	milligram
ml	milliliter
mM	millimolar
$\mu$ l	microliter

## Appendix

---

$\mu\text{M}$	micromolar
MMP2	Matrix metalloprotease 2
MMP9	Matrix metalloprotease 9
mRNA	Messenger Ribonucleic acid
MSPR	Macrophage-stimulating protein receptor
MuSK	Muscle-Specific Kinase
NaCl	Sodium Chloride
NaF	Sodium Fluoride
$\text{Na}_2\text{HPO}_4$	Sodium hydrogenphosphate
$\text{Na}_2\text{HPO}_4 \times 2\text{H}_2\text{O}$	Sodium hydrogenphosphate dihydrate
$\text{Na}_3\text{VO}_4$	Sodium vanadate
$\text{NH}_4\text{Cl}$	Amonium chloride
NF- $\kappa\text{B}$	Nuclear Factor kappa B
NICD	Notch intracellular domain
NIK	NF- $\kappa\text{B}$ -inducing kinase
ng	nanogram
NO	Nitric-oxide
NK	Natural killer cell
NP-40	Nonyl phenoxyethoxyethanol
NSCLC	Non-small cell lung cancer
$\text{ONOO}^\cdot$	Peroxynitrite
PBS	Phosphate buffered saline
PCNA	Proliferating Cell Nuclear Antigen
PDGF	Platelet-derived growth factor
PDGFR $\alpha$	Platelet-derived growth factor receptor alpha

## Appendix

---

PDGFR $\beta$	Platelet-derived growth factor receptor beta
P-Erk1/2	Phosphorylated extracellular-signal-regulated kinases
P-IKK	Phosphorylated I $\kappa$ B kinase
PI-3-K	Phosphatidylinositol – 3 kinase
PKC	Protein kinase C
PMN	Polymorphonuclear cell
PMSF	Phenylmethanesulfonylfluoride
P-STAT3	Phosphorylated - signal transducer and activator of transcription 3
PVDF	Polyvinylidene fluoride
RIP	Receptor interacting protein
ROS	Reactive oxygen species
rpm	revolutions per minute
RT-PCR	Reverse transcription – Polymerase chain reaction
SCFR	Stem cell factor receptor
SDS	Sodium dodecyl sulphate
SDS-PAGE	Sodium dodecyl sulphate – polyacrylamide gel electrophoresis
SDF-1	Stromal cell-derived factor 1
sgp130	Soluble glycoprotein 130
sICAM-1	Soluble Intercellular Adhesion Molecule 1
sIL-6R	Soluble Interleukin 6 Receptor
STAT1	Signal transducer and activator of transcription 1
STAT3	Signal transducer and activator of transcription 3
TACE	TNF- $\alpha$ converting enzyme (ADAM17)
TAE	Tris, Acetic acid, EDTA buffer



## Appendix

---

TCR	T-cell receptor
TEMED	Tetramethylethylenediamine
TGF- $\alpha$	Transforming growth factor alpha
TGF- $\beta$	Transforming growth factor beta
Tie 1	Tyrosine kinase with immunoglobulin-like and EGF-like domains 1
TLR	Toll-like receptor
TRADD	TNFR I associated death domain containing protein
TRAF 2	TNFR associated factor 2
TRAIL	TNF-related apoptosis-inducing ligand
TREM 1	Triggering receptor expressed on myeloid cells 1
Trk A	Neurotrophic tyrosine kinase receptor type 1
TNF- $\alpha$	Tumor necrosis factor alpha
TNFR I	Tumor necrosis factor alpha receptor I
Tris-HCl	tris-(hydroxymethyl)-aminomethane hydrochloric acid
Tyr	tyrosine
V	volt
VCAM-1	Vascular cell adhesion molecule 1
VEGF $\alpha$	Vascular endothelial growth factor alpha
VEGFR 1	Vascular endothelial growth factor receptor 1
VEGFR 2	Vascular endothelial growth factor receptor 2
VEGFR 3	Vascular endothelial growth factor receptor 3
WB	Western Blot

### 9 Publication

Schmidt-Arras, D., M. Müller, **M. Stevanovic**, S. Horn, A. Schütt, J. Bergmann, R. Wilkens, A. Lickert and S. Rose-John. 2013. Oncogenic deletion mutants of gp130 signal from intracellular compartments. *J. Cell Sci. in press*

### 10 Acknowledgement

I would like to thank to Prof. Dr. Stefan Rose-John for giving me a chance to work in a wonderful scientific environment. I am very grateful for many advices, support and constructive criticism which upgraded and inspired my work. Our team meetings were great inspiration for me. Thank you very much!

I would like to thank to Prof. Dr. Röder for his kindness and interest in revising this Thesis.

Thank you, Dirk for passing all the knowledge that you have... and for your endless optimism, which sometimes was even too much for me. Thank you for your support.

This work would not be so successful without my dearest friends and colleagues. Anna Zaslowski who was constantly there for me. I am very lucky that you became the part of my life. Endless Thank you to Silke Horn, whose advices were always coming from the heart and were very helpful without exception. Dr. Kosuke Yamamoto who taught me “Japanese patience” and who was a great support. Nina Hedemann for being a true friend. Olga Schweigert and Dörte Meyer for good advices, many talks and laughs.

I would like to thank to all former and current members of my team: to Dr. Jessica Rabsch who was great support in the very beginning of my work, to Dr. Sven Malchow who thought me i.v. injections which turned out to be indispensable for my work, to Nico Schneider and Dr. Antje Schütt for the great atmosphere in the lab. Dr. To Dr. Juri Bergmann and Miryam Müller, thank you for the never boring moments on a daily basis.

Thank you Ralf and Elsbeth for a wonderful work which you did!

Amazing Petra Voss, who never said NO and who always made things possible.

Thank you, Athena for your time and all answered questions!

Thank you Hannes for a great team spirit and endless scientific talks!

This “triathlon” would not be possible without love and support from my family. Thank you Sasa! You run three quarters of it together with me. Thank you mum and dad! I love you so much! Thank you Tamara!

### 11 Statutory Declaration

I hereby declare that I have authorized this thesis independently, that I have not used other than the declared sourced and that I have cited all literature correctly.

The submitted written version of this work complies on the electronical data medium.

Furthermore, I declare that I have not handed in this paper as final thesis elsewhere.

Hiermit erkläre ich, dass ich die vorliegende Arbeit selbstständig und ohne fremde Hilfe angefertigt und keine anderen als die angegebenen Quellen und Hilfsmittel verwendet habe. Die eingereichte schriftliche Fassung der Arbeit entspricht der auf dem elektronischen Speichermedium.

Weterhin versichere ich, dass ich diese Arbeit noch nicht an anderer Stelle als Abschlussarbeit eingereicht habe.

Kiel, December 2013

-----  
Marija Stevanovic

## **Curriculum vitae**

---

### **12 Curriculum vitae**

#### **Personal data**

---

Name: Marija Stevanović  
Date of birth: 11.06.1983  
Place of birth: Belgrade, Serbia  
Nationality: serbian

#### **Education**

---

March 2010 – February 2014	PhD thesis, Institute of Biochemistry, Medical Faculty, Christian-Albrechts University Kiel, “Analysis of A Disintegrin and Metalloprotease 17 (ADAM17) in the metastatic niche of the lung”
October 2008 – October 2009	Diploma thesis, Institute of Biochemistry, Chemical Faculty, University of Belgrade, “Modification of –SH group of human serum albumin with methylglyoxal”
October 2002 – October 2008	Undergraduate studies, Chemical faculty, University of Belgrade, Serbia

#### **Scientific presentation**

---

Scientific talk at the “5<sup>th</sup> International Conference on Tumor-Host Interaction and Angiogenesis” , 2013 in Ascona, Switzerland